Doctoral Thesis

Regulation of the Cleavage-independent Release of Cohesin in Budding Yeast Meiosis

Ghanim Fajish. V

2017-2023

Laboratory of Genome and Chromosome Functions

Department of Biological Science

Graduate School of Science

Osaka University

TABLE OF CONTENT

Abstract

Meiotic recombination and sister chromatid cohesion maintained by a meiosis specific cohesin complex with Rec8 work together to ensure accurate segregation of chromosomes in budding yeast meiosis. Cleavage of Rec8 by separase enzyme removes bulk of cohesins from arms and centromeres in meiosis I and meiosis II respectively. Recent study led to the discovery of a new step in cohesin removal during meiotic prophase I in a manner independent of cleavage by separase. To delineate the mechanism of regulation of cleavage independent removal of cohesins , I carried out immunostaining and chromatin immunoprecipitation (ChIP) analysis of Rec8 in various mutants. Genome-wide localization of Rec8 confirmed the reduced Rec8 levels on chromosomes in late prophase I compared to mid prophase I. This cohesin removal is region-specific; some regions including centromeres showed the dissociation of Rec8 and the others did not show the dissociation. Furthermore, mutants in meiotic recombination genes; SPO11, MSH5, MLH1, and MLH3 maintained a similar level of Rec8 in late prophase I to that in mid prophase I, suggesting the role of meiotic recombination in cleavage-independent removal of Rec8 .

Mlh1-Mlh3 is involved in the resolution of meiotic recombination intermediates specifically into crossovers as a structure-specific endonuclease. I found out from my analysis that nuclease-defective mlh3 mutant, mlh3- D523N, is also defective in cleavage-independent Rec8 removal. Taken together, my results suggest the coupling of cohesin removal with the formation of crossover formation in meiotic prophase I.

1.Introduction

Meiosis is the central process in sexual reproduction that maintains ploidy in the succeeding generation. Meiotic recombination is a starting point of genetic variations that underlie human evolution. Molecular events during meiotic cell division are being studied in detail by scientists worldwide.

Cohesin is an evolutionarily conserved entrapment (Marston et al 2014) that keeps chromosomes together during these dynamic molecular events. In humans, the cohesin complex entraps and keeps the sister chromatids in female germ cells stable until fertilization. The study of cohesin complex removal regulation in meiosis will lay the foundation for a better scientific understanding of cohesin arrangement and stability in these ageing human maternal oocytes. This understanding is important for drug discovery for coping with infertility in men and conditions like a premature ovarian failure in women (Chiang et al 2010, 2011; Jessberger et al 2012; Herbert et al 2015; Gruhn et al 2019).

Understanding cohesin biology is also essential for other therapeutic interventions for common genetic disorders due to chromosomal abnormalities. Researchers worldwide have shown that cohesin is among the most commonly mutated protein complexes in cancer. In this thesis, I have studied the regulation of cohesin complex dynamics in budding yeast meiotic prophase, particularly its relation with recombination in detail.

1.1.Meiosis and Mitosis

Meiosis and Mitosis are types of cell division in eukaryotes. In Mitosis, the DNA, in the form of chromosomes, is halved so that each daughter cell gets a complete copy of the genetic material. In

meiosis, DNA, in the form of chromosomes, is divided so that each daughter cell gets only half of the copy of genetic material resulting in four haploid germ cells.

Initially, in both Mitosis and meiosis, cells generate a replica of the entire genome through DNA replication during the S phase. Then there is a short G2 phase in which the cell with replicated chromosomes gets ready for segregation. Cell checks the duplicated chromosomes for errors during this phase. G2 is a period of rapid cell growth and protein synthesis.

Mitosis consists of a single round of separation of duplicated chromosomes giving rise to daughter cells with the same amount of genetic information as the parent.

Meiosis is characterized by a single round of DNA replication at the S phase, followed by two successive rounds of chromosome segregation. The net result is four daughter cells with half of the chromosome numbers of an original parent cell. During the first meiotic division, homologous chromosomes different in parental origin get segregated from each other (Figure 1a). Accurate segregation of homologous chromosomes requires recombination at meiotic prophase I.

1.2. Meiotic prophase I

Meiotic prophase I is the most crucial phase in meiosis. It is the most prolonged phase responsible for the proper formation of daughter cells at the end of meiosis.

During this phase, chromosomes search for their homologs and pair with them. Initially in meiotic recombination proteins like Spo11 creates double strand breaks on the DNA. These ends could be repaired by synthesis dependent strand annealing (Figure 1g). This nicks on DNA are then resected by the coordinated action of several nucleases like Exo1 in yeast, resulting in the formation of single stranded 3’ end DNA filaments. These filaments are bound by proteins like Rad51 in yeast (Shinohara et al 1992). This stabilized nucleoprotein filament searches for homologous genomic

regions and pairs with them. When one end of nucleoprotein filament is paired with adjacent homologous DNA strand, these results in the formation of Single-End Invasion Intermediates (SEI). When second strands invasion and capture from a SEI, it then forms double Holliday junctions (dHJs) (Hunter N et al 2001). Synaptonemal complex (SC) (Klein et al 1999) is a structural complex that holds together chromosomes at these junctions. SC contains two chromosome axes called the lateral elements containing two sister chromatids connected through transverse filaments in a central region.

The ring-shaped cohesin complex entraps sister chromatids (Marston et al 2014; Remeseiro et al 2013) forms the structural basis for SC formation (Figure 1b).

Meiotic prophase I is divided into Leptotene, Zygotene, Pachytene, Diplotene, and Diakinesis based on chromosome structures including SCs (Zickler and Kleckner 1998).

Leptotene is the first stage of meiotic prophase I, where cohesin holds sister chromatids together. Chromatids start to condense into a chromosome axis at this stage. Formation of double-strand breaks (DSB) by Spo11 on DNA occurs in this phase. During the late Leptotene stage, the search for the homologs chromosomes starts, and the axial elements of SC begin to assemble onto the chromosomes.

In the Zygotene stage, homologous chromosomes with axial elements initiate pairing with each other, thus SC formation. In this stage, DSBs are converted into an intermediate for recombination. This is referred as to Single-End Invasion (SEI). Chromosomes start to undergo rearrangements inside the nucleus by the attachment of telomeres to the centrosome (yeast spindle pole body (SPB)) to form telomere clusters called bouquet-like structures (Zickler and Kleckner 1999) at the zygotene stage.

In the early pachytene stage, the homologous pairing (synapsis) is complete. SC is now extended to an entire length of the chromosomes, which is described as elongated SC's. At early pachytene, the recombination proceeds from SEIs to double-Holiday Junctions (dHJs) by capturing with the other end of DSB (Kerr et al 2012).

The resolution of dHJs to reciprocal crossover or non-crossover products occurs in the late pachytene accompanied by the disassembly of SCs. A recombination checkpoint controls this transition (Marston and Amon 2004; Kerr et al 2012).

In the diplotene stage, the Synaptonemal complex dissembles completely. Homologous chromosomes are connected loosely to each other except at points called the chiasma, which results from the dissolution of dHJs. Chiasma holds the chromosomes together until the onset of metaphase I (Zickler and Kleckner 1998). In the diakinesis phase following diplotene, the chiasmata are primarily visible between the homologous chromosomes. The Diakinesis stage is followed by the metaphase I stage. Microtubules pull chromosomes at kinetochores to the poles of the cell at this stage. Chiasmata and the cohesin complex provide tension against the pulling force of microtubules at metaphase I.

Metaphase I is followed by Anaphase I. Separase activation at anaphase I lead to arm-cohesin dissociation, while Shugoshin protects sister chromatid cohesion at kinetochores. As a result, at the end of meiosis I homologous chromosomes segregate to the different poles.

In meiosis II, cohesion at the centromere region of sister chromatids is removed, and individual sister chromatids separate. This separation results in the formation of four haploid gametes (Figure 1a).

1.3. Assembly and disassembly of Synaptonemal Complex

SC formation and disassembly events are well defined in budding yeast. The ladder-like structure of the SC comprises of two lateral elements (LEs) that are connected to each other via the central element (CE). The chromatin corresponding to homologous chromosomes is attached to LEs in regular arrays of DNA loops. Meiotic sister chromatids assembled as an axis of SCs consist of cohesin and TopII (Klein et al 1992; Klein et al 1999). At leptotene stage, an Axial Element protein Red1 is associated with the Rec8 cohesin complex (Rockmill et al 1988) on chromosomes, which is followed by the recruitment of Hop1 to form a chromosome axis structure (Hollingsworth et al 1990).

At the zygotene stage, homologues chromosomes are linked together by the deposition of a Zip1 at the central region of SC (Sym et al 1993). In the middle of Synaptonemal Complex, Zip1 protein forms coiled-coil homodimer. Two homodimers overlap at its N terminus forming tetrameric structures. Along with central and lateral elements, axis-associated proteins called of ZMM proteins that include Zip2, Zip3, Msh4, Msh5, Spo22, Mre3 and Spo16 facilitate the formation of SC as well as COs. (Shinohara et al 2008; Tsubouchi et al 2006). After late pachytene stage when SC starts to disassemble between the homologues, Aurora B/Ipl1 kinase plays an essential role in disassembly of SC during meiosis (Jordan et al 2009).

Meiosis-specific kleisin Rec8 plays an essential role in Sister chromatid cohesion. SCC-independent roles of Rec8 in chromosome axis formation during meiosis have been discovered (Buonomo et al 2000; Jin et al 2009). It has been identified by many groups that Rec8 plays a role in Axis Element biogenesis and SC formation in various eukaryotic models. The rec8 deletion mutant show absence of axis assembly and improper localization of various axis proteins in budding yeast (Klein et al 1999; Golubovskaya et al 2006). In C. elegans Rec8 has two paralogs COH-3 and COH-4 and deletion of these genes leads to defective Axis Element formation

(Severson et al., 2009). In mouse REC8 knockdown does not show problem in Axis Element formation (Bannister et al., 2004; Xu et al., 2005). But studies on Rad21L, a variant of meiosis-specific kleisin in mouse demonstrate that Rad21L is required for initiation of synapsis and crossover recombination (Herran et al 2011; Lee et al 2011). Spermatocyte knockdown of both meiosis-specific kleisins Rad21L and Rec8 in mouse showed defect in Axis Element assembly and induces an arrest at leptotene stage.

Along with meiosis-specific kleisin Rec8, cohesion-associated subunit Pds5 also plays a role in SC formation. PDS5 depletion mutant of budding yeast shows failure in homologous pairing with normal localization of Rec8 as well as other Axis Element proteins Hop1 and Red1 (Jin et al 2009). In this particular stage, chromosome appear as short rod-like structures, indicating that Pds5 is required for proper axial compaction of chromosomes.

Hence cohesin and its regulators, together with Red1 and axial elements like Hop1 and Zip1 is responsible for SC assembly and disassembly.

1.4. Homologous recombination

Recombination is a process in which pieces of DNA are exchanged into new DNA strands resulting in a new combination of genetic information. Homologous recombination happens in the meiotic prophase in all sexually reproducing organisms. At meiotic prophase I in budding yeast, homologous chromosomes from each parent pair with each other. The chromosome from one parent aligns and pairs with the respective homologous chromosome from the other parent. Homologous chromosomes contain genetic information for the same set of biological functions, but the type differs according to the lineage of each parent.

Double strand breaks are made at sites across the genome by Spo11 protein (Klapholz et al 1985; Keeney et al 1997; Handel et al 2010). PRDM9 deposits both H3K4me3 and H3K36me3 histone methylation marks at the sites it binds to and plays a role in DSB positioning. These breaks are then resected by removing nucleotides from one of the strands (5' end). This results in the formation of overhangs (3' overhangs). The ssDNA with 3'-overhang is then loaded with RecA-related recombinases Rad51 and Dmc1, forming filament-like structures on the DNA (Shinohara et al 1992; Bishop et al 1992).

Rad51-Dmc1 pair initiate homology search and Rad54 and Tid1/Rdh54 proteins for the homologous duplex DNA sequences (Shinohara et al 1992). After overhangs find the homologous DNA, displacement loop (D-loop) is formed by invasion of the ssDNA into the duplex DNA (Lao et al., 2010). When the invading strand finds the exact homology, it binds to the DNA helix resulting in the displacement of complementary DNA strand and forms displacement loop (D-loop) (Szostak et al 1983). The DNA polymerase further extends the ssDNA using the homolog as a template, releasing a much bigger D-loop. The D-loop could be repaired by a variety of pathways in budding yeast meiosis resulting in either crossovers or non-crossovers (Figure 1g). This depends on the class of DSB protein groups which are acting on the D-loop. Formation of crossovers result in the formation of chiasmata. Crossovers and non-crossovers are the end result of homologous recombination. Hence homologous recombination creates new variants of DNA strands from existing ones through a set of tightly regulated and programmed steps.

1.5. DNA Double-Strand Break Repair Pathway Choice

Double Strand Break repair in budding yeast meiosis can follow a variety of pathways. Steps from DSB formation by spo11 and resection to form Strand Invasion intermediates and ultimately D-loop formation is the same for crossovers as well as non-crossovers.

A variety of DSB repair pathways can act on the intermediate D-loop. At this point, if the helicase Sgs1, Top3 and Rmi1(STR complex with helicases/topoisomerases) disassemble the double Holliday junctions (and other strand invasion intermediates). This disassembly can result in synthesis-dependent strand annealing (SDSA) cross-overs (Figure 1g). The return of events to the original DSB state can also happen from this state (Jessop et al 2008). This form of DSB repair is termed synthesis-dependent strand annealing (SDSA) leads to non-crossovers only. If the D-loop is not dissolved, the ssDNA end is further extended and captures the other side of the DSB, a process termed second end capture, resulting in a joint molecule involving both the chromatids (Szostak et al. 1983). These joint molecules are then turned into crossovers or non-crossovers depending upon the pathway they are acted upon. Local chromosome context is a significant determinant of crossover pathway biochemistry during budding yeast meiosis (Darpan Medhi et al 2016).

If at this step structure selective nucleases (SSNs) such as Mus81-Mms4, Slx1-Slx4, and Yen1 can act on these intermediates, they cut them at specific junctions resulting in a small number of crossovers (Kaur et al 2015).

Nevertheless, most of the joint molecules produced during meiosis escape SSNs and get captured by ZMM proteins (Figure 1g,1h) (Bzymeket al 2010). If capture and protection by the ZMM (Zip1, Spo16, Zip2, Zip3, and Zip4, Mer3, Msh4 and Msh5) proteins happen, stabilization of JMs and dHJ formation happen. The resolution of these dHJs as class I crossovers by Mlh1-Mlh3 and Exo1 is the ultimate result of this pathway (Kaur et al 2015). Biochemical and molecular studies suggest that SIC components and MutS homolog proteins Msh4 and Msh5 are essential to stabilize the joint molecules (JMs) and promote dHJs (Snowden et al 2004). The Msh4-Msh5 and Mlh1-Mlh3 proteins also act as pro-crossover factors that act in opposition to Sgs1 to promote crossing over

at designated chromosome sites and to prevent aberrant crossing over (Jessop et al 2006; Oh et al 2007)

Cross talk between local axis structure and proximity from nearby crossovers influence the formation of crossovers. The presence of a CO at one position decreases the possibility of another CO formation nearby, known as CO interference (Borner et al2004). Only crossovers formed in the ZMM pathway are interference dependent.

Homologous chromosomes undergo at least one CO along the chromosomes, a crossover assurance (Roeder et al 1997). It has been shown that the ZMM proteins distinctly regulate crossover assurance and crossover interference during yeast meiosis (Miki Shinohara et al 2008). These cross-overs are Class I crossovers and form the majority of cross-overs in budding yeast.

Crossover patterning along chromosomes have a mechanical basis. Formation of a crossover at a position creates a mechanical expansional stress at three levels, at DNA/chromatin fiber for recombination, chromosome axis for axis exchange and sister chromatids (for separation) which is distributed along the chromosomes (Kleckner et al 2004).

1.6. MutSγ complex (Msh4-Msh5)

The Msh4 and Msh5 proteins form a hetero-oligomeric structure/heterodimer. It is conserved from yeast and humans (Pochart et al 1997). The Msh4-Msh5 complex binds and stabilizes double Holliday junctions. This stabilization promotes their resolution into crossover products.

In S.cerevisiae, both msh4Δ and msh5Δ mutants show a significant reduction in meiotic viability along with crossover defects and Meiosis I non-disjunction (Hollingsworth et al 1995; Argueso et al 2004). Biochemical and biophysical studies using purified human Msh4 andMsh5 show that they bind specifically to Holliday junction substrates and stabilize them (Snowden et al. 2004).

Similarly, in vitro biochemical and physical studies in S. cerevisiae show that Msh4-Msh5 stabilizes 3'- overhangs, single-end invasion (SEI) intermediates, and Holliday junctions (Borner et al. 2004, Lahiri et al 2018). Taken together, stabilization of double Holliday junctions is a well characterized function of the MutS **γ** complex. As discussed earlier, this stabilization also prevents branch migration and action of other crossover pathways on the D-loops until the resolution of double Holliday junctions (Figure 1g,1h).

1.7. MutLγ complex (Mlh1-Mlh3)

Mlh1-Mlh3 complex is an endonuclease which specifically binds to Holliday junctions (Ranjha et al 2014). It binds to supercoiled dsDNA and creates single strand breaks. The action of Mlh1-Mlh3 complex is characterized in more detail at stages after D-loop formation. Mlh1-Mlh3 complex is believed to polymerize with itself in a filament like fashion on the Holliday junctions and create incisions on DNA away from the double Holliday junctions. MutLγ complex forms a complex with exo1 when it is recruited to double Holliday junctions (Jingqi Dai et al 2021). They create nicks in an asymmetric fashion on D-loop leading to the formation of crossovers. Majority of crossovers in budding yeast arise through this cleavage of recombination intermediates by the Mlh1-Mlh3 (MutLγ) endonuclease and a non-catalytic function of Exo1, and require the Polo kinase Cdc5 (Sanchez et al 2020). Mlh3 has an endonuclease motif which is indispensable for this DNA nicking activity. It is known that a mutation in the putative Mlh3 Endonuclease domain (*mlh3-D523N* mutation) confers a defect in both Mismatch Repair and Meiosis in *Saccharomyces cerevisiae*. The MLH3 homologs in yeast and humans contain the highly conserved metal-binding motif implicated in MutLα endonuclease activity (Kadyrov et al. 2006). Crossovers resulting from Mlh1-Mlh3 pathway are named Class I crossovers.

1.8. Mus81-Mms4 Complex

Mus81 is an evolutionarily conserved endonuclease with homology to the XPF/Rad1 proteins that function in nucleotide excision repair (Haber and Heyer 2001). Mus81-Mms4 is required for only a small subset of crossovers in budding yeast. The Mus81 and Mms4 function together as a complex. It is been found out that the polo like kinase Cdc5 activates the Mus81-Mms4 complex (Erin K Schwartz et al 2012). Mus81-Mms4 cleaves nicked recombination intermediates such as displacement loops, nicked Holliday junctions, or 3′ flaps but not intact Holliday junctions with four uninterrupted strands. This is because it exists as a single heterodimer with only one active site. On the other hand, activity of two catalytic sites is required for resolution of intact double Holliday junctions into crossovers.

Mus81-Mms4 is hence unable to perform coordinated cleavage of double Holliday junctions like Mlh1-Mlh3 complex. Importantly, Crossovers are distributed normally along chromosomes in an *mms4* mutant, indicating that crossovers subject to interference do not require *MUS81/MMS4.*

Observations from various studies have led to the conclusion that dHJ resolution in budding yeast does not require Mus81-Mms4 and that it is a dispensable pathway. Crossovers resulting from Mus81-Mms4 pathway are named Class II crossovers.

1.9. Structure of Cohesin Complex

Chiasmata by crossovers and cohesion by of sister chromatids and homologs provide resistance against pulling force of microtubules leading to accurate segregation of chromosomes. Sister chromatid cohesion is essential component of meiotic cell division. Sister chromatid cohesion (SCC) is maintained by an evolutionarily conserved protein complex called cohesin. Cohesin is a member of the ancient genome-organizing SMC (Structural Maintenance of Chromosomes) family of protein complexes, present from bacteria to humans (Makrantoni V et al 2018). The

structure of the cohesin complex has been well characterized in budding yeast. Cohesin structure is tailor-made for its protein-protein as well as protein-DNA interactions.

In budding yeast, cohesin holds sister chromatids together by forming a ring-shaped complex with three protein subunits, Smc1, Smc3, and kleisin specific subunit Scc1/Mcd1 during Mitosis. Mitosis-specific kleisin subunit of cohesin complex Rad21/Scc1 is replaced by a meiosis-specific kleisin Rec8 in S. cerevisiae and S. pombe during meiosis (Figure 1b).

Smc1 and Smc3 belong to the structural maintenance of the chromosome (SMC) protein family group. These proteins consist of a separated ATPase domain flanking an anti-parallel coiled-coil rod domain with a hinge (Michaelis et al 1997; Strunnikov et al 1993) and form a heterodimer by interacting via hinge domains and between ATPase heads (Melby et al 1998; Haering et al 2002; Hirano et al 2002).

Scc1/Mcd1 (or Rec8 in meiosis) subunit is connected to ATPase heads of both the proteins in both mitosis specific and meiosis specific proteins (Figure 1b). This ring-shaped entrapment has a diameter around 40nm and holds sister chromatids within it (Haering et al 2002). Opening or breaking the ring hinders sister chromatid cohesion. A major subunit of the cohesin complex, Scc3/Irr1, is associated with Scc1/Mcd1. The Scc3 contains HEAT repeats, required for the protein-protein interactions. SA1 and SA2 are isoforms of Scc3. Scc3-Scc1 DNA-binding interface plays a central role in the recruitment of cohesin complexes to chromosomes.

In C. elegans along with Rec8 another two paralogs, called COH3 and COH4 controls sister chromatid cohesion (Severson et al 2009). Meiotic Smc1 is replaced with Smc1β in mammalian cells. In higher eukaryotes, STAG3 replaces SA1/SA2 subunits during meiosis (Pezzi et al 2000; Prieto et al 2001; Revenkova et al 2004). Recent findings in mouse also lead to discovery of a

Rad21-like protein (Rad21L) during meiosis, which has sequence similarity with Rec8 and Rad21 (Gutierrez-Caballero et al 2011). Rad21L gets localized on chromosome axis during meiotic prophase, along with axial elements of Synaptonemal complex and is shown to possess a significant role in homologous recombination (Ishiguro et al 2011).

1.10. Loading and Maintenance of Cohesin Complex

The loading of the cohesin ring happens before the replication of DNA strands at the S phase. Cohesin binds to the chromosomes at the G1 phase to anaphase onset in budding yeast (Michaelis et al 1997; Tanaka et al 1999).

In budding yeast, the cohesin loader is a conserved Scc2/Scc4 complex (Ciosk et al 2000). The proteins of the complex interact with soluble cohesin but do not co-localize with the cohesin complex on the chromosome CAR regions (Arumugam et al 2003; Lengronne et al 2004).

In vertebrates, cohesin stays on chromosomes until the telophase of the preceding cell cycle and remains intact until the anaphase of the subsequent division (Sumara et al 2000; Losada et al 2000).

The cohesin-binding sites have been mapped onto the chromosomes in several species. In budding yeast, a high level of cohesin binding is seen at the centromere, where cohesin plays an essential role. It provides tension against pulling forces of spindle microtubules. This tension plays a crucial role in preventing the mis-segregation of chromosomes. Cohesin binding also peaks at axial sites since it is the primary structural component of the SC complex during the meiotic prophase.

Cohesin loads onto the chromosome arms at every 10 to 15 kb of the genome (Blat et al 1999; Laloraya et al. 2000; Glynn et al. 2004; Lengronne et al. 2004). Cohesin sites are highly conserved in meiosis and mitosis, suggesting that chromosomes share a common underlying structure during different developmental programs. These sites occur with a spacing of 11 kb that correlates with

their AT content (Glynn et al 2004). These sites are around 0.8 to 1.0 kb in length in budding yeast (Laloraya et al 2000). However, no specific DNA sequence has been identified in cohesin associated regions, although AT-rich intergenic regions are between the transcription sites (Lengronne et al 2004; Glynn et al 2004). Strong correlation between cohesin sites and regions between convergent transcription units have been identified (Glynn et al 2004). Cohesin sites avoid sites of meiotic exchange (Ito et al 2004; Glynn et al 2004) in meiosis.

It has been believed that cohesin gets loaded onto intergenic regions first with the help of cohesin loader at temporary sites and is then further moved to other sites by driven by transcription (Sun et al 2015). Recent experiments have shown that cohesin slides along chromosomes towards areas where genes are active (Sun et al 2015).

Cohesin regulator Wapl/Rad61 in humans is required for a role of cohesin in chromatin; DSB repair, implicated in heterochromatin formation, and is also known to promote cohesion dissociation from chromosomes during mitotic prophase (Kueng et al 2006; Gandhi et al 2006). The role of Rad61/Wapl in cohesin removal process was also observed in fission yeast (Bernard et al 2008). However, the loss of WAPL function in humans leads to increase in chromosomal cohesin, while the rad61 deletion in budding yeast shows decreased cohesin on chromosomes (Warren et al 2004; Sutani et al 2009; Rowland et al2009; Gandhi et al2006) In both yeast and mammalian systems deletion of wapl/rad61 bypass the eco1-induced defects (Gandhi et al2006, Kueng et al., 2006). Hence wapl1 and eco1 act oppositely to each other.

The chromatin-associated cohesin needs to acquire the complete ring state to hold the sister chromatids together. This is achieved by establishing sister chromatid cohesion with Eco1 protein, which is coupled with DNA replication. Eco1 protein has the acetyl-transferase activity required for the cohesive state of the complex. The Wpl1-Pds5 complex is inhibitory for cohesion

establishment, but Eco1 establishes cohesion by hindering the function of Wpl1-Pds5 temporally in the S phase (Takashi Sutani et al 2009).

Recent chromosome capture (Hi-C) experiments show precise alignment of sister chromatids at centromeres with cohesion rings. Along arms, sister chromatids are less precisely aligned, with inter-sister connections by cohesins at every ~35 kilobase (kb). Inter-sister interactions occur between cohesin binding sites that are often offset by 5 to 25 kb (Oomen et al 2020). Along sister chromatids, cohesin results in the formation of loops from 3kb to around 20kb (Costantino et al 2020). Hence recent studies show cohesion compact the chromosomes at specific regions yet resulting formation of chromosome loops in different regions once established.

1.11. Removal of the Cohesin Complex in Mitosis

In budding yeast mitosis, cohesin removal does not take place during prophase. All the cohesin rings remain bound to the DNA until the onset of anaphase (Ciosk et al 2000). At the anaphase onset, the entire cohesin is removed by the protease called Separase that cleaves the mitotic kleisin Mcd1/Scc1 (Uhlmann et al 1999) (Figure 1f).

Separase is activated by the degradation of its inhibitor, Securin (Pds1). Anaphase promoting complex/Cyclosome (APC/C) degrades securin at the metaphase to anaphase transition (Sumara et al., 2000) (Figure 1c).

In vertebrate cells, cohesion is removed from chromosomes in a two-step process. Initially, most arm cohesin is removed from the chromosome arms by a process called the 'prophase pathway'. (Figure 1e). However, cohesin on centromere is protected from this pathway. They are only removed at metaphase-to-anaphase transition (Waizenegger et al. 2000; Losada et al. 2000; Warren et al., 2000). The phosphorylation of sororin and Scc3 kick-starts this 'prophase pathway'

for cohesin removal by a series of kinases, namely, the polo-like kinase (PLK), aurora kinase, and cyclin-dependent kinase (CDK). Phosphorylation renders sororin inactive, and it can no longer suppress Wapl activity (Nishiyama et al 2010).

On the other hand, at the centromeres, the phosphorylation that triggers the prophase pathway is blocked by the action of Shugoshin (the name means guardian spirit). Shugoshin recruits a phosphatase, PP2A (Marston AL et al 2015). PP2A dephosphorylate proteins involved in the prophase pathway, such as sororin. Interestingly, sororin is not present in lower eukaryotes such as budding yeast, and hence the prophase pathway of cohesin removal is absent in yeast mitosis (Lopez-Serra et al 2013).

1.12. Removal of the cohesin complex in Meiosis

Cohesin dynamics in meiosis is crucial because it is directly involved in critical chromosomal events such as homologous recombination and chromosome motion in the meiotic prophase-I (Yoon SW et al 2016). Protection of SCC at the kinetochores is essential for proper sister chromatids segregation at Meiosis II (Figure 1a).

A two-step pathway regulates cohesin removal during meiosis. Arm cohesin is removed through the cleavage of Rec8 by a protease Separase at metaphase I-to anaphase I-transition while the action of Sgo1/PP2A protects centromeric cohesin. Separase remains inactive by the action of securing until the onset of anaphase. At the onset of anaphase, Anaphase Promoting Complex (APC) and CDC20 complex ubiquinates and degrades securing making separase active (Figure 1c). At meiosis II, centromeric cohesin is also cleaved by the Separase. It has been previously reported that Scc1 is phosphorylated by Polo-like kinase-dependent manner and this phosphorylation promotes Scc1 cleavage in yeast mitosis (Alexandru et al 2001, Lengronne et al

2004). Like Mitosis, during meiosis, Rec8 is phosphorylated by multiple kinases such as Polo-like kinase/Cdc5, casein kinase I δ/ε (CK1), Dbf4-dependent Cdc7 kinase (DDK) (Clyne et al 2003; Lee et al 2003; Katis et al 2010; Brar et al 2006; Attner et al 2013). Importantly, DDK and CK1-dependent phosphorylation of Rec8 remains inevitable for the separase cleavage (Katis et al 2010)

Like yeast, in most higher organisms, cohesin removal during meiosis is regulated by a two-step process. In Xenopus egg extracts, APC/C activation and separase-mediated cleavage are not required for first meiotic division but for centromeric cohesin cleavage at second meiotic division (Peter et al., 2001). It has been reported that temperature-sensitive mutants of APC/C in C. elegans showed defects in homologs segregation, suggesting that separase-mediated cleavage of cohesin is required for first meiotic division (Furuta et al 2000). Interestingly, in higher eukaryotes decrease in the amount of cohesin bound to chromosome arms during prophase was also observed, suggesting the presence of cleavage-independent removal of cohesin (Prieto et al 2001,2002; Revenkova et al 2001).

1.13. Cleavage-independent Removal of the Cohesin Complex in Budding Yeast Meiosis

At late meiotic prophase-I of budding yeast, approximately half of the full-length of Rec8 molecules are released from meiotic chromosomes in a cleavage-independent manner (Challa et al 2019; Yu and Koshland 2005). In addition to Cdc5/PLK, it was shown that this “prophase-like” removal of cohesin during meiotic prophase-I requires phosphorylation by Rad61/Wpl1 and DDK. The Rec8 release is coupled to changes in chromosome compaction. This new model was discovered from previous studies in our laboratory (Challa et al 2019) (Figure 1d). This chromosome compaction is strong compaction facilitating chiasmata to emerge, preparing chromosomes for segregation. In meiosis I, the chiasmata are essential for chromosome

segregation. Indeed, loss of cohesion around chiasmata sites has been observed in various organisms (Kleckner et al. 2006).

Similarly, in worms, Wapl-dependent cohesin removal promotes the recombination-mediated change of meiotic chromosome structure. It has been shown that removal of cohesion at the site of chiasmata may be a necessary step in the formation of normal diplotene bivalents (Kleckner et al. 2006). A possible function of cohesin release before could be to facilitate chiasmata formation. I have studied in detail which proteins involved in chiasmata formation are indispensable for this cleavage-independent cohesin release.

2.Aim of Project

Sister chromatid cohesion dynamics must be tightly regulated in budding yeast meiosis to ensure accurate segregation of chromosome pairs in meiosis I and sister chromatids in meiosis II. Our previous study (Challa et al 2019) reported the existence of a novel step in cohesin removal before anaphase I in a manner independent of Separase. We retrieved Rec8 intact from meiotic prophase cells showing this removal is cleavage-independent. This removal requires phosphorylation of wapl1, the regulatory protein of cohesin. It was also showed this removal is coupled with the synaptonemal complex breakdown in prophase. However, the regions from where cohesin rings are removed or are protected from removal are unknown. The molecular determinants that influence this dynamic rearrangement of the cohesin ring are studied in this project, focusing on recombination.

My aim is to independently validate this observation and importantly to find the relationship of this removal with meiotic recombination. In addition to relationship with recombination, spatial patterning of cleavage independent removal of cohesin proteins is not understood till date. I want to address this problem also in my study. I want to check if the binding locations of cohesin differ drastically before and after cleavage independent removal to delineate the relationship of cleavage independent cohesin removal with meiotic recombination. I wish to check if the binding pattern of cohesins overlap with meiotic recombination proteins.

It has been long hypothesized that crossing over and chiasmata formation in meiotic prophase could be critical in this cleavage independent Rec8 removal. I analyzed a range of proteins

responsible for chiasmata formation to elucidate the candidate genes responsible for tight regulation of this removal. I am interested in the Class I crossovers (ZMM dependent) because those proteins create incisions on recombination intermediates and exchange long stretches of DNA, leading to the majority of crossovers in S.cerevisiae. If these crucial proteins of recombination influence Rec8 dynamics in meiotic prophase is studied upon in my study in detail.

3.Materials and methods

3.1. Yeast Genomic DNA preparation

Yeast cells are cultured in 1-2 ml of YPAD liquid medium overnight. Cells are harvested in Eppendorf tubes. Pellets are then suspended in 500 µl of Zymolase buffer (10mM NaPO4, 10mM EDTA, 0.1 M β-Mercaptoethanol, 100mg/ml Zymolase 100T), vortexed for mixing, and then incubated at 37° for 30 min. Cells are lysed by adding 5 µl of Proteinase-K (10 mg/ml) and 100 µl of Lysing buffer (0.25 M EDTA, 0.5 M Tris base, 2.5% (w/v) SDS), mixed well, and incubated at 65°C for 1 hour. During this period, tubes are mixed at least 2 times. 100 µl of 5 M potassium acetate solution is added to the cell suspension, mixed well by shaking, and cell suspensions are incubated on ice for 15 min. Cells are centrifuged at 15000 rpm for 10 min. Supernatants are transferred to new Eppendorf tubes containing 500 µl of cold 100% (V/V) EtOH (ethanol). Samples are inverted 5times gently and centrifuged at 12000 rpm for 30 sec. Supernatants were removed and pellets were washed with 1 ml of 70% (V/V) EtOH. Furthermore, supernatants were removed and washed the pellets with 1 ml 100%(V/V) EtOH. Samples are dried for 10 min by the centrifugal concentrator. DNAs are suspended with 500 ml of 1X TE, which is followed by RNase A treatment with 10 µg/ml RNaseA at room temp for 30 min. 0.5 ml of 2-propanol is added to samples, inverted gently 5 times, and centrifuged at 15000 rpm. Resultant supernatants were removed, and pellets were washed with 70% (V/V) EtOH followed by washing with 100% (V/V) EtOH. Samples are dried up for 10 min, and DNAs are suspended with 100-200 µl of 1X TE buffer.

3.2. Meiosis Time Course

Initially, yeast cells are spread on the YPG (1% Bacto Yeast Extract, 2% Bacto Peptone,2% Glycerol) plate from freezing stock (-80°C), incubated at 30°C for 12 hours, and then streaked on

YPAD plates and incubated for further 2 days at 30°C for producing single colonies. A single diploid colony was inoculated in 3 ml of liquid YPAD medium and incubated overnight in a rotator at 30°C. 1 ml of the culture was added to 100 ml of SPS (0.5% Bacto Yeast Extract, 1% Bacto Peptone, 0.17% Yeast nitrogen base, 1% Potassium acetate, 1% Potassium hydrogen phthalate, 0.5% Ammonium sulfate) and incubated for 16-17 hours at 30°C with 230 rpm, shaker (Innova® 44). The next day, after 16–17 hour overnight incubation, the SPS culture was centrifuged using a 50 ml screw-cap tube, and then pellets were washed twice with sterilized distilled water.

Yeast cells were suspended in 100 ml of SPM (0.3% Potassium acetate,0.02% Raffinose) and incubated at 30°C at 230 rpm to initiate meiosis, and samples were collected at each time point.

3.3. Slide Preparation for Chromosome Spreads (Lipsol method)

From meiotic time course samples,5 ml of SPM culture containing yeast cells were collected in a 15 ml conical screwcap tube, centrifuged, and pellets were resuspended in 1 ml of ZK buffer (25 mM Tris- HCl [pH 7.5], 0.8 M KCl). Furthermore, 20 µl of 1 M DTT (Dithiothreitol) was added, and samples were incubated for 2 min at room temperature with gentle mixing. The samples were centrifuged again, and pellets were recorded and resuspended in fresh 1 ml of ZK buffer. 5ml of Zymolase buffer (5 µg/ml Zymolase 100T, 2% glucose, 50 mM Tris [pH 7.5]) was added, and then samples were incubated for 30 min in a 30°C incubator with rotating. To check the status of spheroblasting, Milli Q water was added to an aliquot of samples on a glass slide, and cells were watched under a light microscope to ensure that cells showed bursting. After ensuring that more than 80% of cells became a spheroblast (burst/like a black dot in microscope view), samples were centrifuged and washed with 1 ml MES/Sorbitol (0.1M MES [pH6.5], 1M sorbitol) using a glass pipette (Pasteur pipette).

The samples were centrifuged again, pellets were resuspended in 1 ml MES/Sorbitol, kept at 4°C for the usage of spreading later. For chromosome spreads, using a micropipette, 20 µl of above-prepared cell suspension was spotted on a clean glass slide (S2441 micro slide glass, Matsunami glass IND., LTD). To cell suspension, 40 µl of PFA/sucrose (4%PFA (Paraformaldehyde [SIGMA-ALDRICH], 3.4% sucrose, freshly-prepared) was added and swirled carefully for few minutes. Then, 80 µl of 1% Lipsol was added and swirled again, cells were incubated for 30 seconds and watched under the light microscope until about 80-90% of cells were lysed. After confirming complete lysis, 80 µl of the PFA/sucrose was added to fix the cells. A glass pasture pipette was passed lengthwise along the top of the drop to spread liquid all over the entire surface of the slide. The slides were dried from 4 hours to overnight and were stored in a plastic black microscope box at -20°C.

3.4. Immunostaining of Chromosome Spreads

Slides prepared by the lipsol method mentioned above were dipped gently in 0.2% photo flow (Photo-Flow 200 solution Kodak) for 2 min using a Coplin jar. The slides were air-dried for 5-10 min, and were blocked for 15 min using 0.5 ml TBS/BSA (1x TBS [20mM Tris pH7.5, 0.15M NaCl], 1% BSA [albumin from bovine serum, SIGMA]). Then, the blocking buffer was drained onto a paper towel, and 90 µl of TBS/BSA solution with primary antibody was added to slides. Slide glasses with the antibody solution were covered with a coverslip and incubated overnight at 4°C or 2 hours at room temperature in a moist chamber. The coverslip was removed by submersion at a 45° angle in the washing buffer (1x TBS). The slides were washed for 10 min 3 times in 1xTBS using a Coplin jar. 90µl of TBS/BSA solution with secondary antibody solution (1/2000) dilution of fluorochrome-conjugated IgG (corresponding secondary antibody) was added to slides. The slides were incubated for 2 hours at room temperature in a dark, moist chamber. The coverslip was

removed, slides were washed as described above and then washed with water for 2 min. Once slides were completely dry, ~15 µl (three drops) of mounting medium (Vecta Shield with 0.2 µg/ml DAPI) was added to slides and covered with a coverslip, followed by sealing with nail polish and storing in a dark box. Stained samples were observed using an epi-fluorescence microscope (BX51; Olympus, Japan) with a 100X objective (NA1.3). Images were captured by CCD camera (CoolSNAP; Roper, USA), and afterwards processed using IP lab and iVision (Silicon, USA) and Fiji-ImageJ software tools.

3.5. Intensity Quantification from Chromosome Spreads

The area of nuclear spread was defined and the mean fluorescence intensity was measured within this area. Quantification was performed using unprocessed raw images. The final fluorescence intensity data were normalized with DAPI intensity for each nucleus. Fluorescence intensity refers to pixel intensity per unit area on the chromosome spreads.

3.6. Tetrad Dissection

Tetrads were dissected to check the spore viability and strain construction. The haploid parental strains were patched together on YPAD plates for 4 hours at least for mating and then spread on sporulation plates (0.3% Potassium acetate, 0.02% Raffinose). After incubation at 30℃ overnight, tetrads were dissected manually using Zeiss Axioskop 40 microscope. The plates were incubated for two days, and viable spores were counted for viability. For strain construction, genotypes of each colony were determined by replica plating to appropriate plates.

3.7. Chromatin Immunoprecipitation (Agarose beads method)

For synchronized meiotic progression or meiotic time course, yeast cells were streaked on YPG plate and cells from grown colonies were inoculated YPD overnight. OD600 (10x dilution) was

calculated using bio spectrometer. Cells were inoculated in YPD culture in 25 mL SPS in a 125 mL flask at a final concentration of about 5 x 10^6 cells/ml (OD600 = 0.8). Cells were then cultured at 30°C at 250 rpm for 7 h. After 7h, OD600 was measured. Inoculated SPS culture in 900 mL of SPS in a 2.8 L baffled flask (BELLCO) at a final concentration of about 3 x 10^5 cells/ml (OD600 = 0.05). Cells were then cultured at 30°C at 250 rpm for 12-16 h. After 12 h, measured OD600. Cells were grown until the density reaches 3-4 x 10^7 cells/ml (OD600 = 4.5-6). Cells were collected by a 1000 mL filter unit (NARGEN) and washed with 400 mL of SPM. Cells were then resuspended at 4 x 10^7 cells/ml in 610 mL of SPM supplemented with amino acids and PPG (time point t = 0 h).

From time course sporulation samples, collect 50 ml aliquots in 100 ml conical flask at each time point (rpm: 245rpm, 30°C). Add 1.35 ml formaldehyde (37.5%) [final concentration-1 %]. (Sigma Aldrich , F8775). Incubate at dancing platform shaker for 30 minutes (full speed During this time, take Aprotinin (1.4mg/ml), Protease inhibitor cocktail (Dissolve 1 tab in 2ml autoclaved dH_20) and PMSF.

Take screwcap tubes and add 900 µl (with 7.5mg of Protein A-Sepharose beads dissolved in each). Fixation is stopped by adding 2.7 ml (131mM) Glycine (Sigma Aldrich , G7126) and shaking on a dancing platform shaker for 5 more minutes. Collect cells in 50ml falcon and spin in centrifuge pre-cooled at four °C and 400 rpm, 5 min. Wash cells with 40 ml ice-cold TBS twice at 4000rpm, 5 min, 4°C.After TBS wash, transfer cells by dissolving in 1ml TBS to 2ml Eppendorf and centrifuge at 8000 rpm,5 min,4°C.Now, make a complete lysis buffer(filter lysis buffer through the filter unit and add other components to 14ml of it).Transfer the cell pellet to the screw cap tube containing glass beads by dissolving in 850 µl complete lysis buffer (3 scoops). Break the cells by shaking in 1 minute, 18 times with 2 min on ice in between each step to maintain cell lysate

temperature at 4 °C on a mini bead beater. Take 15 ml tubes, clean the screw cap tube with 70% ethanol, put a hole on each cap using a thumbnail, and keep inverted on 15ml tube and centrifuge at 4000 rpm, 5 min, 4°C.Take screw cap tubes using forceps and gently tap on the tissue paper to avoid dripping on the cap and tap to loop beads in the bottom position. Tap the cell lysate from the regular 15ml tube to the SUMILION tube. Add 1ml lysis buffer complete (LBC) to screw-cap tubes with glass beads and loop them inverted to 15 ml tubes Transfer lysate in SUMILION tubes after removing screw cap tubes using forceps. Take 15ml SUMILION TUBES and label them. Fill the bio-ruptor with ice to make it 4 °C, one layer of ice on top (intensity low 30 sec ON/ 30 sec OFF). After every ten cycles, replace the water in the tank with chilled water with a monolayer of ice. Once the cells are sonicated three times, ten cycles each, transfer entire lysate to fresh 2ml tubes and centrifuge at 13000 rpm, 5 min, 4°C.Transfer the supernatant to freshly labelled 15ml SUMILION TUBES. Again, sonicate 20 cycles more with the same described setting as above. Transfer the lysate to 1.5 ml Eppendorf tubes in duplicates (900µl each tube). Wash beads twice with 1ml per vial MIlliQ (after dividing beads into tubes). Remove supernatant water only and add approx. same water removed while washing) Wash two times with 1 ml lysis buffer (not complete) and carefully remove supernatant only. Divide tubes into two equal sets (3 each if total 6). Add lysate (sonicated) to one set of wash beads (set 1). Add or suspend another set of beads in a 1 ml lysis buffer (set 2). Keep at 4°C rotators for 1 hour for pre-cleaning. Centrifuge both sets at 1000rpm, 1 min, 4°C. Set 1 - transfer lysate (supernatant of set 1 of 25.) to new Eppendorf (1.5 ml). From this, take 20 µl input, take ten µl for western I (lysate before pulldown).

Add antibody to cell lysate of 900 µl each and incubate at 6 hours at 4°C with rotator for one set. The Rec8 antibody was generated in rabbit and is polyclonal (Shinohara et al 2008). For the second set, wash with 1ml PBS/BSA (Sigma Aldrich, A4503) twice and re-suspend in 400 µl PBS/BSA

along with first set for 6 hours. Centrifuge at 1000 rpm 1 min 4°C after 6 hours. Wash beads two times with 1ml PBS/BSA. Discard supernatant. Carefully transfer the lysate from first set to PBS/BSA-washed beads and inoculate at 4°C for 6 hours on a rotating platform. Centrifuge at 1000rpm, 1 min 4°C.Carefully remove all supernatant and take 10 µl for western II (lysate after pulldown). Add 900 µl of lysis buffer, gently mix the beads and transfer the entire mixture to a protein L_o bind tube. Wash once again with 1ml of lysis buffer. Sequentially, wash with 1 ml lysis buffer + 360 mM NaCl twicein the same PBT. Then wash twice with 1ml washing buffer. Add 900 µl of TE wash buffer, mix gently and transfer to new protein L_o bind tube (PBT). Centrifuge at 13000 rpm for 15 seconds but do not vortex. Altogether remove all the supernatant carefully. Add 40 µl elution buffer (vortex) and incubate at 65° C for 25 min shaking. (1200 rpm). Centrifuge at max speed for 15 sec and transfer supernatant to new PBT. (13000 rpm for 15 seconds at 4° C). Add 160 µl TE/ 1% SDS to beads, vortex,20 min heating at 65° C, spin down at max speed and transfer this to previous eluate (40 µl) and take an aliquot for analysis by western blot. To the 20 µl Input sample, add 380 µl of TE/ 1% SDS and split the sample into two. Add 1µl RNAase and incubate all samples overnight at 65° C to digest RNA and reverse crosslinks. Incubate at 50° C for two hours with 5µl proteinase K per vial/tube on the following day.DNA purification through QIAGEN quick Column Kit. Mix two vials per time-point into one while passing through the column. Store at -20° C until analysis.

I optimized chromatin immunoprecipitation technique from early and late meiotic prophase against Rec8 polyclonal rabbit antibody (Shinohara et al 2008). Initial experiments were carried out to see if Rec8 rabbit or Rec8 Guinea pig is ideal for the maximum pull down in wild-type meiotic cells. Lysate (Figure 3) refers to the Rec8 concentration in cell lysate before the addition of Rec8 specific antibody for pulldown of Rec8 associated regions. ‘Lysate after pull down' refers to the Rec8

concentration left in the cell lysate after Rec8 specific antibody is added to the cell lysate and pull down is performed. Ideally, there should be no protein left in 'lysate after pulldown'. Eluate refers to the final eluate fraction which is the amount of Rec8 in the pulldown sample. In Rec8 rabbit the difference between 'lysate after pull down' and 'lysate before pulldown' was high and Rec8 rabbit was then used for further optimization. The goal was to further reduce the concentration of Rec8 in 'lysate after pulldown' to the minimum so that a very high percentage of Rec8 gets pulled down on the agarose beads. Agarose beads were chosen because of their larger size and better compatibility with polyclonal lab-developed antibodies (Krishnaprasad et al 2021). I optimized the volume of anti-Rec8 antibody (2.5 microliter per vial) and agarose beads to maximize the concentration of Rec8 in the eluate fraction. The concentration of Rec8 in lysate after pull down needs to be minimum for efficient pull down of Rec8 from the cells (Figure 3). The resultant eluate fraction was treated with RNAase and protease-K, purified through QIAGEN quick DNA purification column.

The whole-genome sequencing of this DNA was performed and the fold change of Rec8 between early and late time points was estimated as mentioned in methods. This purified DNA was also used for ChIP-qPCR experiments. Library preparation and sequencing of the ChIP sample by illumina method Hi-seq/Mi-seq sequencing is done by *FASTERIS*, Switzerland.

3.8. Yeast Transformation

Pick up a patch from YPD- lactate plate and inoculate into 10ml YPD-glucose overnight at 30C. Use 1 ml of overnight culture (3ml for EAY1112) to inoculate into 50 ml YPD glucose and grow 3-4 hours (4-5 hr for EAY1112) such that O.D 600 is between 0.3 – 0.5 (mid-log phase with cell density 10^7 cells/ml). Decant culture into 50ml tubes and pellet the cells at 3500 rpm / 5 min. In

the meantime, denature carrier DNA (50 µg / transformation, use the PCR machine for denaturation- 100C for 10min). Wash the cells in 20ml ddH2O, spin down at 3500 rpm / 5min. In the meantime, make 5ml each of 40% PEG (Sigma Aldrich, 81240) and TE/LiAc.(Himedia , RM1507) (Flame pipettes before use to maintain sterility). Re-suspend cells in 1ml H2O (vortex mildly once), transfer to Eppendorf tube and pellet again at 5000 rpm for 5 min R suspend in 1ml TE/ LiAc using a P1000 and pellet at 5000 rpm for 5 min. (Do not vortex for resuspension unless in water). Re-suspend in 50 µl × no. of transformations required (not more than 10 for a 50 ml culture so that high cell density is maintained). Add carrier DNA to this. For example, for eight transformations, 400 µg carrier DNA is required. So re suspend in 400 µl TE/LiAc + 40 µl carrier. Add 55 µl cells to transforming DNA (1 µg < DNA< 5 µg). Transforming DNA (ideally amplified PCR product of the corresponding gene to amplified) volume should not exceed 20 µl to avoid diluting Li concentration. Add 300 µl 40% sterile PEG and mix thoroughly with P1000. Tape the tubes on to Eppendorf stand and incubate at 30^{0C} for 30 min in a shaker. Switch on 42 degrees Celsius water bath in the meantime. Heat shock cells at 42^{0}C for 15 minutes. Spin down cells at 5000 rpm for 5 min and remove as much PEG as possible with P1000. Re-suspend cells in 1 ml ddH2O and again pellet. Now re-suspend in about 0.5 ml water. If plating on amino acid selection plates, one can plate straight away after adjusting for volume. If plating for antibiotic resistance, re-suspend the pellet in 1 ml YPD and transfer to snap cap tube having 3ml YPD and incubate 30^{0}C for 4-6 hours. Pellet cells at 3500 rpm for 5 min and re-suspend in 500 ul ddH2O. Use 150 µl for plating to avoid satellite colonies. Plate using autoclaved glass beads or a spreader. Colonies may take 2-5 days to appear.

3.9. Western Blotting

For the western blotting semi-dry transfer method,5 to 15 ml of SPM culture was collected. Cell precipitates were initially washed with water and then washed twice with 20% (w/v) tri chloro acetic acid (TCA). Cells were suspended in 1 ml of TCA and then were disrupted using a bead shaker (60Sec on-60Sec off repeated five times) (Yasui Kikai Co. Ltd., Osaka, Japan). Precipitated proteins were recovered by centrifugation and then suspended in 150µl of sodium dodecyl sulfate-polyacrylamide gel electrophoresis (SDS-PAGE) sample buffer. After adjusting the pH to8.8 with 1M Tris- HCL [pH 9.5], samples were boiled at 95°C for 5 min. Following SDS-PAGE, proteins were transferred from gel to Nylon membrane (Immobilon, MILLIPORE) with a semi-dry transfer unit from ATTO-TRANSWESTERN. Antibodies against Rec8 (1:2000), Hop1 (1:3000), Zip1 (1:1000), Rec8 (1:1000), and Tubulin (1:10000) (Serotec, UK) were used (Shinohara et al., 2008; Zhu et al., 2010). Secondary antibodies conjugated Alkaline Phosphatase (Promega) were used at (1:7500) dilution. And finally, proteins on the blots were detected by BCIP/NBT reaction with a kit (Nacalai Tesque).

For the western blotting fully wet transfer method, trichloroacetic acid was added for the preparation of protein extracts described (Penkner et al 2005). The antibody against the Rec8 protein (Rabbit polyclonal antibody) was used at 1:4000 dilution and anti- Rabbit secondary horseradish peroxidase-conjugated antibody at 1: 20000 (Jackson Immuno Research) dilutions.

To analyze the samples collected during the ChIP experiment, 5 µL 2x sample buffer was added to the 10 µL Western blotting samples (eluate fraction, Supernatant after IP, and before IP). Samples were de-crosslinked by boiling at 100°C for 30 minutes using a thermal cycler.15µL of this sample was used for western blotting.

3.10. Quantitative Real-time PCR (qPCR)

Input DNA is collected during ChIP at each time points (lysate before pulldown). Serial dilutions of Input DNA are made (after purification with kit) into 1/10th,1/100th,1/1000th, and 1/10000th in Milli-Q water. In ChIP DNA, 1/20th of DNA is made as three technical replicates at each time point. In the seven wells of the RT PCR machine, the first four are serial dilutions of input DNA. This is standard. Its value is set as 1/10th,1/100th,1/1000th, and 1/10000th of a standard value to machine manually before running PCR. Three technical replicates of ChIP DNA are unknown samples in the last three wells. Cq values of these are calculated from each sigmoid curve, and where these values are falling on the slope of Input DNA slope will be shown as output. Starting template concentrations for each primer sets hence back-calculated will also be available as output of the machine.

We multiplied each Starting template concentration (estimated from Cq) for each primer set by 2000 for volume correction. The final ChIP DNA was divided by 20 and 100 to turn from percentage to final absolute value.

Hence internal control is Input DNA here of each time point. The final value is absolute DNA present representing that genomic region where antibody had bound. Error bars are standard errors, that is standard deviation from three replicates divided by the square root of the number of biological replicates, and the average is plotted.

We used kit of Takara (Sybergreen) and Quantstudio PCR machine for the analysis. 5uM of primer stock concentration and 10ul of TB Green Premix Ex Taq (Tli RNase H Plus) (SYBR Premix from Takara) for each reaction.

3.11. Strain Construction

Yeast strains used in my study are derived from Saccharomyces cerevisiae SK1 strain (MSY832/833 (*MATα/MAT**a**,ho*::*LYS2/”*, *lys2/”*, *ura3/”*, *leu2*::*hisG/”*, *trp1*::*hisG/”*) and are listed in the Table 01. Yeast strains were grown on either yeast extract–peptone–dextrose (YPD) or synthetic complete media at 30 ° (Mortimer and Johnston 1986; Rose et al 1990; Mccusker et al 1994). Sporulation medium was prepared as described earlier (Argueso et al 2004). *cdc20mn* is previously mentioned in Lee et al 2003. Both *mlh3Δcdc20mn* and *spo11-Y135F-cdc20mn* were taken from Dr.Kiran Challa's strain list (Challa et al 2019). To make null mutants of Mlh1 , Mms4 and Msh5 in *cdc20mn* background , regions specific to *mlh1Δ::HPHMX4 , mms4Δ:: KANMX4* and *msh5Δ::cloNATMX4* were amplified with corresponding primer sets MLH1F/R , MMS4F/R and MSH5F/R (Table 02) respectively from their deletion strains GYS 75*76 , GYS77*78 and GYS 81*82 respectively after DNA isolation and restriction digestion.These amplicons were then transformed via yeast transformations (See 3.8) into *cdc20mn* strain. Mutants were generated in *cdc20mn* by direct transformation using standard techniques mentioned above (Gietz et al. 1995). As required, drugs geneticin (Invitrogen), nourseothricin (Werner BioAgents, Germany), and hygromycin (Sigma) were added to the media at prescribed concentrations (Goldstein and Mccusker 1999). Inorder to make *mlh3-D523N cdc20mn* cells , *mlh3-D523N :KANMX* was amplified from GYS 79*80 (KTY 31*32 in Dr.Nishant KT laboratory strain list) mentioned in Nishant et al 2008 and yeast transformed into *cdc20mn :HPHMX4* (GYS 85*86) strain and confirmed by selection on drug plates and amplification with primer set MLH3F/R.

3.12. Antisera and Antibodies

Anti-Red1, Anti-Hop1 and Anti-Rec8 antisera for cytology, immunoprecipitation and western blotting are original lab grown antibodies and have been described previously (Shinohara et al 2008). Secondary antibodies conjugated with Alexa 488 and Alexa594 dyes (Molecular Probes,

Life Technologies, UK) were used for the detection of the primary antibodies in cytology and western blotting for Rec8 phosphorylation analysis. Anti-rabbit HRP conjugate substituted antibody was used as secondary antibody for western blotting to visualize Rec8 Immuno-precipitated fractions.

4.Bioinformatic analysis of ChIP-seq data

Bioinformatic analysis of ChIP-seq data was done in collaboration with Dr Ajith V.P in the laboratory of Dr Nishant K.T. (School of Biology, Indian Institute of Science Education and Research Thiruvananthapuram, India). FastQC (version 0.11.5) was used to analyze the quality and statistics of raw reads from sequencing of ChIP DNA. Preprocessing was done based on the FastQC report summary. Trimmomatic (version 0.36) was used to remove Illumina adapters and trimming of raw sequence reads. Processed reads (~2-8 million reads per sample) were aligned to the S288c reference genome (version R64-1-1) using bowtie2 (version 2.3.0) since the SK1 reference genome assembly is incomplete. Previous studies have used both S288c and SK1 as genomes as a reference, and they have shown that the results are similar in both cases (Pan et al. 2011; Sun et al. 2015).

We used only samples with more than 75% alignment rate and more than 2 million aligned reads for the downstream analysis. Statistics of the mapped reads generated from the alignment program were analyzed for uniquely mapped reads and multiple mapped reads. Samples having an alignment rate of less than 30% and less than 0.5 million reads were not used for the analysis. Unmapped reads were analyzed using blast to detect any contamination in the sample. Conversion of aligned file format (SAM) to its compressed file format (BAM), indexing, and sorting was done

using samtools (version 1.3.1) after completely analyzing the alignment statistics; All the downstream analyses were done using R (version 3.3).

Genome-wide profile normalization using MACS

Before mapping the reads to the genome, we partitioned the S288c reference genome into equal-sized bins (1 bp) each. Reads per bin were calculated from the sequencing output received for the samples. Reads mapped to N locations were assigned a score of 1/N for each read in the case of multi-mapped reads.

\In this study, we performed normalizations with the Input sample as background for normalization. After normalizing the counts using MACS, backgrounds were subtracted from their respective control samples. They were then averaged, and a genome-wide smoothening by ksmooth with a bandwidth of 1 kb was performed across all control samples.

Peak calling using MACS

To correctly identify Rec8 peaks, only reads that are uniquely aligned were taken into account. MACS (Model-based Analysis for ChIP-Seq) (http://liulab.dfci.harvard.edu/MACS/) (74. Zhang et al. 2008) was used to identify peaks from the sample. MACS uses a dynamic Poisson distribution to identify local biases in peak detection.

Rec8 peaks are called from the pooled set of two replicates. Rec8 peaks with a p-value more significant than 10^{-5} are filtered out.

5.Results

5.1. Cleavage-independent Cohesin Removal in Budding Yeast Meiosis

It was reported from earlier research from our lab that a novel step in cohesin removal before the anaphase entry happens at meiotic prophase (Challa et al 2019). Around half of the cohesins were removed from chromosomes in *CDC20* meiotic null cells (with inactive Cdc20/inactive anaphase entry). *CDC20* meiotic null (hereafter *cdc20mn*) strain is arrested at metaphase as *CDC20* is inactive. Cleavage-dependent (Separase-dependent) cohesin removal is absent in *cdc20mn* cells (Lee et al 2003). I have checked the *cdc20mn* cells meiotic progression on my own first and found out that *cdc20mn* cells are indeed arrested prior to anaphase I nor do they complete meiosis I and enter meiosis II.

Further , I performed immunostaining analysis of chromosome spreads for DAPI (blue/nuclear stain) , Rec8 (green/ axis element part of cohesin complex) and Red1 (red /axis element part of synaptonemal complex) at two different time points in time course progression, 5 hour (5h)and 8 hour (8h) corresponding to pachytene and diplotene cell stages respectively *cdc20mn* cells. (Figure 2a , 2b). Red1 is a central component of Synaptonemal complex and Rec8 is subunit of cohesin complex.

In early time points (5 h) of *cdc20mn* cells undergoing synchronous meiotic progression, Rec8 show continuous bright localization (termed long localization from now on in this text) on chromosomes and in late time points (8 h), show discontinuous, diffused and faint localization (termed dotty localization from now on) (Figure 2a). The intensity of Rec8 was calculated at each time point from a population of cells from each time point statistically using Image J software to measure individual intensity of each cell. The average intensity from the population of cells at each time point is plotted in Figure 2b.

When a cell is Red1 positive, it means Red1 protein is indeed bound on the chromosomes at the stage of cell cycle. When a cell is Red1 negative, this means that Red1 is no longer bound on chromosomes. In early time points (5 h), majority of cells are Red1 positive indicative of intact Synaptonemal complex whereas in late time point (8 h), 90 percentage of cells are Red1 negative indicative of dissolution of synaptonemal complex (Figure 1c). I found out that the intensity of Rec8 in Red1-positive cells (5 h) is double than that in Red1-negative cells (8 h). Hence Rec8 is getting removed from chromosomes concomitant to synaptonemal complex breakdown.

This indicates that cleavage-independent removal of cohesins happens in budding yeast meiosis. I revisited and confirmed earlier finding (Challa et al 2019) in my study.

5.2. Regulation of Cleavage-independent Cohesin Removal

The main aim of my study is to elucidate the spatial and temporal mechanism of the cleavage-independent removal of cohesins with special focus on recombination.

I hypothesized that Class I and Class II crossover formation could play a role in cohesin removal in budding yeast meiotic prophase. Hence, I created several null mutations of genes responsible for meiotic crossover recombination pathways in *cdc20mn* background. I found novel observations

in my study when I deleted several genes important for recombination in *cdc20mn* background. I compared the Rec8 intensity from each individual cells of a population of cells in early with mean individual Rec8 intensity at late time points in *cdc20mn* cells. I perfomed the same comparison for new strains I created with null mutations on specific genes and plotted the average intensity for each strain at each time point (Figure 2a(i),(ii), 2b). Red1 and Rec8 kinetics at early and late time points for each strain is shown to show the percentage of cells which are Red1 positive and Red1 negative in the population selected for intensity comparison (Figure 2c, 2d).

I wanted to check in class II cross overs play a role in cleavage independent Rec8 removal in meiotic prophase. I compared the mean Rec8 intensity of an individual cell in the representative population of cells to find the regulatory proteins for Rec8 removal.

In the *mms4Δ cdc20mn* strain, I found out that the Rec8 intensity was reduced to half in diplotene (8 h) at Red1-negative cells showing Rec8 removal is independent of Mms4 activity (Class II pathway) (Figure 2a,2b). In the absence of Mms4, the class II type of crossovers cannot happen to recombination intermediates but class I is present. Mus81- Mms4 pathway is responsible for a small subset of crossovers in meiosis. They are structure selective endonucleases which binds to a subset of double-Holliday junctions they can act upon. They cannot act upon all the Holliday junctions since they have one active site on the Mms4 enzyme. Moreover, the double-Holliday junction is cleaved in a different pattern, with only one catalytic site, as compared to class I crossovers. In Class I crossovers, asymmetric cleavage at two two catalytic sites simultaneously of the double-Holliday junctions happen. This cleavage gives rise to a majority of crossovers in budding yeast.

Since Mlh1 and Mlh3 form a complex which specifically binds to double-Holliday junctions and nicks them to form Class I crossovers, I deleted *MLH1* and *MLH3* gene in *cdc20mn* background

and compared Rec8 intensity among two time points. In *mlh1Δ cdc20mn* cells, *MLH1* gene was replaced with an antibiotic resistance gene (marker for selection, for e.g., kanamycin) in *cdc20mn* background. The results from immunostaining in these cells were interesting. I found no reduction into half in Rec8 intensity at early time point indicative of pachytene (Red1-positive) and late time point indicative of diplotene (Red1-negative). In In *mlh3Δ cdc20mn* cells, Rec8 intensity did not reduce to half like in control *cdc20mn* cells (Figure 2a,2b). This shows that removal of Rec8 in a cleavage-independent manner do not occur in the absence of Mlh1 and Mlh3. I concluded from statistical analysis of my cytological studies that Mlh1-Mlh3 complex is inevitable for cleavage independent cohesin removal (Figure 2a,2b). In other words, in the absence of Class I crossovers, Rec8 intensity reduction resulting from genome wide cleavage-independent cohesin removal was absent.

A mutation in the Mlh3 endonuclease domain confers a defect in endonuclease activity of Mlh1-Mlh3 in budding yeast. Interaction between Mlh1 and Mlh3 is however not compromised in this *mlh3-D523N cdc20mn* mutant (Nishant KT et al., 2008). I created this mutation in *cdc20mn* background, resulting in *mlh3-D523N cdc20mn* with defective endonuclease activity of Mlh1-Mlh3 complex. When I performed similar analysis in *mlh3- D523N cdc20mn*, it showed no reduction into half in Rec8 intensity in pachytene and diplotene. Endonuclease activity of Mlh1-Mlh3 complex is important for Rec8 removal from chromosomes. Taken together this shows that Mlh1-Mlh3 dependent Class I crossover formation play a role in Rec8 removal (Figure 2a,2b).

Msh5 stabilizes Class I crossovers in budding yeast (Nishant KT et al 2010). When I analyzed Rec8 intensity at early and late time points in *msh5 Δ cdc20mn*, Rec8 intensity remains unchanged in pachytene (5h) and diplotene (8h) (Figure 2a,2b). This supports the finding that cleavage-independent removal of cohesin is absent in Class I crossover defective background.

Spo11 initiates DSB formation in budding yeast. *spo11-Y135F* mutation creates a catalytic dead version of Spo11 where the DSB forming activity is compromised. I created *spo11-Y135F cdc20mn* strain and analyzed Rec8 intensity at early and late time points. I found out that the Rec8 intensity is not reduced to half in *spo11-Y135F cdc20mn*. Hence catalytic DSB forming activity of Spo11, which precedes meiotic crossover recombination is inevitable for Rec8 removal in budding yeast meiosis. Taken together, these results indicate that Rec8 removal is largely reduced or absent in the absence of Class I crossovers.

The percentage of Red1 negative cells at late time points is high in in *msh5 Δ cdc20mn* and *spo11-Y135F cdc20mn* cells. It is shown that some fractions of the CDC20mn spo11Y135F get into meiosis I (Katis et al. Current Biology, 2004). Msh5 and Spo11 are known to be inevitable for proper SC formation. These could have influenced the Red 1 and Rec8 kinetics. Hence only Rec8 positive Red1 positive cells from 5 hour and Rec8 positive Red1 negative cells from 8 hour are used for analysis.

5.3. Spatial Patterning of Cleavage-independent Cohesin Removal

In order to find out the spatial patterning of cleavage independent cohesin removal, I have performed Chromatin immunoprecipitation (ChIP) of Rec8 in *cdc20mn* background (Figure 3) from an early time point (5h, pachytene) and compared the Rec8 distribution it with that from a late time point in meiotic prophase (8h, diplotene) in *cdc20mn* cells using whole genome sequencing of precipitated DNA. We need an internal control to normalize the analysis of 5h and 8h. ‘Lysate before pull down’ consists of the cell lysate after fixing of proteins with DNA using formaldehyde and its sonication and just before pulldown with Rec8 antibody. Hence ‘lystae before pull down’ fraction contains fragmented DNA-protein complexes prior to antibody treatment. When ‘lysate before pull down’ fraction (Figure 03) is treated with proteinase, we get

'Input DNA' which we use for normalization of our comparison for Rec8 distribution between two time points. Qualitatively in Figure 3 the quantity of immunoprecipitated Rec8 (Eluate fraction after immunoprecipitation) at 5 hour seems to be higher than in 8 hour. I performed ChIPseq quantitatively to delineate the differences spatial patterning in Rec8 distribution at the nucleotide level with Input DNA as internal control.

Since *cdc20mn* cells do not enter anaphase I, the removal of cohesins by separase will not affect my analysis. Following chromatin immunoprecipitation against Rec8, library preparation and sequencing of the ChIP sample by illumina method Hi-seq/Mi-seq sequencing is done by *FASTERIS*, Switzerland.

After alignment of the sequenced Rec8 reads following my ChIP to the parent SK1 genome, comparison the Rec8 intensity and generation of plots showing Rec8 distribution across chromosomes was done by bio-informatician, Dr Ajith V. P (School of Biology, IISER Thiruvananthapuram) (see Chapter 04). Combined data from duplicates (mean of two biological replicates) was used for analysis and generation of chromosome wise plots by Dr Ajith VP (Figure 04). The black dot represents the centromere of each chromosome. I define peak as the region where the Rec8 binding is more after normalization to the input sample (methods in Chapter 04). Top 200 peaks from which Rec8 show maximum removal at 8h when compared to 5h is marked with green dots on top of them and Lowest 200 peaks showing minimum removal of Rec8 is denoted with pink dots on top of the corresponding peaks (Figure 4a). The blue line (dots) represents the Rec8 enrichment at 5 hour and red line (dots) represent the Rec8 enrichment at late time point of 8 hour.

Rec8 was found to be removed from all the centromeres of all 16 chromosomes. Centromere is represented as the black dot towards the middle of each chromosome. The pericentromeric regions

are represented for a closer view (Figure 4b). Rec8 initial enrichment at 5 hour (blue) is higher than that of 8h enrichment (red). There is enrichment at 8h even after cleavage independent cohesion removal.

Rec8 was removed from selected axis sites in all the chromosomes in meiotic prophase I. This trend was seen on all 16 chromosomes (Figure 4a). In chromosome IX for example, Rec8 is removed from centromere. On the arms of chromosome IX, Rec8 is removed only from some of the regions (blue peak is higher than red peak). Rec8 is protected from the removal on other chromosome regions (blue peak and red peak are of the same height) (Figure 4c). Hence there is regional variation in cohesin removal in cleavage independent pathway. Some regions of the chromosome were resistant to removal while others are sensitive to removal of Rec8.

Rec8 ChIP-seq data is already published by Ito et al in 2014 and Sun et al in 2015. I checked the correlation of my Rec8 ChIP-seq data with Sun et al 2014 published data set and found good correlation between the two data (Figure 4d). In addition, I checked the correlation between the 5 h and 8 h data points from my data points with the help of bio informatician Dr Ajith V.P.

The number peaks that are unique to 5 h and 8 h and common to both 5h and 8h is depicted (Figure 4e). When a peak is unique to a time point, there exist no peak on the other time point at that particular position. When a peak is common to both the time points, it means that there exists a peak at the same position in both the time points. 2019 peaks were common to both 5 h and 8 h. 538 peaks were unique to 5h time point and 616 peaks were unique to 8h time point (Figure 4e). Majority of peaks were common to 5h and 8h showing the Rec8 binding sites do not change appreciably during the meiotic prophase specific cleavage-independent removal of cohesins. Peaks which were common to both 5h and 8h showed maximum fold enrichment when compared peaks

unique to only one of the time points. Our analysis is currently focused at common peaks at 5h and 8h.

I was curious to find if the peaks which show removal of Rec8 are away from or close to DSB initiation sites. From common peaks of 5 h and 8 h, I selected the top 200 peaks which show the difference in 5h and 8h (High removal/green dots over chromosome peaks in Figure 4a) and 200 peaks with no difference in 5h and 8h (Low removal/pink dots over chromosome peaks in Figure 04) and plotted their distance from DSB and axis sites (Table 03).The median line of the highest 200 peaks (red line in Figure 4f) and median line of lowest 200 peaks (blue line in Figure 4f) was not significantly different (p value = 0.18 , p value > 0.05). However, when the distance from the nearest hotspot was plotted (Figure 4g), median line for distribution for the highest 200 peaks (red/ representing top 200 regions of maximum removal) was farther away from hotspots when compared to line of lowest peaks (blue/representing 200 regions of minimum removal) (p value = 0.02, p value < 0.05).The median of two these two skewed distributions were statistically compared using Wilcoxon t test by suing R script. We concluded that maximum removal of Rec8 happens from locations away from DSB hotspots.

To delineate the relationship between chromosome size and Rec8 removal, we correlated the enrichment of Rec8 versus the size of chromosomes in budding yeast. I classified the Rec8 peaks into two categories, the category Rec8 5h >8h from which Rec8 removal is seen and category 5h = 8h from which Rec8 is not removed. I found out that Rec8 is enriched and removed prominently from the smallest chromosomes (4h, A). The initial enrichment of Rec8 and removal at late time points is less pronounced as the size of chromosomes increases. Moreover, in the category 5h = 8h from which Rec8 is protected from removal (4h, B)., the initial enrichment itself is very less compared to the its 5h>8h counterpart (~Rec8 read density 15-25 in 5h=8h versus ~Rec8 read

density of 35-55). We can visualize that a minimum threshold level of Rec8 is retained at chromosomes. The Rec8 enrichment at 5h was divided at Rec8 enrichment at same corresponding region at 8h to get Rec8 5h/ Rec8 8h value (4i). This is a measure of the strength of Rec8 removal. I correlated this with the Spo11 density across the genome. I found out that removal of Rec8 is also not correlated to the spo11 density in the genome (4i,A,B). Removal happens from selected axis sites in mostly small chromosomes where initial Rec8 enrichment is high and from regions within chromosomes with maximum initial enrichment of Rec8 like centromere.

Based on the whole genome enrichment data of Rec8 in pachytene and diplotene, I selected distinctive regions for ChIP-qPCR. (Figure 5). Quantitative PCR independently validates our observations from ChIPseq analysis.

Following were kept as the basis for primer selection. Primers for peaks that show maximum removal and minimum removal in *cdc20mn* need to be included.Peaks from centromere regions is inevitable for our analysis as well. Our primer selection must inculcate small as well as large chromosomes. Based on these criteria the regions mentioned were selected for ChIP-qPCR analysis in different backgrounds. I selected four primer regions. First one from an axis region which show maximum removal of Rec8 from ChIP-seq data, **axis c5** (72 kb axis region in chromosome V, black arrow, Figure 4a). Second primer region is from a centromeric region of chromosome III, **centromere c3** (110kb centromere region in chromosome III, black arrow, Figure 4a,4b).

Third primer region is from an Axis region which showed retention of Rec8 from *cdc20mn* ChIP-seq data near CCT6 hotspot on chromosome IV , **axis c4** (850kb axis region on chromosome IV, black arrow, Figure 4a). As an internal control to normalize my values, I chose a region inside CCT6 hotspot locus where Rec8 ChIP-seq binding is minimum at both early and late time points.

I selected *cdc20mn* as the control background for ChIP-qPCR analysis since only cleavage-independent removal is present in the absence of Cdc20.

In *spo11-Y135F cdc20mn,* I found out that in the **axis c5** which show removal of Rec8 in *cdc20mn* cells and chosen centromere region **centromere c3**, Rec8 enrichment did not reduce to half in the early and late time points from qPCR. In axis region which show retention of Rec8 in *cdc20mn* cells **axis c4** also, Rec8 remained the same (Figure 5).

In addition, I analyzed Rec8 removal in *mms4*Δ *cdc20mn*. In the absence of Mms4, the class II type of crossovers cannot happen to recombination intermediates but Class I is present. I found out from my ChIP-qPCR analysis that Rec8 intensity gets reduced at late time points for *mms4*Δ *cdc20mn* similar to control wild type *cdc20mn* cells in the centromere region **centromere c3**. Axis region **axis c5** which showed Rec8 removal in *cdc20mn* showed similar reduction into half of Rec8 enrichment in *mms4*Δ *cdc20mn* as well (Figure 5)

I also had created Mlh1 and Mlh3 deletions in *cdc20mn* background to create *mlh1Δ cdc20mn* cells and in *mlh3Δ cdc20mn* cells respectively. With no Mlh1 and Mlh3 proteins, Class 1 crossover pathway is suppressed in these mutants. I checked the Rec8 enrichment in early and late time points and found out that it is not reduced to half in **axis c5**, **centromere c3** and **axis c4**. Similarly, I used *mlh3-D523N cdc20mn* cells which is Mlh3 catalysis dead mutant in CDC20mn background with no endonuclease activity of Mlh3. In *mlh3-D523N cdc20mn* cells also I found no significant difference in Rec8 enrichment in early and late time point in the axis which showed removal of rec8 in cdc20mn cells **axis c5** and the centromere region **centromere c3** (Figure 5). This shows that endonuclease activity of Mlh3, responsible for creating nicks in Holliday junctions is essential for cohesin release.

Since Mhs4-Msh5 complex stabilizes joint molecules in the class I crossovers, I also checked Rec8 enrichment difference in *msh5Δ cdc20mn* cells. I found similar results in *msh5Δ cdc20mn* as well. Rec8 intensity was statistically different from two time points in the axis site which showed removal in *cdc20mn* cells and in the axis site but I did not observe large 50% reduction like in *cdc20mn* cells for **axis c5**, **centromere c3** and **axis c4** (Figure 5)

Nevertheless, It was not reduced into half in *mlh3-D523N cdc20mn* and *spo11-Y135F cdc20mn*. Rec8 was not removed when early events like DSB formation were compromised. Rec8 was also not removed when the Class I crossover pathway was specifically absent. Rec8 was removed normally like in control *cdc20mn* cells when the Class II pathway was specifically absent and Class I/ZMM proteins are functional. Most importantly, Rec8 enrichment did not get reduced into half in early and late time points in all the three primer regions selected (axis which show removal, axis which show retention, centromere region) in *mlh1*Δ *cdc20mn*, *mlh3*Δ *cdc20mn* and *msh5*Δ *cdc20mn* strains.

Hence my ChIP-qPCR results show that class I crossing over is playing a direct role in cleavage independent Rec8 removal in budding yeast meiosis. These results are in line with the earlier results from immunostaining of chromosome spreads from these mutants.

5.4 Rec8 enrichment do not change in late time points in Mlh3Δ Background.

I performed Chromatin Immunoprecipitation followed by sequencing (ChIP-seq) of Rec8 in the absence of Mlh3 in *cdc20mn* background. I found out that in the absence of Mlh3 activity, Rec8 enrichment remains unperturbed even at 8h, late time point of meiotic prophase corresponding to diplotene. The Rec8 enrichment at 5h and 8h overlap in *mlh3Δ cdc20mn* showing that Mlh3 activity is inevitable for cohesin removal prior to anaphase entry. This trend is seen uniformly in

all the 16 chromosomes. I have shown representative figures of Chromosome 01 and Chromosome 07 (Figure 06). This confirms that Mlh3 indeed play a global role in Rec8 removal along chromosomes. Taken together with my previous results, I propose Class I crossover formation by Mlh3 perturbs the Rec8 distribution

5.5. Global Phosphorylation Status of Rec8 is Unaffected in Mlh3Δ Background

Rec8 and its accessory protein Rad61 is phosphorylated at multiple sites in meiotic prophase by a spectrum of kinases like casein kinase, polo kinase, Dbf4-dependent kinase and aurora kinase (SW Yoon et al 2016) and this phosphorylation is essential for removal for Rec8 in a cleavage independent manner (Challa et al 2019).I was curious if Mlh3 directly affects the phosphorylation status of Rec8 and its accessory protein Rad61 for removal of cohesin from chromosomes.

I checked the global phosphorylation status of Rec8 and Rad61 in *mlh3 Δ cdc20mn* using western blotting technique and compared it with phosphorylation status in *cdc20mn* wild type cells by checking for phosphorylation specific bands in western blotting. I found out that the Rec8 phosphorylation status remains unchanged in Mlh3 null backgrounds (Figure 7). In order to confirm there is no delay in the meiotic progression, I checked the phosphorylation status of Hop1 from same progression. Hop1 is readily phosphorylated and removed in meiosis. Hop1p phosphorylation pattern was similar in *mlh3Δ cdc20mn* and *cdc20mn* showing no delay in early phosphorylation events in meiosis. Phosphorylation of Rec8 and Rad61 by Polo like Kinase (PLK)/Dbf4 dependent Kinase (DDK) is essential for release of Rec8 prior to anaphase (Challa et al 2019). The results of this experiment indicate that Mlh3 either act downstream or independent of the phosphorylation events essential for cohesin release.

6.Discussions and Model

My study revisited and independently validated the observation that cohesins are removed before the onset of anaphase in a cleavage-independent manner in budding yeast meiosis. In addition, I found out the spatial patterning and molecular determinants of this removal using a ChIP-seq based approach.

I found out that Rec8 is removed in a more pronounced manner from smaller chromosomes in my genome wide analysis of ChIP-seq data. Moreover, Rec8 is enriched heavily at smaller chromosomes of the genome. When I analyzed the regions of genome which show retention of Rec8 (5h=8h), I found out that these regions showed less enrichment when compared regions which showed removal. There must exist an independent mechanism for protection of Rec8 from removal, especially at regions where its initial binding itself is less. Cells maintain a threshold of Rec8 until anaphase entry. This could be important because active cohesin is essential to provide resistance against pulling force of microtubules and accurate segregation of chromosomes. The regions from which cohesins are removed were found to be centromere and selected axis sites across genome. Even though there existed no correlation between Spo11 density and sites of Rec8 removal, I was curious to find the molecular determinants of this removal. I suspected crossover recombination and subsequent transmission of forces across the chromosomes could play a role in this cohesin removal. It was long assumed but not properly investigated that cohesins get removed as a result of homologous chromosomes undergoing crossover and subsequent chiasmata formation.

Further investigation was aimed at finding the relationship of this cohesin removal with chiasmata formation. It was found out that DSB initiation by spo11 was inevitable for Rec8 dynamics in the late meiotic prophase. If the major crossover pathway (Class I) plays a role in this cohesin removal

was studied upon in great detail in this study. Several candidate genes were chosen and several deletion strains were created in *cdc20mn* control background to answer this question. *cdc20mn* control background was chosen to block cleavage dependent cohesin removal by Cdc20/separase at the onset of anaphase.

I found out in my study that Rec8 removal is absent in the absence of Mlh1 and Mlh3. Mlh1-Mlh3 form filament and create asymmetric incisions at DNA creating class I crossovers.

Msh5 stabilize double Holliday junctions in the class I pathway. Rec8 removal was hindered in the absence of Msh5 as well. All this points out that the tightly regulated Class I crossover formation is inevitable for Rec8 removal in meiotic prophase. This also shows that the long-assumed model of cohesin getting displaced from chromosomes due to crossing over is true (Figure 8a). I made a model summarizing my results which schematically show how cohesion gets removed as a result of Class I crossover formation (Figure 8b) highlighting the proteins selected for my candidate-based approach.

In addition, I checked the Rec8 enrichment using whole genome ChIP-seq in the absence of Mlh3. I found out that Rec8 enrichment across the genome remains the same in both early and late time in the absence of Mlh3. Mlh3 activity is essential for removal of cohesin from chromosomes prior to anaphase I entry.

My results indicate that cohesin get removed genome-wide in a manner dependent on chiasmata formation. However, some amount of cohesin is getting removed from the centromeres of all chromosomes before anaphase I in control cells. The mechanism of cohesin removal from centromere remains to be studied in detail. It has to be noted here that the centromeric region has an independent mechanism to repress crossover formation. The Ctf19 complex prevents meiotic

DNA break formation, the initiating event of recombination, proximal to the centromere (Nadine et al 2015).

Indeed, there must exist a distinct mechanism for cohesin regulation at the centromere region before anaphase I. Both centromeric cohesion and chiasmata formation provide resistance against pulling force by microtubules at the onset of anaphase. One possibility why cohesin at the centromere get removed when there is Class I chiasmata formation with the exchange of chromosome arms, due to tension release as a result of chiasmata formation. Nicking of DNA strands by Mlh1-Mlh3 and subsequent Class I crossover formation indeed causes tension release along chromosomes (Figure 8c).

I propose a tension-based mechanical model to explain my findings. It has been earlier proposed that DSB formation releases tension along chromosomes on both sides and this tension release is instrumental in crossover patterning along chromosomes (Kleckner et al 2004). Formation of double Holliday junction precedes crossover formation. When Class I crossovers are formed, double Holliday junctions get dissolved and chromosome arms get exchanged by Mlh1-Mlh3. Nicking of DNA helix by endonucleases result in stress release of the chromatin loop. In other words, crossover formation results in a release of tension along both sides of chromosomes. Hence cohesins gets removed globally from chromosome arms as well as centromere to physically enable the chromosome morphogenesis associated with crossover formation. Some regions are resistant to this removal of cohesins. These regions are essential for holding together chromosome arms when crossover happen at chromosomes. (Figure 8c)

Biophysical approaches using optical tweezers for studying the forces on chromosomes in the presence and absence of cohesion proximal to crossovers need to be undertaken to study the change

in tension on chromosomes with and without the presence of class I crossovers. Motility forces on isolated chromosomes have been determined with laser tweezers (Nima Khatibzadeh et al 2014). Centromere cohesin is enriched by the Ctf19 complex (Nadine et al 2015) and Shugoshin protects cohesin from separase-dependent removal. However, my results show cohesin is indeed removed if not completely from centromere regions prior to anaphase onset.

We need to check how does the chromatin in the centromeric region interact with Mlh1-Mlh3 which were known to specifically bind to double Holliday junctions, using Hi-C and chromosome capture experiments.

Chromosome conformation capture techniques like Hi-C should be performed at the centromere region to uncover the spatial interactions of the genome at the centromere regions in the *cdc20mn* background. This will give us the interaction profile of chromosome arms with specific proteins at the late meiotic prophase. Since SK1 background is homozygous (both strands are the same), I propose using heterozygous hybrid genomes (for e.g., S288C/YJM789) with efficient synchronous meiotic progression in *cdc20mn* background for chromosome conformation capture techniques to help us identify the proteins which bind to each arm of the chromosome in the presence and absence of class I crossovers in a strand-specific manner.

Another future direction would be to introduce an artificial crossover site in the chromosome and monitor the Rec8 dynamics with and without crossover from the locations proximal to that crossover site. The DNA sequence of regions which show maximum crossover is known. We can transform yeast genome with pieces of these crossover specific regions. If the transformation is successful, a new crossover site can be introduced in the genome. After a new crossover site is introduced artificially like this, cohesion enrichment locally around this new locus can be

monitored. If the local cohesion distribution changes as a result of new crossover site, we can confirm independently that cohesin is indeed removed as a result of crossover formation.

Taken together, the relationship between crossing over of chromosomes and loss of cohesins from proximal regions needs to be studied in detail with a special focus on both chromosome arms and centromere regions. In the bigger picture, cohesion and crossover formation are essential mechanisms providing forces against pulling forces by microtubules. The further study of their relationship will help in improving our understanding of the loss of cohesion with aging in both oocytes and artificial reproductive techniques.

Figure labels and description

Figure 1 Introduction a) A diagram of meiosis. Four haploid gametes result from two rounds of chromosome segregation in meiosis I and meiosis II b) Structure of mitosis specific and meiosis specific cohesin complex. Smc1 and Smc3 are two main structural components. Accessory protein Rad61/Wapl antagonizses the ring closing of cohesin and leads to its dissociation. The acetylation of Smc3 by Eco1 locks the gate and antagonizes Wapl activity.Eco1 activity is essential for loading and maintenance. Accessory protein Pds5 antagonzies Wapl. The kleisin specifc sub unit that bridges gap between Smc1 and Smc3 is Scc1 in mitosis and Rec8 in meiosis c) Cohesin removal in budding yeast meiosis at Anaphase. In both anaphase I and anaphase II cohesin gets removed with separase enzyme. Sepearase remains inhibited by a protein called securing.Securin is degraded by ubiquitination by Anapahase promoting complex /cyclosome rendering seprase active at the onset of anaphase.Separase cleaves Rec8 opening the ring-shaped complex. d) Cleavage independent cohesin removal in meiotic prophase I of budding yeast meiosis. Recent discovery by Challa et al 2019 lead to a new step in cohesin removal prior to anaphase I in a cleavage independent manner. The regulation of this cleavage independent removal of cohesin is unknown. e) Cohesin removal in vertebrate mitosis is initiated by Plk1 and Wapl at mitotic prophase. Cohesin is opened at the Scc1-Smc3 junction without cleavage of Scc1 by separase. In mitosis II, sister chromatids get separated by cleavage of centromeric cohesin by separase f) In budding yeast mitosis, prophase pathway is absent and cohesin remains bound on chromosomes until onset of anaphase when Scc1 is cleaved by Separase. In mitosis II, sister chromatids get separated by cleavage of centromeric cohesin by separase g) Diagram for DNA Double-Strand Break repair choice pathways in meiotic prophase I. DSB formation and strand resection lead to intermediates which follow different pathways depending upon proteins they are acted upon. If Mus81-Mms4 act on them before stabilization by ZMM group of proteins, it will follow Mus81-Mms4 pathway giving rise to non-crossovers and crossovers (Class II). If ZMM proteins stabilize the intermediates, then Mlh1-Mlh3 act on them giving rise exclusively to crossovers (Class I). The formed DSB can also be repaired by SDSA pathway giving only non-crossovers.

Figure 2 Cleavage independent removal of Rec8 requires class I crossover pathway: a) Immunostaining from chromosome spreads to compare Rec8 intensity in cdc20mn cells (control) cells and mutants in *cdc20mn* background defective in recombination. The bar represents 2 µm. Order of mutants (top to bottom): *mms4Δ cdc20mn, mlh1Δ*

cdc20mn, mlh3Δ cdc20mn, mlh3-D523N cdc20mn, msh5Δ cdc20mn, spo11-Y135F cdc20mn. b) Bar graph comparing mean Rec8 intensity between early (5 hour) and late (time) point in synchronized meiotic progression. There is significant decrease to half of the initial value only in *cdc20mn* and *mms4Δ cdc20mn*. In other strains there is statistically significant difference between two time points but intensity is not reduced to half like *cdc20mn* and *mms4Δ cdc20mn*. Order of mutants (left to right) : *cdc20mn* (three replicates , p value <0.001), *mms4Δ cdc20mn* (three replicates , p value <0.001) , *mlh1Δ cdc20mn* (three replicates , p value <0.001) , *mlh3Δ cdc20mn* (three replicates , p value <0.001) , *mlh3-D523N cdc20mn* (three replicates , p value <0.001) , *spo11-Y135F cdc20mn* (two replicates , p value <0.001). In *msh5Δ cdc20mn* (two replicates, p value =0.5818, p value > 0.05), there was not even statistically significant difference between early and late time points in Rec8 enrichment. Error bar is standard deviation. p value is calculated using paired students t test c) Cells were classified into three classes. Red1 positive -Rec8 positive and , Red1 negative -Rec8 positive and Red1-negative Rec8 negative cells (from three replicates for *mms4Δ cdc20mn , mlh1Δ cdc20mn , mlh3Δ cdc20mn* , MLH3 D523N *cdc20mn ,* from two replicates for *msh5Δ cdc20mn ,* SPO11 Y135F *cdc20mn*) and the percentage of cells in each class were plotted. In early time points majority of cells are red1 positive rec8 positive and in late time points majority of cells are red1 negative rec8 positive.

Figure 3 Chromatin Immunoprecipitation of Rec8: Fractions of cell lysate before and after pull down (immunoprecipitation) with Anti-Rec8 antibody as well as fraction after elution was visualized by performing western blotting. Ladder was visualized under white light. Cell lysate fractions were treated with HRP (Horse radish peroxidase) conjugated antibody and chemiluminescence was detected.

Figure 4: Spatial patterning of Rec8 removal from 16 chromosomes of S cerevisiae. a) The black dot on each chromosome represents its centromere. Blue line represents Rec8 distribution at 5h (pachytene /early time point) and red line represent Rec8 distribution at 8h (diplotene/late time point) in *cdc20mn* strain. Rec8 gets removed from centromere as well as some axis sites in all the 16 chromosomes. The binding pattern of Rec8 remains the same at pachytene and diplotene. b) Comparison of Rec8 enrichment at early and late time points at all the centromeres. Black dot represents centromere of each chromosome. Blue line represents Rec8 distribution at 5h (pachytene /early time point) and red line represent Rec8 distribution at 8h (diplotene/late time point) in *cdc20mn* strain. c) Magnified view of chromosome arms. Some regions are resistant and some regions are sensitive to Rec8 removal. Chromosome IX is shown as a representative one.d) Correlation of Rec8 ChIP-seq data with previously published data. A. Correlation

between two biological replicates of Rec8 5 h in this study B. Correlation between two biological replicates of Rec8 8 h in this study.C. Correlation between Sun et al 2015 Rec8 3 h data with Rec8 5 h first biological replicate *a* data generated in this study. D. Correlation between Sun et al 2015 Rec8 data with Rec8 5 h second biological replicate *b* data generated in this study. E. Correlation between Sun et al 2015 Rec8 3 h data with Rec8 8 h first biological replicate *a* data generated in this study. F. Correlation between Sun et al 2015 Rec8 data with Rec8 8 h second biological replicate *b* data generated in this study. G. Correlation between 5 h of first biological replicate *a* and 8 h of first biological replicate *a* of my study. H. Correlation between 5 h of first *a* biological replicate and 8 h of second biological *b* replicate of my study. I. Correlation between 5 h of second biological replicate *b* and 8 h of first biological replicate *a* of my study. J. Correlation between 5 h of second biological replicate *b* and 8 h of second biological replicate *b* of my study. b) Venn diagram showing unique and common peaks of Rec8 5 h and 8 h. f) Rec8 gets removed maximum from sites proximal to Red1 binding sites X-axis: Distance in base pairs from end-point of nearest red1 peak, Y-axis: Density of peaks at a particular nucleotide position at x axis. Vertical lines indicate the median. Red line represents the density distribution of Highest 200 peaks which show maximum removal of Rec8 when 5h and 8h enrichment is compared (see Table 03), Blue line represent the density distribution of Lowest 200 peaks which show minimum removal of Rec8 when 5h and 8h enrichment of Rec8 is compared. g) X-axis: Distance in base pairs from mid-point of nearest spo11 peak, Y-axis: Density of peaks at a particular nucleotide position at x axis. Vertical lines indicate the median. Red line represents the density distribution of Highest 200 peaks which show maximum removal of Rec8 when 5h and 8h enrichment is compared (see Table 03), Blue line represent the density distribution of Lowest 200 peaks which show minimum removal of Rec8 when 5h and 8h enrichment of Rec8 is compared. Median line of lowest peaks (blue) is closer to origin and median line of highest peaks (red) is away from origin showing Rec8 gets removed away from spo11 sites.4h) A, B Comparison of Rec8 enrichment at early and late time points with chromosome size. Y-axis: Rec8 read density (Rec8 5h in red, Rec8 8h in blue). X-axis: size of chromosome in Mb. R is Pearson correlation coefficient. Rec8 enrichment and removal is less pronounced as chromosome size increases. Regions which show retention of Rec8 (5h =8h) seem to show less initial enrichment of Rec8.4i) A, B. Correlation of strength of Rec8 removal with spo11 density in the genome. Y-axis is Rec8 5h value / Rec8 8h value at corresponding position in the genome. X-axis is Spo11 density at corresponding position in the genome. R is Pearson correlation coefficient There exist no strong correlation with Spo11 density and Rec8 removal strength throughout genome from this correlation study.

Figure 5: Chromatin Immunoprecipitation followed by quantitative real-time PCR shows class I crossovers are inevitable for cleavage dependent cohesin removal. The order of mutants (left to right top panel) : *cdc20mn* cells, SPO11 Y135F *cdc20mn , mms4Δ cdc20mn ,* MLH3 D523N *cdc20mn* . The order of mutants (left to right bottom panel) : *cdc20mn* cells *,mlh1Δ cdc20mn , msh5Δ cdc20mn , mlh3Δ cdc20mn.* The DNA enrichment of each locus with reference to an internal control was calculated. A DSB hotspot CCT6 was selected as internal control as Rec8 binding is minimal/absent at DSB hotspots from our ChIP-seq data. Two time points, 5h representing early time point (pachytene) and 8h representing late time point (diplotene) was used for analysis. At axis peak locus at chromosome V (blue bar graphs) , Rec8 was removed into half the initial enrichment at late time point (diplotene) in *cdc20mn* cells (Three biological replicates ,N=3 , p value is 0.0001 , p <0.05) but in this same locus at chromosome V (axis c5) , there was no significant reduction of Rec8 in *spo11- Y135F cdc20mn ,mlh3 D523N cdc20mn , mlh1Δ cdc20mn , , mlh3Δ cdc20mn* (Three biological replicates ,N=3 , p value > 0.05, p values are respectively 0.8309,0.0515,0.5383,0.2821,0.8724).In *msh5Δ cdc20mn ,* there was statistically significant difference between enrichment at two time points but the reduction into half like *cdc20mn* was absent. In *mms4Δ cdc20mn*, Rec8 enrichment was reduced in late time point similar to control *cdc20mn* cells. Similarly, at the qPCR locus from centromere of chromosome III (orange bar graph) , Rec8 enrichment was reduced significantly to almost half in *cdc20mn* control cells and *mms4Δ cdc20mn* cells (Three biological replicates ,N=3 , p value ,0.00012 ,0.00031 ,p < 0.05). But there was no significant reduction of Rec8 from centromere of chromosome III in *spo11- Y135F cdc20mn ,mlh3- D523N cdc20mn , mlh1Δ cdc20mn , msh5Δ cdc20mn* and *mlh3Δ cdc20mn* (Three biological replicates ,N=3 , p value > 0.05 p values are respectively 0.4705,0.0579,0.9182 and 0.9350).An axis region near CCT6 hotspot , chromosome IV , axis c14 (grey bar graph) showed retention of Rec8 in all the backgrounds analyzed in early and late time points with no significant difference in Rec8 enrichment (Three biological replicates ,N=3 , p value > 0.05). In *msh5Δ cdc20mn* there was statistically significant reduction in axis (p value <0.05 , 0.0028) and centromere locus (p value <0.05, 0.0010) but the difference is not significant when compared to difference in *cdc20mn* and *mms4Δ cdc20mn.*Primer information in the oligonucleotide list table.p values .

Figure 6: Rec8 enrichment remains the same in the absence of Mlh3. In the representative chromosomes shown (chromosome 01 and 07) , the Rec8 enrichment remains the same in early time point 5h (light blue line) and late time

point 8h (light red line) throughout the chromosome. Spo11 peaks (grey line) from Pan et al 2011 and Red1 peaks (pink line) from Sun et al 2015 are also overlapped.

Figure 7: Rad61 and Rec8 global phosphorylation status is unchanged in *mlh3Δcdc20mn* a) Rad61 phosphorylation status is compared in *cdc20mn* and *mlh3Δcdc20mn* strains at 0h,2h,4h,6h,8h,10,12h and 24h time points from the initiation of meiotic progression. Primary phosphorylation of Rad61 happened at 4h time point in both the strains giving a phosphorylated band above the Rad61 band. Secondary phosphorylation band appeared at 6h in both in *cdc20mn* and *mlh3Δcdc20mn* strains. Hence the global phosphorylation status of Rad61 remains the same in absence of Mlh3. To check if there is any technical delay in meiotic progression experiment, I checked the phosphorylation status of Hop1p which is readily phosphorylated in early meiosis in the same samples. I found out that Hop1p phosphorylation status is also the same in *cdc20mn* and *mlh3Δcdc20mn* indicating there is no delay in early events in meiosis. b) Rec8 phosphorylation status is compared in *cdc20mn* and *mlh3Δcdc20mn* strains at 2h, 3h, 5h, 7h, 8h, 9h and 10h time points from the initiation of meiotic progression. Primary phosphorylation of Rec8 happened at 3h time point in both the strains in my analysis giving a phosphorylated band above the Rec8 band. Secondary phosphorylation band appeared at 5h in both in *cdc20mn* and *mlh3Δcdc20mn* strains. Hence the global phosphorylation status of Rec8 remains the same in absence of Mlh3.

Figure 8: Model for regulation of cleavage independent cohesin removal. a) (Top to bottom) DSB formation followed by formation of strand invasion intermediates (SEI). The formation of double Holliday junctions (dHJ) and further dissolution resolution accompanied by localized removal of cohesins from the chromosome arms b) Spo11 initiates DSB formation in the loop structure of the loop-axis conformation. Resection and formation of double Holliday junction follows this. Msh4-Msh5 stabilizes the double Holliday junctions. Mlh1-Mlh3 forms a filament on the Holliday junctions and create ssDNA nicks away from Holliday junctions resulting in the dissolution of dHJs into class I crossovers. Cohesin entraps and keeps DNA strands together. Class I crossover formation is accompanied by removal of cohesin from the homologs and sister chromatids.c) A mechanical model for cohesin removal as a result of Class I crossover formation. Cohesin is loaded on the chromosome arms and centromere before the cells enter meiotic prophase I. Double Strand Break formation by spo11 initiates meiotic crossover recombination. Crossover positioning is dictated by stress relief by DSB formation on the chromosome arms (Nancy Kleckner 2004). Similarily stress created on the chromosomes when double Holliday junction formation occur is released when Mlh1-Mlh3

endonucleases cut DNA strands and exchange genomic regions. This stress release gets transmitted globally along the chromosomes resulting in removal and retention of cohesins from chromosomes.

References

Pan J, Sasaki M, Kniewel R, Murakami H, Blitzblau HG, Tischfield SE, Zhu X, Neale MJ, Jasin M, Socci ND, Hochwagen A, Keeney S. A hierarchical combination of factors shapes the genome-wide topography of yeast meiotic recombination initiation. Cell. 2011 Mar 4;144(5):719-31. doi: 10.1016/j.cell.2011.02.009. PMID: 21376234; PMCID: PMC3063416.

Klein F, Mahr P, Galova M, Buonomo SB, Michaelis C, Nairz K, Nasmyth K. A central role for cohesins in sister chromatid cohesion, formation of axial elements, and recombination during yeast meiosis. Cell. 1999 Jul 9;98(1):91-103. doi: 10.1016/S0092-8674(00)80609-1. PMID: 10412984.

Marston AL. Chromosome segregation in budding yeast: sister chromatid cohesion and related mechanisms. Genetics. 2014 Jan;196(1):31-63. doi: 10.1534/genetics.112.145144. PMID: 24395824; PMCID: PMC3872193.

Chiang T, Duncan FE, Schindler K, Schultz RM, Lampson MA. Evidence that weakened centromere cohesion is a leading cause of age-related aneuploidy in oocytes. Curr Biol. 2010 Sep 14;20(17):1522-8. doi: 10.1016/j.cub.2010.06.069. PMID: 20817534; PMCID: PMC2939204.

Teresa Chiang, Richard M. Schultz, Michael A. Lampson, Age-Dependent Susceptibility of Chromosome Cohesion to Premature Separase Activation in Mouse Oocytes, *Biology of Reproduction*, Volume 85, Issue 6, 1 December 2011, Pages 1279–1283, https://doi.org/10.1095/biolreprod.111.094094

Jessberger R. Age-related aneuploidy through cohesion exhaustion. EMBO Rep. 2012 Jun 1;13(6):539-46. doi: 10.1038/embor.2012.54. PMID: 22565322; PMCID: PMC3367239.

Prakash Arumugam, Stephan Gruber, Koichi Tanaka, Christian H. Haering, Karl Mechtler, Kim Nasmyth,ATP Hydrolysis Is Required for Cohesin's Association with Chromosomes,Current Biology,Volume 13, Issue 22,2003,Pages 1941-1953,ISSN 0960-9822,https://doi.org/10.1016/j.cub.2003.10.036.

Lopez-Serra L, Lengronne A, Borges V, Kelly G, Uhlmann F. Budding yeast Wapl controls sister chromatid cohesion maintenance and chromosome condensation. Curr Biol. 2013 Jan 7;23(1):64-9. doi: 10.1016/j.cub.2012.11.030. Epub 2012 Dec 6. PMID: 23219725.

Sutani T, Kawaguchi T, Kanno R, Itoh T, Shirahige K. Budding yeast Wpl1(Rad61)-Pds5 complex counteracts sister chromatid cohesion-establishing reaction. Curr Biol. 2009 Mar 24;19(6):492-7. doi: 10.1016/j.cub.2009.01.062. Epub 2009 Mar 5. PMID: 19268589.

Sumara I, Vorlaufer E, Gieffers C, Peters BH, Peters JM. Characterization of vertebrate cohesin complexes and their regulation in prophase. J Cell Biol. 2000 Nov 13;151(4):749-62. doi: 10.1083/jcb.151.4.749. PMID: 11076961; PMCID: PMC2169443.

Kleckner N. Chiasma formation: chromatin/axis interplay and the role(s) of the synaptonemal complex. Chromosoma. 2006 Jun;115(3):175-94. doi: 10.1007/s00412-006-0055-7. Epub 2006 Mar 23. PMID: 16555016.

Laloraya S, Guacci V, Koshland D. Chromosomal addresses of the cohesin component Mcd1p. J Cell Biol. 2000 Nov 27;151(5):1047-56. doi: 10.1083/jcb.151.5.1047. PMID: 11086006; PMCID: PMC2174344.

Gruhn JR, Zielinska AP, Shukla V, Blanshard R, Capalbo A, Cimadomo D, Nikiforov D, Chan AC, Newnham LJ, Vogel I, Scarica C, Krapchev M, Taylor D, Kristensen SG, Cheng J, Ernst E, Bjørn AB, Colmorn LB, Blayney M, Elder K, Liss J, Hartshorne G, Grøndahl ML, Rienzi L, Ubaldi F, McCoy R, Lukaszuk K, Andersen CY, Schuh M, Hoffmann ER. Chromosome errors in human eggs shape natural fertility over reproductive life span. Science. 2019 Sep 27;365(6460):1466-1469. doi: 10.1126/science.aav7321. PMID: 31604276; PMCID: PMC7212007.

Yu HG, Koshland D. Chromosome morphogenesis: condensin-dependent cohesin removal during meiosis. Cell. 2005 Nov 4;123(3):397-407. doi: 10.1016/j.cell.2005.09.014. PMID: 16269332.

Marston AL. Chromosome segregation in budding yeast: sister chromatid cohesion and related mechanisms. Genetics. 2014 Jan;196(1):31-63. doi: 10.1534/genetics.112.145144. PMID: 24395824; PMCID: PMC3872193.

Makrantoni V, Marston AL. Cohesin and chromosome segregation. Curr Biol. 2018 Jun 18;28(12):R688-R693. doi: 10.1016/j.cub.2018.05.019. PMID: 29920258; PMCID: PMC6013277.

Lengronne A, Katou Y, Mori S, Yokobayashi S, Kelly GP, Itoh T, Watanabe Y, Shirahige K, Uhlmann F. Cohesin relocation from sites of chromosomal loading to places of convergent transcription. Nature. 2004 Jul 29;430(6999):573-8. doi: 10.1038/nature02742. Epub 2004 Jun 30. PMID: 15229615; PMCID: PMC2610358.

Ciosk R, Shirayama M, Shevchenko A, Tanaka T, Toth A, Shevchenko A, Nasmyth K. Cohesin's binding to chromosomes depends on a separate complex consisting of Scc2 and Scc4 proteins. Mol Cell. 2000 Feb;5(2):243-54. doi: 10.1016/s1097-2765(00)80420-7. PMID: 10882066.

Blat Y, Kleckner N. Cohesins bind to preferential sites along yeast chromosome III, with differential regulation along arms versus the centric region. Cell. 1999 Jul 23;98(2):249-59. doi: 10.1016/s0092-8674(00)81019-3. PMID: 10428036.

Christine Michaelis, Rafal Ciosk, Kim Nasmyth,Cohesins: Chromosomal Proteins that Prevent Premature Separation of Sister Chromatids,Cell,Volume 91, Issue 1,1997,Pages 35-45,ISSN 0092-8674,https://doi.org/10.1016/S0092-8674(01)80007-6.

Miki Shinohara, Steve D Oh, Neil Hunter ,Akira Shinohara , Crossover assurance and crossover interference are distinctly regulated by the ZMM proteins during yeast meiosis, Nature Genetics volume 40, pages 299–309 (2008) https://doi.org/10.1038/ng.83

G.Valentin Börner, Nancy Kleckner, Neil Hunter,Crossover/Noncrossover Differentiation, Synaptonemal Complex Formation, and Regulatory Surveillance at the Leptotene/Zygotene Transition of Meiosis, Cell,
Volume 117, Issue 1,2004,Pages 29-45,ISSN 0092-8674, https://doi.org/10.1016/S0092-8674(04)00292-2.

Costantino L, Hsieh TS, Lamothe R, Darzacq X, Koshland D. Cohesin residency determines chromatin loop patterns. Elife. 2020 Nov 10;9:e59889. doi: 10.7554/eLife.59889. PMID: 33170773; PMCID: PMC7655110.

Douglas K. Bishop, Demian Park, Liuzhong Xu, Nancy Kleckner,DMC1: A meiosis-specific yeast homolog of E. coli recA required for recombination, synaptonemal complex formation, and cell cycle progression,
Cell,Volume 69, Issue 3,1992,Pages 439-456,ISSN 0092-8674,https://doi.org/10.1016/0092-8674(92)90446-J.

Bzymek M, Thayer NH, Oh SD, Kleckner N, Hunter N. Double Holliday junctions are intermediates of DNA break repair. Nature. 2010 Apr 8;464(7290):937-41. doi: 10.1038/nature08868. Epub 2010 Mar 28. PMID: 20348905; PMCID: PMC2851831.

Ivanov D, Schleiffer A, Eisenhaber F, Mechtler K, Haering CH, Nasmyth K. Eco1 is a novel acetyltransferase that can acetylate proteins involved in cohesion. Curr Biol. 2002 Feb 19;12(4):323-8. doi: 10.1016/s0960-9822(02)00681-4. PMID: 11864574.

Furuta T, Tuck S, Kirchner J, Koch B, Auty R, Kitagawa R, Rose AM, Greenstein D. EMB-30: an APC4 homologue required for metaphase-to-anaphase transitions during meiosis and mitosis in Caenorhabditis elegans. Mol Biol Cell. 2000 Apr;11(4):1401-19. doi: 10.1091/mbc.11.4.1401. PMID: 10749938; PMCID: PMC14855.

Handel, Mary Ann and John C. Schimenti. “Genetics of mammalian meiosis: regulation, dynamics and impact on fertility.” Nature Reviews Genetics 11 (2010): 124-136. doi: 10.1038/nrg2723

Glynn EF, Megee PC, Yu HG, Mistrot C, Unal E, Koshland DE, DeRisi JL, Gerton JL. Genome-wide mapping of the cohesin complex in the yeast Saccharomyces cerevisiae. PLoS Biol. 2004 Sep;2(9):E259. doi: 10.1371/journal.pbio.0020259. Epub 2004 Jul 27. PMID: 15309048; PMCID: PMC490026.

Snowden T, Acharya S, Butz C, Berardini M, Fishel R. hMSH4-hMSH5 recognizes Holliday Junctions and forms a meiosis-specific sliding clamp that embraces homologous chromosomes. Mol Cell. 2004 Aug 13;15(3):437-51. doi: 10.1016/j.molcel.2004.06.040. PMID: 15304223.

Jessop L, Rockmill B, Roeder GS, Lichten M (2006) Meiotic Chromosome Synapsis-Promoting Proteins Antagonize the Anti-Crossover Activity of Sgs1. PLoS Genet 2(9): e155. https://doi.org/10.1371/journal.pgen.0020155

Oh SD, Lao JP, Taylor AF, Smith GR, Hunter N. RecQ helicase, Sgs1, and XPF family endonuclease, Mus81-Mms4, resolve aberrant joint molecules during meiotic recombination. Mol Cell. 2008 Aug 8;31(3):324-36. doi: 10.1016/j.molcel.2008.07.006. PMID: 18691965; PMCID: PMC2587322.

Ana Losada, Tomoki Yokochi, Ryuji Kobayashi, Tatsuya Hirano; Identification and Characterization of Sa/Scc3p Subunits in the *Xenopus* and Human Cohesin Complexes. *J Cell Biol* 7 August 2000; 150 (3): 405–416. doi: https://doi.org/10.1083/jcb.150.3.405

Tanaka T, Cosma MP, Wirth K, Nasmyth K. Identification of cohesin association sites at centromeres and along chromosome arms. Cell. 1999 Sep 17;98(6):847-58. doi: 10.1016/s0092-8674(00)81518-4. PMID: 10499801.

Medhi D, Goldman AS, Lichten M. Local chromosome context is a major determinant of crossover pathway biochemistry during budding yeast meiosis. Elife. 2016 Nov 18;5:e19669. doi: 10.7554/eLife.19669. PMID: 27855779; PMCID: PMC5222560.

Börner GV, Kleckner N, Hunter N. Crossover/noncrossover differentiation, synaptonemal complex formation, and regulatory surveillance at the leptotene/zygotene transition of meiosis. Cell. 2004 Apr 2;117(1):29-45. doi: 10.1016/s0092-8674(04)00292-2. PMID: 15066280.

Lahiri S, Li Y, Hingorani MM, Mukerji I. MutSγ-Induced DNA Conformational Changes Provide Insights into Its Role in Meiotic Recombination. Biophys J. 2018 Dec 4;115(11):2087-2101. doi: 10.1016/j.bpj.2018.10.029. Epub 2018 Nov 6. PMID: 30467025; PMCID: PMC6289823.

Pochart P, Woltering D, Hollingsworth NM. Conserved properties between functionally distinct MutS homologs in yeast. J Biol Chem. 1997 Nov 28;272(48):30345-9. doi: 10.1074/jbc.272.48.30345. PMID: 9374523.

Ranjha L, Anand R, Cejka P. The Saccharomyces cerevisiae Mlh1-Mlh3 heterodimer is an endonuclease that preferentially binds to Holliday junctions. J Biol Chem. 2014 Feb 28;289(9):5674-86. doi: 10.1074/jbc.M113.533810. Epub 2014 Jan 17. PMID: 24443562; PMCID: PMC3937642.

Jingqi Dai, Aurore Sanchez, Céline Adam, Lepakshi Ranjha, Giordano Reginato, Pierre Chervy, Carine Tellier-Lebegue, Jessica Andreani, Raphaël Guérois, Virginie Ropars, Marie-Hélène Le Du, Laurent Maloisel, Emmanuelle Martini, Pierre Legrand, Aurélien Thureau, Petr Cejka, Valérie Borde, Jean-Baptiste Charbonnier. Molecular basis of the dual role of the Mlh1-Mlh3 endonuclease in MMR and in meiotic crossover formation. Proceedings of the National Academy of Sciences Jun 2021, 118 (23) e2022704118; DOI: 10.1073/pnas.2022704118

Sanchez A, Adam C, Rauh F, Duroc Y, Ranjha L, Lombard B, Mu X, Wintrebert M, Loew D, Guarné A, Gnan S, Chen CL, Keeney S, Cejka P, Guérois R, Klein F, Charbonnier JB, Borde V. Exo1 recruits Cdc5 polo kinase to MutLγ to ensure efficient meiotic crossover formation. Proc Natl Acad Sci U S A. 2020 Dec 1;117(48):30577-30588. doi: 10.1073/pnas.2013012117. Epub 2020 Nov 16. PMID: 33199619; PMCID: PMC7720183.

Farid A. Kadyrov, Leonid Dzantiev, Nicoleta Constantin, Paul Modrich, Endonucleolytic Function of MutLα in Human Mismatch Repair,Cell,Volume 126, Issue 2,2006,Pages 297-308,ISSN 0092-8674,https://doi.org/10.1016/j.cell.2006.05.039.

Haber JE, Heyer WD. The fuss about Mus81. Cell. 2001 Nov 30;107(5):551-4. doi: 10.1016/s0092-8674(01)00593-1. PMID: 11733053.

Schwartz EK, Wright WD, Ehmsen KT, Evans JE, Stahlberg H, Heyer WD. Mus81-Mms4 functions as a single heterodimer to cleave nicked intermediates in recombinational DNA repair. Mol Cell Biol. 2012 Aug;32(15):3065-80. doi: 10.1128/MCB.00547-12. Epub 2012 May 29. PMID: 22645308; PMCID: PMC3434506.

Prieto I, Suja JA, Pezzi N, Kremer L, Martínez-A C, Rufas JS, Barbero JL. Mammalian STAG3 is a cohesin specific to sister chromatid arms in meiosis I. Nat Cell Biol. 2001 Aug;3(8):761-6. doi: 10.1038/35087082. PMID: 11483963.

Herbert M, Kalleas D, Cooney D, Lamb M, Lister L. Meiosis and maternal aging: insights from aneuploid oocytes and trisomy births. Cold Spring Harb Perspect Biol. 2015 Apr 1;7(4):a017970. doi: 10.1101/cshperspect.a017970. PMID: 25833844; PMCID: PMC4382745.

Keeney, Scott, Craig N. Giroux and Nancy Kleckner.]Meiosis-Specific DNA Double-Strand Breaks Are Catalyzed by Spo11, a Member of a Widely Conserved Protein Family. Cell 88 (1997): 375-384.

Challa K, Fajish V G, Shinohara M, Klein F, Gasser SM, Shinohara A. Meiosis-specific prophase-like pathway controls cleavage-independent release of cohesin by Wapl phosphorylation. PLoS Genet. 2019 Jan 3;15(1):e1007851. doi: 10.1371/journal.pgen.1007851. PMID: 30605471; PMCID: PMC6317811.

Marston, Adèle L. and Angelika Amon.Meiosis: cell-cycle controls shuffle and deal.Nature Reviews Molecular Cell Biology 5 (2004): 983-997.

Roeder GS. Meiotic chromosomes: it takes two to tango. Genes Dev. 1997 Oct 15;11(20):2600-21. doi: 10.1101/gad.11.20.2600. PMID: 9334324.

Nancy M. Hollingsworth, Loretta Goetsch, Breck Byers,The HOP1 gene encodes a meiosis-specific component of yeast chromosomes,Cell,Volume 61, Issue 1,1990,Pages 73-84,ISSN 0092-8674, https://doi.org/10.1016/0092-8674(90)90216-2.

Mary Sym, JoAnne Engebrecht, G.Shirleen Roeder,ZIP1 is a synaptonemal complex protein required for meiotic chromosome synapsis,Cell,Volume 72,Issue 3,1993,Pages 365-378,ISSN 0092-8674,https://doi.org/10.1016/0092-8674(93)90114-6.

Shinohara M, Oh SD, Hunter N, Shinohara A. Crossover assurance and crossover interference are distinctly regulated by the ZMM proteins during yeast meiosis. Nat Genet. 2008 Mar;40(3):299-309. doi: 10.1038/ng.83. Epub 2008 Feb 24. PMID: 18297071.

Tomomi Tsubouchi, Hongyu Zhao, G. Shirleen Roeder,The Meiosis-Specific Zip4 Protein Regulates Crossover Distribution by Promoting Synaptonemal Complex Formation Together with Zip2,Developmental Cell,Volume 10, Issue 6,2006,Pages 809-819,ISSN 1534-5807,https://doi.org/10.1016/j.devcel.2006.04.003.

Jordan P, Copsey A, Newnham L, Kolar E, Lichten M, Hoffmann E. Ipl1/Aurora B kinase coordinates synaptonemal complex disassembly with cell cycle progression and crossover formation in budding yeast meiosis. Genes Dev. 2009 Sep 15;23(18):2237-51. doi: 10.1101/gad.536109. PMID: 19759266; PMCID: PMC2751982.

Buonomo SB, Clyne RK, Fuchs J, Loidl J, Uhlmann F, Nasmyth K. Disjunction of homologous chromosomes in meiosis I depends on proteolytic cleavage of the meiotic cohesin Rec8 by separin. Cell. 2000 Oct 27;103(3):387-98. doi: 10.1016/s0092-8674(00)00131-8. PMID: 11081626.

Hui Jin, Vincent Guacci, Hong-Guo Yu; Pds5 is required for homologue pairing and inhibits synapsis of sister chromatids during yeast meiosis. *J Cell Biol* 7 September 2009; 186 (5): 713–725. doi: https://doi.org/10.1083/jcb.200810107

Inna N. Golubovskaya, Olivier Hamant, Ljuda Timofejeva, Chung-Ju Rachel Wang, David Braun, Robert Meeley, W. Zacheus Cande; Alleles of *afd1* dissect REC8 functions during meiotic prophase I. *J Cell Sci* 15 August 2006; 119 (16): 3306–3315. doi: https://doi.org/10.1242/jcs.03054

Severson AF, Ling L, van Zuylen V, Meyer BJ. The axial element protein HTP-3 promotes cohesin loading and meiotic axis assembly in C. elegans to implement the meiotic program of chromosome segregation. Genes Dev. 2009 Aug 1;23(15):1763-78. doi: 10.1101/gad.1808809. Epub 2009 Jul 2. PMID: 19574299; PMCID: PMC2720254.

Bannister, L.A., Reinholdt, L.G., Munroe, R.J. and Schimenti, J.C. (2004), Positional cloning and characterization of mouse *mei8*, a disrupted allele of the meiotic cohesin *Rec8*. Genesis, 40: 184-194. https://doi.org/10.1002/gene.20085

Huiling Xu, Matthew D. Beasley, William D. Warren, Gijsbertus T.J. van der Horst, Michael J. McKay,Absence of Mouse REC8 Cohesin Promotes Synapsis of Sister Chromatids in Meiosis,Developmental Cell,Volume 8, Issue 6,2005, Pages 949-961,ISSN 1534-5807, https://doi.org/10.1016/j.devcel.2005.03.018.

Herrán Y, Gutiérrez-Caballero C, Sánchez-Martín M, Hernández T, Viera A, Barbero JL, de Álava E, de Rooij DG, Suja JÁ, Llano E, Pendás AM. The cohesin subunit RAD21L functions in meiotic synapsis and exhibits sexual dimorphism in fertility. EMBO J. 2011 Jul 8;30(15):3091-105. doi: 10.1038/emboj.2011.222. PMID: 21743440; PMCID: PMC3160193.

Jibak Lee, Tatsuya Hirano; RAD21L, a novel cohesin subunit implicated in linking homologous chromosomes in mammalian meiosis. *J Cell Biol* 24 January 2011; 192 (2): 263–276. doi: https://doi.org/10.1083/jcb.201008005

Yoon, Sang-Wook, Min-Su Lee, Martin Xaver, Liangran Zhang, Soogil Hong, Yoon-Ju Kong, Hong-Rae Cho, Nancy Kleckner and Keun P. Kim. "Meiotic prophase roles of Rec8 in crossover recombination and chromosome structure." Nucleic Acids Research 44 (2016): 9296 - 9314.

Haering CH, Löwe J, Hochwagen A, Nasmyth K. Molecular architecture of SMC proteins and the yeast cohesin complex. Mol Cell. 2002 Apr;9(4):773-88. doi: 10.1016/s1097-2765(02)00515-4. PMID: 11983169.

Jessop L, Lichten M. Mus81/Mms4 endonuclease and Sgs1 helicase collaborate to ensure proper recombination intermediate metabolism during meiosis. Mol Cell. 2008 Aug 8;31(3):313-23. doi: 10.1016/j.molcel.2008.05.021. PMID: 18691964; PMCID: PMC2584117.

Revenkova E, Eijpe M, Heyting C, Gross B, Jessberger R. Novel meiosis-specific isoform of mammalian SMC1. Mol Cell Biol. 2001 Oct;21(20):6984-98. doi: 10.1128/MCB.21.20.6984-6998.2001. PMID: 11564881; PMCID: PMC99874.

Alexandru G, Uhlmann F, Mechtler K, Poupart MA, Nasmyth K. Phosphorylation of the cohesin subunit Scc1 by Polo/Cdc5 kinase regulates sister chromatid separation in yeast. Cell. 2001 May 18;105(4):459-72. doi: 10.1016/s0092-8674(01)00362-2. PMID: 11371343.

Attner, Michelle A., Matthew P. Miller, Ly-sha Ee, Sheryl K Elkin and Angelika Amon. "Polo kinase Cdc5 is a central regulator of meiosis I." Proceedings of the National Academy of Sciences 110 (2013): 14278 - 14283.

Clyne RK, Katis VL, Jessop L, Benjamin KR, Herskowitz I, Lichten M, Nasmyth K. Polo-like kinase Cdc5 promotes chiasmata formation and cosegregation of sister centromeres at meiosis I. Nat Cell Biol. 2003 May;5(5):480-5. doi: 10.1038/ncb977. PMID: 12717442.

Shinohara A, Ogawa H, Ogawa T. Rad51 protein involved in repair and recombination in S. cerevisiae is a RecA-like protein. Cell. 1992 May 1;69(3):457-70. doi: 10.1016/0092-8674(92)90447-k. Erratum in: Cell 1992 Oct 2;71(1):following 180. PMID: 1581961.

Brar GA, Kiburz BM, Zhang Y, Kim JE, White F, Amon A. Rec8 phosphorylation and recombination promote the step-wise loss of cohesins in meiosis. Nature. 2006 May 25;441(7092):532-6. doi: 10.1038/nature04794. Epub 2006 May 3. PMID: 16672979.

Katis VL, Lipp JJ, Imre R, Bogdanova A, Okaz E, Habermann B, Mechtler K, Nasmyth K, Zachariae W. Rec8 phosphorylation by casein kinase 1 and Cdc7-Dbf4 kinase regulates cohesin cleavage by separase during meiosis. Dev Cell. 2010 Mar 16;18(3):397-409. doi: 10.1016/j.devcel.2010.01.014. PMID: 20230747; PMCID: PMC2994640.

Krogh BO, Symington LS. Recombination proteins in yeast. Annu Rev Genet. 2004;38:233-71. doi: 10.1146/annurev.genet.38.072902.091500. PMID: 15568977.

Remeseiro S, Cuadrado A, Kawauchi S, Calof AL, Lander AD, Losada A. Reduction of Nipbl impairs cohesin loading locally and affects transcription but not cohesion-dependent functions in a mouse model of Cornelia de Lange Syndrome. Biochim Biophys Acta. 2013 Dec;1832(12):2097-102. doi: 10.1016/j.bbadis.2013.07.020. Epub 2013 Aug 3. PMID: 23920377; PMCID: PMC3825806.

Uhlmann, Frank, Friedrich Lottspeich and Kim A. Nasmyth. “Sister-chromatid separation at anaphase onset is promoted by cleavage of the cohesin subunit Scc1.” Nature 400 (1999): 37-42.

Hirano T. SMC proteins and chromosome mechanics: from bacteria to humans. Philos Trans R Soc Lond B Biol Sci. 2005 Mar 29;360(1455):507-14. doi: 10.1098/rstb.2004.1606. PMID: 15897176; PMCID: PMC1569466.

Pezzi, N., Prieto, I., Kremer, L., Jurado, L.A.P., Valero, C., Del Mazo, J., Martínez-A., C. And Barbero, J.L. (2000), *STAG3*, a novel gene encoding a protein involved in meiotic chromosome pairing and location of *STAG3*-related genes flanking the Williams-Beuren syndrome deletion. FASEB J, 14: 581-592. https://doi.org/10.1096/fasebj.14.3.581

Strunnikov, Alexander, Vladimir L. Larionov and Douglas E Koshland. “SMC1: an essential yeast gene encoding a putative head-rod-tail protein is required for nuclear division and defines a new ubiquitous protein family.” The Journal of Cell Biology 123 (1993): 1635 - 1648.

Cristina Gutiérrez-Caballero, Yurema Herrán, Manuel Sánchez-Martín, José Ángel Suja, José Luis Barbero, Elena Llano & Alberto M. Pendás (2011) Identification and molecular characterization of the mammalian α-kleisin RAD21L, Cell Cycle, 10:9, 1477-1487, DOI: 10.4161/cc.10.9.15515

Nishiyama, Tomoko, Rene Ladurner, Julia Schmitz, Emanuel Kreidl, Alexander Schleiffer, Venugopal Bhaskara, Masashige Bando, Katsuhiko Shirahige, Anthony A. Hyman, Karl Mechtler and Jan-Michael Peters. “Sororin Mediates Sister Chromatid Cohesion by Antagonizing Wapl.” Cell 143 (2010): 737-749.

Prieto I, Pezzi N, Buesa JM, Kremer L, Barthelemy I, Carreiro C, Roncal F, Martinez A, Gomez L, Fernandez R, Martinez-A C, Barbero JL. STAG2 and Rad21 mammalian mitotic cohesins are implicated in meiosis. EMBO Rep. 2002 Jun;3(6):543-50. doi: 10.1093/embo-reports/kvf108. Epub 2002 May 24. PMID: 12034751; PMCID: PMC1084142.

Lee J, Iwai T, Yokota T, Yamashita M. Temporally and spatially selective loss of Rec8 protein from meiotic chromosomes during mammalian meiosis. J Cell Sci. 2003 Jul 1;116(Pt 13):2781-90. doi: 10.1242/jcs.00495. Epub 2003 May 20. PMID: 12759374.

Peter M, Castro A, Lorca T, Le Peuch C, Magnaghi-Jaulin L, Dorée M, Labbé JC. The APC is dispensable for first meiotic anaphase in Xenopus oocytes. Nat Cell Biol. 2001 Jan;3(1):83-7. doi: 10.1038/35050607. PMID: 11146630.

Szostak , Jack W., Terry L Orr-Weaver, Rodney Rothstein and Franklin William Stahl. “The double-strand-break repair model for recombination.” Cell 33 (1983): 25-35.

Warren, William D., Søren Steffensen, Enmoore Lin, Paula A Coelho, M L Loupart, Neville Cobbe, Janice Y Lee, Michael J McKay, Terry L Orr-Weaver, Margarete M. S. Heck and Claudio E Sunkel. “The Drosophila RAD21 cohesin persists at the centromere region in mitosis.” Current Biology 10 (2000): 1463-1466.

Vincenten N, Kuhl LM, Lam I, Oke A, Kerr AR, Hochwagen A, Fung J, Keeney S, Vader G, Marston AL. The kinetochore prevents centromere-proximal crossover recombination during meiosis. Elife. 2015 Dec 14;4:e10850. doi: 10.7554/eLife.10850. PMID: 26653857; PMCID: PMC4749563.

Klein F, Laroche T, Cardenas ME, Hofmann JF, Schweizer D, Gasser SM. Localization of RAP1 and topoisomerase II in nuclei and meiotic chromosomes of yeast. J Cell Biol. 1992 Jun;117(5):935-48. doi: 10.1083/jcb.117.5.935. PMID: 1315786; PMCID: PMC2289479.

B Rockmill, G S Roeder , RED1: a yeast gene required for the segregation of chromosomes during the reductional division of meiosis , Proceedings of the National Academy of Sciences Aug 1988, 85 (16) 6057-6061; DOI: 10.1073/pnas.85.16.6057

Zickler D, Kleckner N. The leptotene-zygotene transition of meiosis. Annu Rev Genet. 1998;32:619-97. doi: 10.1146/annurev.genet.32.1.619. PMID: 9928494.

Klapholz S, Waddell CS, Esposito RE. The role of the SPO11 gene in meiotic recombination in yeast. Genetics. 1985 Jun;110(2):187-216. doi: 10.1093/genetics/110.2.187. PMID: 3891509; PMCID: PMC1202559.

Neil Hunter, Nancy Kleckner,The Single-End Invasion: An Asymmetric Intermediate at the Double-Strand Break to Double-Holliday Junction Transition of Meiotic Recombination,Cell,Volume 106, Issue 1,2001,Pages 59-70,ISSN 0092-8674,https://doi.org/10.1016/S0092-8674(01)00430-5.

Melby TE, Ciampaglio CN, Briscoe G, Erickson HP. The symmetrical structure of structural maintenance of chromosomes (SMC) and MukB proteins: long, antiparallel coiled coils, folded at a flexible hinge. J Cell Biol. 1998 Sep 21;142(6):1595-604. doi: 10.1083/jcb.142.6.1595. PMID: 9744887; PMCID: PMC2141774.

Kaur H, De Muyt A, Lichten M. Top3-Rmi1 DNA single-strand decatenase is integral to the formation and resolution of meiotic recombination intermediates. Mol Cell. 2015 Feb 19;57(4):583-594. doi: 10.1016/j.molcel.2015.01.020. PMID: 25699707; PMCID: PMC4338413.

Sun X, Huang L, Markowitz TE, Blitzblau HG, Chen D, Klein F, Hochwagen A. Transcription dynamically patterns the meiotic chromosome-axis interface. Elife. 2015 Aug 10;4:e07424. doi: 10.7554/eLife.07424. PMID: 26258962; PMCID: PMC4530585.

Kueng S, Hegemann B, Peters BH, Lipp JJ, Schleiffer A, Mechtler K, Peters JM. Wapl controls the dynamic association of cohesin with chromatin. Cell. 2006 Dec 1;127(5):955-67. doi: 10.1016/j.cell.2006.09.040. Epub 2006 Nov 16. PMID: 17113138.

Gandhi, Rita, Silvia Bonaccorsi, Diana Wentworth, Stephen Doxsey, Maurizio Gatti, and Andrea Pereira. "The Drosophila kinesin-like protein KLP67A is essential for mitotic and male meiotic spindle assembly." *Molecular biology of the cell* 15, no. 1 (2004): 121-131.

Bernard, P., Schmidt, C.K., Vaur, S., Dheur, S., Drogat, J., Genier, S., Ekwall, K., Uhlmann, F. and Javerzat, J.-P. (2008), Cell-cycle regulation of cohesin stability along fission yeast chromosomes. The EMBO Journal, 27: 111-121. https://doi.org/10.1038/sj.emboj.7601955

Rowland, Benjamin D., Maurici B. Roig, Tatsuya Nishino, Alexander Kurze, Pelin Uluocak, Ajay Mishra, Frédéric Beckouët et al. "Building sister chromatid cohesion: smc3 acetylation counteracts an antiestablishment activity." *Molecular cell* 33, no. 6 (2009): 763-774.

Lao JP, Hunter N. Trying to avoid your sister. PLoS Biol. 2010 Oct 19;8(10):e1000519. doi: 10.1371/journal.pbio.1000519. PMID: 20976046; PMCID: PMC2957405.

Waizenegger IC, Hauf S, Meinke A, Peters JM. Two distinct pathways remove mammalian cohesin from chromosome arms in prophase and from centromeres in anaphase. Cell. 2000 Oct 27;103(3):399-410. doi: 10.1016/s0092-8674(00)00132-x. PMID: 11081627.

Oomen ME, Hedger AK, Watts JK, Dekker J. Detecting chromatin interactions between and along sister chromatids with SisterC. Nat Methods. 2020 Oct;17(10):1002-1009. doi: 10.1038/s41592-020-0930-9. Epub 2020 Sep 23. PMID: 32968250; PMCID: PMC7541687.

.Nancy Kleckner, Denise Zickler, GarethH. Jones, Job Dekker, Ruth Padmore, Jim Henle, John Hutchinson. A mechanical basis for chromosome function .Proceedings of the National Academy of Sciences Aug 2004, 101 (34) 12592-12597; DOI: 10.1073/pnas.0402724101

Table 01: Strains used in this study

Serial number	Strain number	Mating type	Ploidy	Genotype
1	GYS 23	α	haploid	*MAT α, ho::LYS2, ura3, leu2::hisG, trp1::hisG, lys2 cdc20::pCLB2-CDC20::KanMX6,mlh3::trp1*
2	GYS 24	a	halpoid	*MAT a, ho::LYS2, ura3, leu2::hisG, trp1::hisG, lys2 cdc20::pCLB2-CDC20::KanMX6,mlh3::trp1*
3	GYS 1	a	haploid	*MAT a, ho::LYS2, ura3, leu2::hisG, trp1::hisG, lys2*
4	GYS 2	α	haploid	*MAT α, ho::LYS2, ura3, leu2::hisG, trp1::hisG, lys2*
5	GYS 30	a	haploid	*MAT a, ho::LYS2, ura3, leu2::hisG, trp1::hisG, lys2 cdc20::pCLB2-CDC20::KanMX6*

6	GYS 31	α	haploid	*MAT α, ho::LYS2, ura3, leu2::hisG, trp1::hisG, lys2 cdc20::pCLB2-CDC20::KanMX6*
7	GYS 59	a	haploid	*MAT a, ho::LYS2, ura3, leu2::hisG, trp1::hisG, lys2 cdc20::pCLB2-CDC20::KanMX6,msh5::cloNAT*
8	GYS 60	α	haploid	*MAT α, ho::LYS2, ura3, leu2::hisG, trp1::hisG, lys2 cdc20::pCLB2-CDC20::KanMX6, msh5::cloNAT*
9	GYS 61	a	haploid	*MAT a, ho::LYS2, ura3, leu2::hisG, trp1::hisG, lys2 cdc20::pCLB2-CDC20::KanMX6,mlh1:: HPHMX4*
10	GYS 62	α	haploid	*MAT α, ho::LYS2, ura3, leu2::hisG, trp1::hisG, lys2 cdc20::pCLB2-*

				CDC20::KanMX6,mlh1:: HPHMX4
11	GYS 65	a	haploid	*MAT a, ho::LYS2, ura3, leu2::hisG, trp1::hisG, lys2 cdc20::pCLB2-CDC20:: HPHMX4,mms4::KanMX6*
12	GYS 66	α	haploid	*MAT* α *, ho::LYS2, ura3, leu2::hisG, trp1::hisG, lys2 cdc20::pCLB2-CDC20:: HPHMX4,mms4::KanMX6*
13	GYS 67	a	haploid	*MAT a , ho::LYS2, ura3, leu2::hisG, trp1::hisG, lys2 cdc20::pCLB2-CDC20::HPHMX4,mlh3D523N::KanMX6*
14	GYS 68	α	haploid	*MAT* α *, ho::LYS2, ura3, leu2::hisG, trp1::hisG, lys2 cdc20::pCLB2-CDC20:: HPHMX4,mlh3D523N::KanMX6*

15	GYS 69	a	haploid	*MAT* a , *ho::LYS2, ura3, leu2::hisG, trp1::hisG, lys2 cdc20::pCLB2-CDC20:: HPHMX4,spo11Y135F::KanMX6*
16	GYS 70	α	haploid	*MAT* α , *ho::LYS2, ura3, leu2::hisG, trp1::hisG, lys2 cdc20::pCLB2-CDC20:: HPHMX4,SPO11y135f::KanMX6*
17	GYS 71	a	haploid	*ho::hisG, lys2, ura3, leu2::hisG,trp1::hisG, URA3-cenXVi, LEU2-chXVi, LYS2-chXVi*
18	GYS 72	α	haploid	*ho::hisG,lys2, ura3, leu2::hisG, trp1::hisG, ade2::hisG, his3::hisG, TRP1-cenXVi*
19	GYS 73	a	haploid	*MAT a, ho::LYS2, ura3, leu2::hisG, trp1::hisG, lys2*

				cdc20::pCLB2-CDC20::HPHMX4
20	GYS 74	α	haploid	*MAT a, ho::LYS2, ura3, leu2::hisG, trp1::hisG, lys2 cdc20::pCLB2-CDC20::HPHMX4*
21	GYS 75	a	haploid	*mlh1Δ:: HPHMX4* (GYS 71 background)
22	GYS 76	α	haploid	*mlh1Δ::HPHMX4* (GYS 72 background)
23	GYS 77	a	haploid	*mms4Δ:: KANMX4* (GYS 71 background)
24	GYS 78	α	haploid	*mms4Δ:: KANMX4* (GYS 72 background)
25	GYS 79	a	haploid	*mlh3-D523N::KANMX4* (GYS 71 background)

26	GYS 80	α	haploid	*mlh3-D523N::KANMX4* (GYS 72 background)
27	GYS 81	a	haploid	*msh5Δ::cloNATMX4* (GYS 71 background)
28	GYS 82	α	haploid	*msh5Δ::cloNATMX4* (GYS 72 background)
29	GYS 83	a	haploid	*mlh3Δ:: KANMX4* (GYS 71 background)
30	GYS 84	α	haploid	*mlh3Δ:: KANMX4* (GYS 72 background)
31	GYS 85	a	haploid	*MAT a, ho::LYS2, ura3, leu2::hisG, trp1::hisG, lys2 cdc20::pCLB2-CDC20::HPHMX4*

32	GYS 86	α	haploid	*MAT a, ho::LYS2, ura3, leu2::hisG, trp1::hisG, lys2 cdc20::pCLB2-CDC20::HPHMX4*

Table 02 : Oligonucleotide list

MLH3F:	CGCCAACGAGAAGGCTGAAC
MLH3R:	GCTCGGTATGTTATGCACTG
MSH5F:	ACTTGTGGGTGCAGCCTCAC
MSH5R:	ACGTAGCACAATCACGTCTGC
Mms4F:	GAACAGCCATCTATGGAGCAC
Mms4R:	CAGTGTGCTGAGAAAGGATGG
MLH1F :	GCTGACGGGAAGGAGCCTAACAT
MLH1R:	GCGTGGTCTCTTTCATCTCC
AXIS5 F:	TCGAGTCATCTGCCAGTGAA
AXIS5 R:	AC GGA TTT CCT CTC CTC ATC
AXIS4 F:	GGTGCGACAATGACAGCTTTT
AXIS4 R	AACTCCTGTACAGCAAAAGACT
CEN3 F:	CTAAGCTATATGTTGATGGG
CEN3 R:	GGACATTAAGGACGAACAG
CCT6 F:	GTGACTGGACCTGAGCTGTC
CCT6 R:	GCTCACTGCAATGGGAAACG

Table 03 : Peak information of Rec8 at 5h and 8h along with distance to nearest Spo11, Red1, Mlh3 peaks.

peakID_5h	peakID_8h	ratio_of_FE	FEATURE	red1_ Distance	mlh3_ Distance	Spo11- Distance
rec8_5h_peak_1630	rec8_8h_peak_1789	12.68948593	CENTROMERE	5502	5502	2801
rec8_5h_peak_2271	rec8_8h_peak_2463	12.15385824	CENTROMERE	10590	10590	5042
rec8_5h_peak_1711	rec8_8h_peak_1871	11.36238816	CENTROMERE	1009	1009	1800
rec8_5h_peak_2394	rec8_8h_peak_2587	11.34202084	NA	3406	3406	771
rec8_5h_peak_1546	rec8_8h_peak_1709	10.76674088	NA	7	7	2390
rec8_5h_peak_1712	rec8_8h_peak_1874	9.050593621	CENTROMERE	1091	1091	1577
rec8_5h_peak_285	rec8_8h_peak_306	8.966492818	NA	1387	1387	3629
rec8_5h_peak_107	rec8_8h_peak_126	7.951161931	CENTROMERE	988	988	1981
rec8_5h_peak_777	rec8_8h_peak_850	7.699286957	CENTROMERE	2033	2033	3220
rec8_5h_peak_2278	rec8_8h_peak_2470	7.562856422	NA	371	371	491
rec8_5h_peak_936	rec8_8h_peak_1032	7.490256339	NA	466	466	3249
rec8_5h_peak_106	rec8_8h_peak_122	7.224658377	CENTROMERE	1516	1516	883
rec8_5h_peak_37	rec8_8h_peak_34	7.212651713	NA	395	395	3332
rec8_5h_peak_1778	rec8_8h_peak_1939	7.021341807	NA	224	224	2577
rec8_5h_peak_1632	rec8_8h_peak_1795	6.98475397	NA	863	863	2038
rec8_5h_peak_1998	rec8_8h_peak_2178	6.910466383	NA	933	933	3454
rec8_5h_peak_2266	rec8_8h_peak_2458	6.54010202	NA	198	198	2408
rec8_5h_peak_288	rec8_8h_peak_312	6.487642982	NA	4234	4234	4242
rec8_5h_peak_485	rec8_8h_peak_500	6.272569365	NA	137	137	1752
rec8_5h_peak_967	rec8_8h_peak_1067	6.191950969	NA	113	113	455
rec8_5h_peak_68	rec8_8h_peak_73	6.116862725	NA	618	618	826
rec8_5h_peak_1267	rec8_8h_peak_1382	5.895649394	NA	1572	1572	588
rec8_5h_peak_1274	rec8_8h_peak_1389	5.89515872	NA	1562	1562	1313
rec8_5h_peak_541	rec8_8h_peak_565	5.887608012	NA	310	310	2685
rec8_5h_peak_908	rec8_8h_peak_1008	5.816207329	NA	205	205	2730
rec8_5h_peak_41	rec8_8h_peak_42	5.807814821	NA	1554	1554	424

rec8_5h_peak_100	rec8_8h_peak_106	5.780036513	NA	10	10	2689
rec8_5h_peak_1996	rec8_8h_peak_2175	5.739183927	CENTROMERE	9794	9794	2648
rec8_5h_peak_1109	rec8_8h_peak_1213	5.711981026	NA	399	399	1781
rec8_5h_peak_1642	rec8_8h_peak_1801	5.620098244	NA	267	267	2644
rec8_5h_peak_2340	rec8_8h_peak_2533	5.594098236	NA	452	452	2821
rec8_5h_peak_1358	rec8_8h_peak_1492	5.531426647	NA	582	582	211
rec8_5h_peak_474	rec8_8h_peak_491	5.506340277	NA	971	971	471
rec8_5h_peak_2349	rec8_8h_peak_2542	5.503248289	NA	458	458	2919
rec8_5h_peak_962	rec8_8h_peak_1062	5.428296881	NA	3547	3547	1075
rec8_5h_peak_1477	rec8_8h_peak_1617	5.420181665	CENTROMERE	264	264	8110
rec8_5h_peak_2044	rec8_8h_peak_2221	5.419552816	NA	336	336	2214
rec8_5h_peak_823	rec8_8h_peak_910	5.323953881	NA	297	297	515
rec8_5h_peak_2700	rec8_8h_peak_2908	5.258573189	NA	2739	2739	598
rec8_5h_peak_780	rec8_8h_peak_859	5.203531088	NA	878	878	3864
rec8_5h_peak_2415	rec8_8h_peak_2607	5.155964501	NA	19112	19112	2195
rec8_5h_peak_1110	rec8_8h_peak_1214	5.094111462	NA	5961	5961	1468
rec8_5h_peak_36	rec8_8h_peak_31	4.930144783	NA	167	167	961
rec8_5h_peak_1580	rec8_8h_peak_1746	4.873295602	NA	767	767	2722
rec8_5h_peak_1276	rec8_8h_peak_1393	4.536859601	CENTROMERE	1362	1362	1410
rec8_5h_peak_1470	rec8_8h_peak_1609	4.420680284	NA	153	153	1809
rec8_5h_peak_979	rec8_8h_peak_1084	4.348415133	NA	900	900	2646
rec8_5h_peak_752	rec8_8h_peak_821	4.328356318	NA	1320	1320	2850
rec8_5h_peak_1158	rec8_8h_peak_1268	4.312760337	NA	992	992	2894
rec8_5h_peak_1146	rec8_8h_peak_1251	4.209375	NA	1309	1309	2323
rec8_5h_peak_1210	rec8_8h_peak_1332	4.180166494	NA	209	209	1467
rec8_5h_peak_646	rec8_8h_peak_692	4.167387802	NA	794	794	2357
rec8_5h_peak_2578	rec8_8h_peak_2789	4.118078976	NA	469	469	1751
rec8_5h_peak_192	rec8_8h_peak_214	4.099597415	NA	840	840	3954
rec8_5h_peak_2082	rec8_8h_peak_2263	4.098371713	NA	316	316	671
rec8_5h_peak_1677	rec8_8h_peak_1829	4.079959235	NA	828	828	2202
rec8_5h_peak_34	rec8_8h_peak_28	3.995742973	NA	1008	1008	1561
rec8_5h_peak_572	rec8_8h_peak_608	3.952482174	NA	706	706	527
rec8_5h_peak_961	rec8_8h_peak_1060	3.922251655	NA	2968	2968	870
rec8_5h_peak_2447	rec8_8h_peak_2651	3.915891407	NA	1215	1215	207
rec8_5h_peak_830	rec8_8h_peak_916	3.898613154	NA	73	73	495
rec8_5h_peak_493	rec8_8h_peak_517	3.894841019	NA	326	326	1241
rec8_5h_peak_2631	rec8_8h_peak_2846	3.88598717	NA	167	167	2789
rec8_5h_peak_2792	rec8_8h_peak_2995	3.84651818	NA	269	269	1826
rec8_5h_peak_844	rec8_8h_peak_933	3.837734612	NA	491	491	2840

rec8_5h_peak_974	rec8_8h_peak_1078	3.798476033	NA	432	432	827
rec8_5h_peak_1262	rec8_8h_peak_1377	3.789455661	NA	230	230	2006
rec8_5h_peak_1937	rec8_8h_peak_2121	3.775785778	NA	176	176	1118
rec8_5h_peak_72	rec8_8h_peak_77	3.747388532	NA	142	142	2068
rec8_5h_peak_1023	rec8_8h_peak_1128	3.658756545	NA	262	262	3211
rec8_5h_peak_1149	rec8_8h_peak_1253	3.656928992	NA	1144	1144	2976
rec8_5h_peak_2261	rec8_8h_peak_2449	3.620697355	NA	1063	1063	736
rec8_5h_peak_1951	rec8_8h_peak_2142	3.591364247	NA	119	119	846
rec8_5h_peak_672	rec8_8h_peak_718	3.574172837	NA	402	402	1707
rec8_5h_peak_2379	rec8_8h_peak_2569	3.573860656	NA	1319	1319	3796
rec8_5h_peak_2692	rec8_8h_peak_2902	3.550837465	NA	502	502	1525
rec8_5h_peak_2745	rec8_8h_peak_2942	3.536439085	NA	372	372	2256
rec8_5h_peak_1545	rec8_8h_peak_1705	3.523807205	NA	35	35	2593
rec8_5h_peak_1300	rec8_8h_peak_1421	3.497239716	NA	110	110	1683
rec8_5h_peak_2115	rec8_8h_peak_2298	3.490324271	NA	290	290	895
rec8_5h_peak_1702	rec8_8h_peak_1860	3.429682945	NA	994	994	3782
rec8_5h_peak_1727	rec8_8h_peak_1892	3.427431492	NA	453	453	451
rec8_5h_peak_845	rec8_8h_peak_935	3.382403315	NA	2525	2525	1446
rec8_5h_peak_636	rec8_8h_peak_678	3.366847064	NA	582	582	1534
rec8_5h_peak_1433	rec8_8h_peak_1574	3.259695084	NA	319	319	1836
rec8_5h_peak_784	rec8_8h_peak_864	3.243056705	NA	562	562	277
rec8_5h_peak_1482	rec8_8h_peak_1623	3.223175858	NA	5613	5613	135
rec8_5h_peak_1948	rec8_8h_peak_2136	3.193938894	NA	360	360	45
rec8_5h_peak_1551	rec8_8h_peak_1714	3.184150738	NA	684	684	469
rec8_5h_peak_941	rec8_8h_peak_1042	3.172526303	NA	859	859	2381
rec8_5h_peak_2067	rec8_8h_peak_2248	3.143343582	NA	388	388	1206
rec8_5h_peak_67	rec8_8h_peak_70	3.137005108	NA	535	535	3268
rec8_5h_peak_846	rec8_8h_peak_937	3.121183668	NA	1364	1364	1541
rec8_5h_peak_1251	rec8_8h_peak_1371	3.114001028	NA	318	318	3026
rec8_5h_peak_2006	rec8_8h_peak_2185	3.112628499	NA	283	283	2828
rec8_5h_peak_1288	rec8_8h_peak_1408	3.110662992	NA	220	220	2521
rec8_5h_peak_1375	rec8_8h_peak_1515	3.101758541	NA	569	569	3185
rec8_5h_peak_2544	rec8_8h_peak_2752	3.08973916	NA	734	734	1961
rec8_5h_peak_1683	rec8_8h_peak_1843	2.997286543	NA	722	722	2075
rec8_5h_peak_1655	rec8_8h_peak_1811	2.97909429	NA	857	857	800
rec8_5h_peak_559	rec8_8h_peak_590	2.944175936	NA	871	871	135
rec8_5h_peak_2391	rec8_8h_peak_2581	2.927017887	NA	454	454	2563
rec8_5h_peak_120	rec8_8h_peak_138	2.910587226	NA	977	977	6330
rec8_5h_peak_680	rec8_8h_peak_731	2.862123157	NA	573	573	1537

rec8_5h_peak_1809	rec8_8h_peak_1982	2.832035537	NA	153	153	2694
rec8_5h_peak_2279	rec8_8h_peak_2475	2.823477472	NA	211	211	1499
rec8_5h_peak_314	rec8_8h_peak_336	2.806743975	NA	943	943	1949
rec8_5h_peak_191	rec8_8h_peak_211	2.80669453	NA	698	698	753
rec8_5h_peak_1458	rec8_8h_peak_1599	2.804255955	NA	213	213	1320
rec8_5h_peak_1283	rec8_8h_peak_1402	2.799278676	NA	38	38	53
rec8_5h_peak_1273	rec8_8h_peak_1388	2.785770707	NA	4653	4653	1776
rec8_5h_peak_1432	rec8_8h_peak_1572	2.774830375	NA	87	87	596
rec8_5h_peak_40	rec8_8h_peak_38	2.770613706	NA	1379	1379	842
rec8_5h_peak_1781	rec8_8h_peak_1947	2.767397411	NA	434	434	1852
rec8_5h_peak_2528	rec8_8h_peak_2728	2.760638058	NA	16712	16712	3295
rec8_5h_peak_1870	rec8_8h_peak_2041	2.746596712	NA	768	768	4200
rec8_5h_peak_1564	rec8_8h_peak_1730	2.746228591	NA	999	999	1903
rec8_5h_peak_2477	rec8_8h_peak_2676	2.739881166	NA	932	932	319
rec8_5h_peak_2702	rec8_8h_peak_2911	2.72304964	NA	9544	9544	7403
rec8_5h_peak_2296	rec8_8h_peak_2489	2.680763974	NA	315	315	587
rec8_5h_peak_2785	rec8_8h_peak_2986	2.675646763	NA	45	45	2125
rec8_5h_peak_841	rec8_8h_peak_928	2.671186516	NA	22565	22565	2213
rec8_5h_peak_1142	rec8_8h_peak_1245	2.666555838	NA	475	475	2396
rec8_5h_peak_1104	rec8_8h_peak_1209	2.640649398	NA	198	198	1350
rec8_5h_peak_105	rec8_8h_peak_120	2.621803006	NA	1154	1154	2617
rec8_5h_peak_2433	rec8_8h_peak_2629	2.587166228	NA	677	677	400
rec8_5h_peak_2606	rec8_8h_peak_2818	2.574156567	NA	949	949	1180
rec8_5h_peak_2752	rec8_8h_peak_2952	2.571382927	NA	637	637	2756
rec8_5h_peak_488	rec8_8h_peak_504	2.549531206	CENTROMERE	7809	7809	4213
rec8_5h_peak_1244	rec8_8h_peak_1358	2.535215425	NA	350	350	1285
rec8_5h_peak_2177	rec8_8h_peak_2360	2.522318572	NA	360	360	1236
rec8_5h_peak_492	rec8_8h_peak_511	2.515584776	NA	1011	1011	1851
rec8_5h_peak_2016	rec8_8h_peak_2193	2.508635598	NA	486	486	1920
rec8_5h_peak_1875	rec8_8h_peak_2049	2.481727291	NA	2192	2192	1389
rec8_5h_peak_946	rec8_8h_peak_1049	2.465634581	NA	993	993	2240
rec8_5h_peak_2608	rec8_8h_peak_2820	2.455806893	NA	1033	1033	1590
rec8_5h_peak_677	rec8_8h_peak_725	2.431275655	NA	2276	2276	337
rec8_5h_peak_549	rec8_8h_peak_578	2.379273475	NA	166	166	2637
rec8_5h_peak_2598	rec8_8h_peak_2809	2.339570138	NA	502	502	1534
rec8_5h_peak_1731	rec8_8h_peak_1896	2.338624194	NA	219	219	1519
rec8_5h_peak_428	rec8_8h_peak_450	2.333765759	NA	738	738	1767
rec8_5h_peak_2475	rec8_8h_peak_2673	2.333045558	NA	307	307	1811
rec8_5h_peak_2032	rec8_8h_peak_2211	2.315172016	NA	72	72	2609

rec8_5h_peak_1474	rec8_8h_peak_1613	2.303419001	NA	10184	10184	2505
rec8_5h_peak_1544	rec8_8h_peak_1704	2.273411292	NA	556	556	2780
rec8_5h_peak_509	rec8_8h_peak_534	2.272726682	NA	239	239	1104
rec8_5h_peak_892	rec8_8h_peak_980	2.256500687	NA	129	129	1407
rec8_5h_peak_614	rec8_8h_peak_646	2.252046379	NA	254	254	99
rec8_5h_peak_1187	rec8_8h_peak_1296	2.236416004	NA	9220	9220	4612
rec8_5h_peak_172	rec8_8h_peak_188	2.228541259	NA	207	207	1238
rec8_5h_peak_1694	rec8_8h_peak_1850	2.216011774	NA	404	404	1344
rec8_5h_peak_1412	rec8_8h_peak_1552	2.189055058	NA	1914	1914	446
rec8_5h_peak_875	rec8_8h_peak_959	2.172839242	NA	1005	1005	1663
rec8_5h_peak_1820	rec8_8h_peak_1994	2.172467213	NA	1292	1292	1570
rec8_5h_peak_1592	rec8_8h_peak_1759	2.170515938	NA	10516	10516	3387
rec8_5h_peak_442	rec8_8h_peak_467	2.145002487	NA	79	79	1736
rec8_5h_peak_1367	rec8_8h_peak_1504	2.142038601	NA	1881	1881	2040
rec8_5h_peak_114	rec8_8h_peak_132	2.133734773	NA	92	92	1039
rec8_5h_peak_1033	rec8_8h_peak_1136	2.105731675	NA	77	77	475
rec8_5h_peak_116	rec8_8h_peak_135	2.077952227	NA	63	63	2472
rec8_5h_peak_863	rec8_8h_peak_949	2.077452701	NA	614	614	1258
rec8_5h_peak_2718	rec8_8h_peak_2925	2.071775124	NA	776	776	2217
rec8_5h_peak_13	rec8_8h_peak_9	2.071526364	NA	1150	1150	1516
rec8_5h_peak_945	rec8_8h_peak_1045	2.060273973	NA	80	80	856
rec8_5h_peak_108	rec8_8h_peak_127	2.055137834	NA	1936	1936	298
rec8_5h_peak_2708	rec8_8h_peak_2915	2.046577087	NA	457	457	1453
rec8_5h_peak_1724	rec8_8h_peak_1888	2.032680596	NA	4064	4064	357
rec8_5h_peak_1844	rec8_8h_peak_2016	2.001035571	NA	1380	1380	3770
rec8_5h_peak_2532	rec8_8h_peak_2735	1.986480312	NA	2404	2404	367
rec8_5h_peak_235	rec8_8h_peak_256	1.978963854	NA	546	546	712
rec8_5h_peak_1272	rec8_8h_peak_1386	1.965512968	NA	9034	9034	2257
rec8_5h_peak_634	rec8_8h_peak_674	1.930040513	NA	259	259	2020
rec8_5h_peak_2089	rec8_8h_peak_2273	1.917780691	NA	422	422	1535
rec8_5h_peak_712	rec8_8h_peak_778	1.908891645	NA	470	470	476
rec8_5h_peak_1914	rec8_8h_peak_2096	1.903939123	NA	6960	6960	4019
rec8_5h_peak_562	rec8_8h_peak_594	1.903317043	NA	214	214	1093
rec8_5h_peak_843	rec8_8h_peak_931	1.896104737	CENTROMERE	9471	9471	2387
rec8_5h_peak_1913	rec8_8h_peak_2093	1.888863744	NA	5243	5243	2943
rec8_5h_peak_1079	rec8_8h_peak_1183	1.886901566	NA	965	965	661
rec8_5h_peak_2592	rec8_8h_peak_2802	1.848262545	NA	1129	1129	2428
rec8_5h_peak_97	rec8_8h_peak_103	1.847921286	NA	1088	1088	1794
rec8_5h_peak_2416	rec8_8h_peak_2613	1.828529672	NA	1865	1865	4333

rec8_5h_peak_1497	rec8_8h_peak_1638	1.827047431	NA	392	392	2162
rec8_5h_peak_667	rec8_8h_peak_713	1.825862723	NA	183	183	2834
rec8_5h_peak_2430	rec8_8h_peak_2626	1.807499218	NA	323	323	1962
rec8_5h_peak_869	rec8_8h_peak_953	1.79308827	NA	18689	18689	1627
rec8_5h_peak_1448	rec8_8h_peak_1588	1.791196994	NA	3189	3189	1388
rec8_5h_peak_205	rec8_8h_peak_230	1.785301623	NA	1077	1077	2319
rec8_5h_peak_2256	rec8_8h_peak_2441	1.783379321	NA	8059	8059	820
rec8_5h_peak_891	rec8_8h_peak_979	1.778426062	NA	1060	1060	476
rec8_5h_peak_547	rec8_8h_peak_575	1.772447008	NA	3273	3273	1231
rec8_5h_peak_2146	rec8_8h_peak_2332	1.747959463	NA	752	752	1662
rec8_5h_peak_274	rec8_8h_peak_296	1.740638835	NA	1712	1712	1191
rec8_5h_peak_1673	rec8_8h_peak_1823	1.738464286	NA	1530	1530	1447
rec8_5h_peak_1484	rec8_8h_peak_1625	1.736930372	NA	1643	1643	254
rec8_5h_peak_484	rec8_8h_peak_499	1.736597694	NA	5094	5094	3499
rec8_5h_peak_75	rec8_8h_peak_82	1.73545362	NA	1366	1366	569
rec8_5h_peak_1117	rec8_8h_peak_1220	1.733023948	NA	5365	5365	2439
rec8_5h_peak_928	rec8_8h_peak_1025	1.731620344	NA	424	424	863

Acknowledgements

I would like to thank my PhD supervisor, Prof. Akira Shinohara for being kind and supportive with my PhD research at every step. Without his timely scientific advices and positive interventions, it would have been really hard for me to complete experiments for this thesis. I feel truly blessed to have chosen to work under him for my PhD.

I would like to thank my seniors in Shinohara lab, particularly Dr. Kiran Challa for his instructions during the initial days of PhD. I would like to extend my gratitude to my colleagues Ms.Faiza Az Zahra and Dr Hana Subhan in training me with the lab techniques in the first month of my PhD. I would also like to thank faculty Dr.Kenichiro Matzusaki for his support and guidance during my stay in Japan. I would like to thank my colleague from Shinohara lab, Mr. Stephen Mwaniki for being a good friend always ready to help.

I would like to thank the secretaries in Shinohara lab, especially Ms. Yoshiko Kamata san for patiently helping me with Japanese documents and assisting my travel in and outside Japan amidst the covid-19 pandemic. Their kindness is the sole reason why I could complete experiments from India and Japan on time.

I would like to thank our collaborator, Dr Nishant KT from IISER Thiruvananthapuram for his immense enthusiasm and interest towards this project. I thank him for kindly letting me work peacefully at his lab until completion of the experiments. I shall always cherish his supportive words during my stay in India. I would like to thank Ms.Suman Dash and Dr Ajith V.P for their help and warm atmosphere in the lab. I cannot forget helps from Mr. Sagar Salim in setting up the ChIP experiment initially from IISER.

I would like to thank my father Mr Saleem, my mother Ms Shahina , my brother Mr Naizam , my sister Ms Nainu and my wife Ms Sulthana for their support . I remain forever indebted to them.

Figure 1

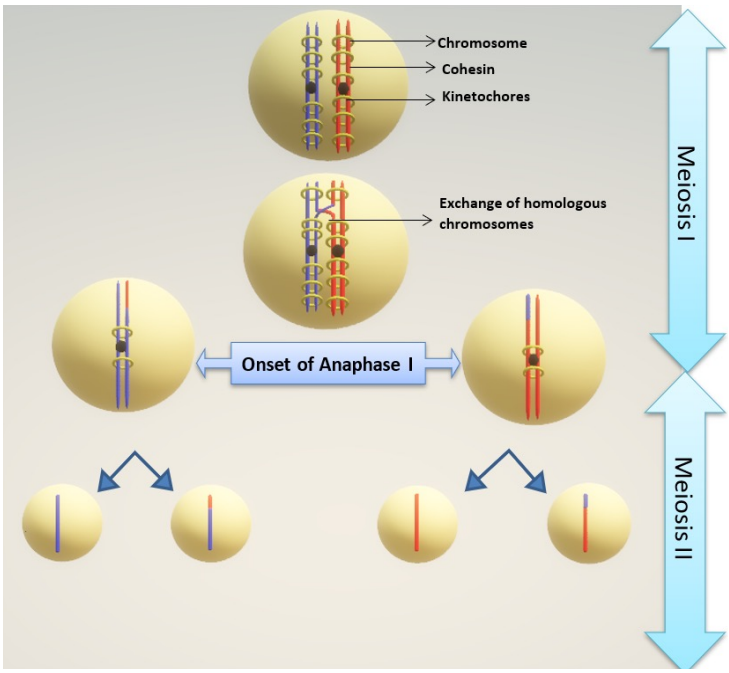

Figure 1a

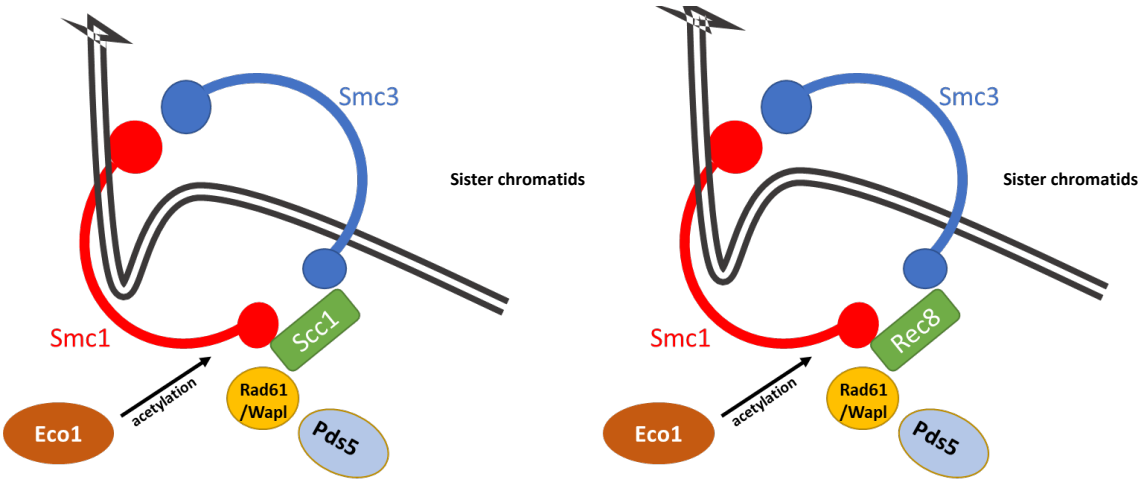

Mitosis-specific cohesin

Meiosis-specific cohesin

Figure 1b

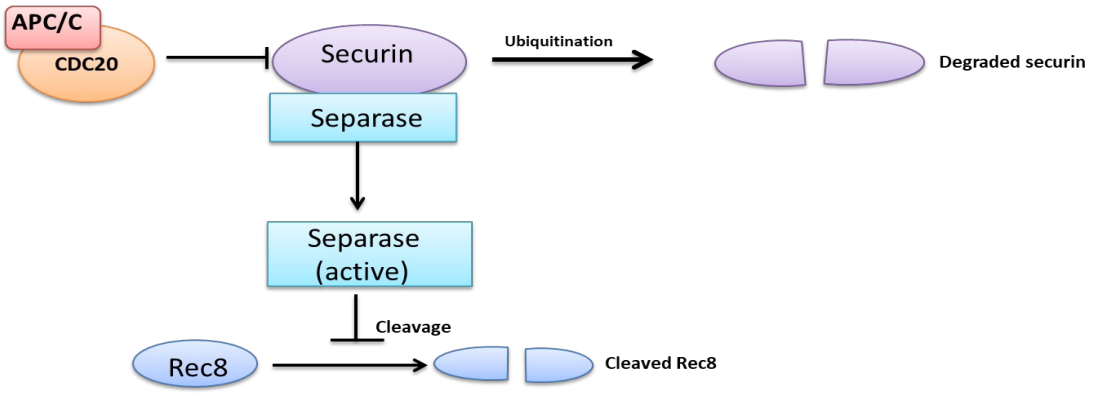

Figure 1c

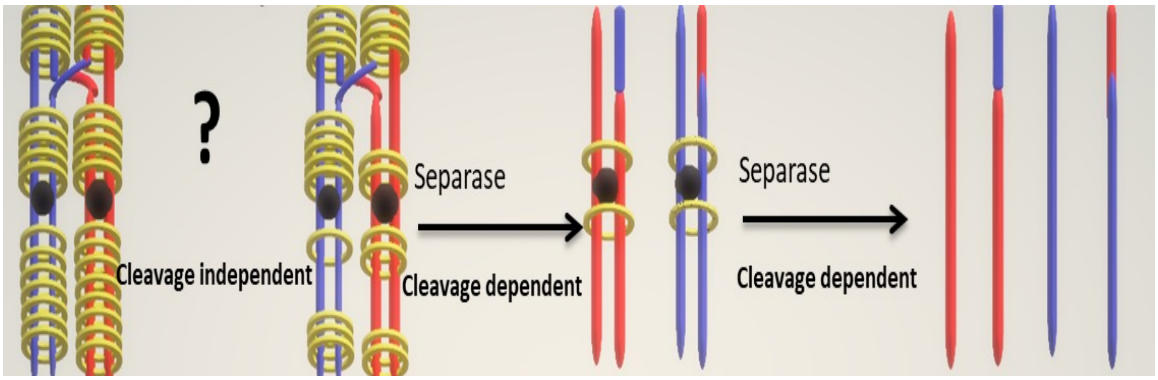

Figure 1d

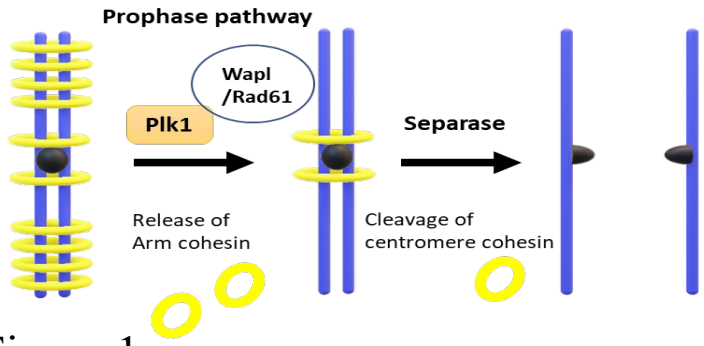

Figure 1e

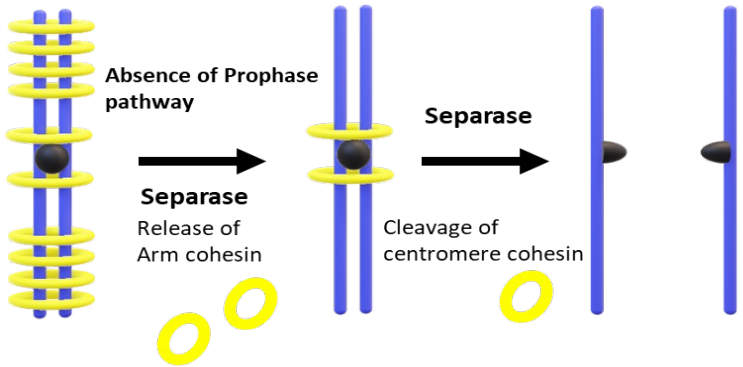

Figure 1f

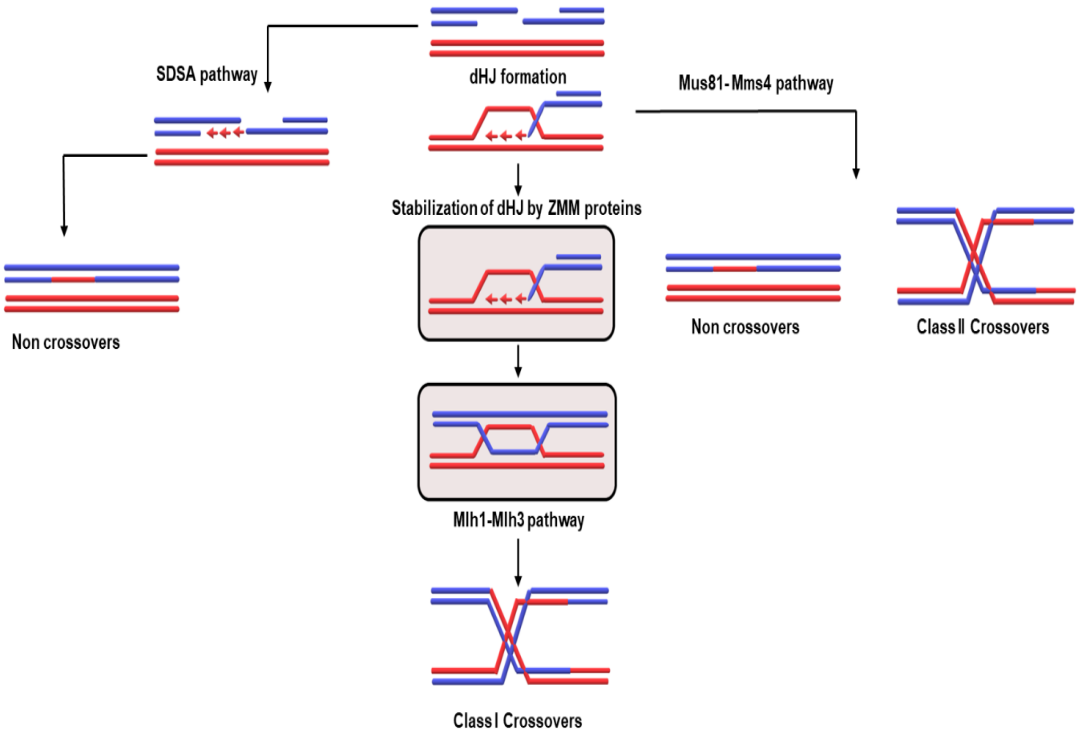

Figure 1g

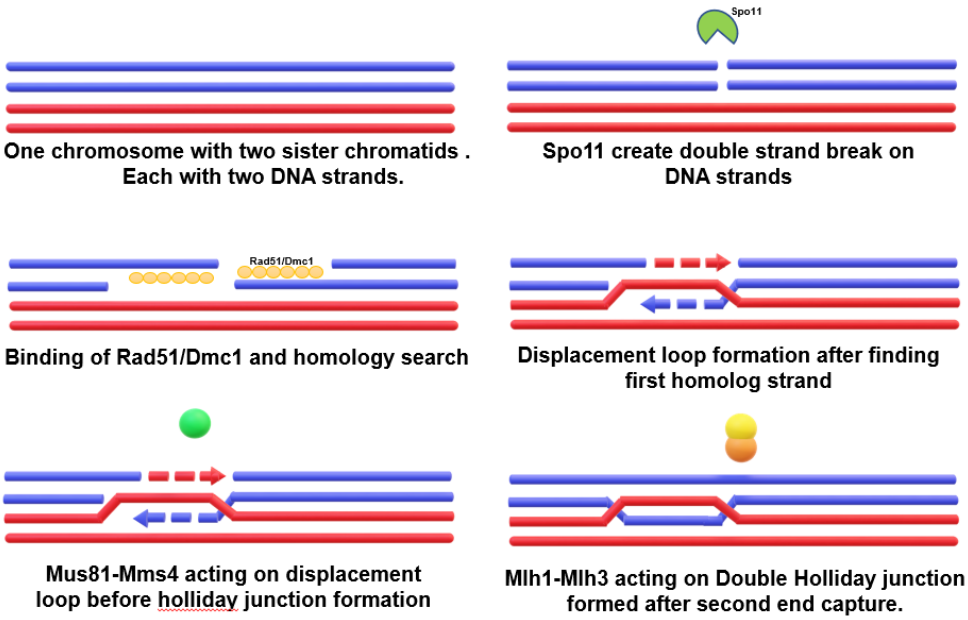
One chromosome with two sister chromatids . Each with two DNA strands.
Spo11
Spo11 create double strand break on DNA strands
Rad51/Dmc1
Binding of Rad51/Dmc1 and homology search
Displacement loop formation after finding first homolog strand
Mus81-Mms4 acting on displacement loop before holliday junction formation
Mlh1-Mlh3 acting on Double Holliday junction formed after second end capture.

Figure 1h

Figure 2

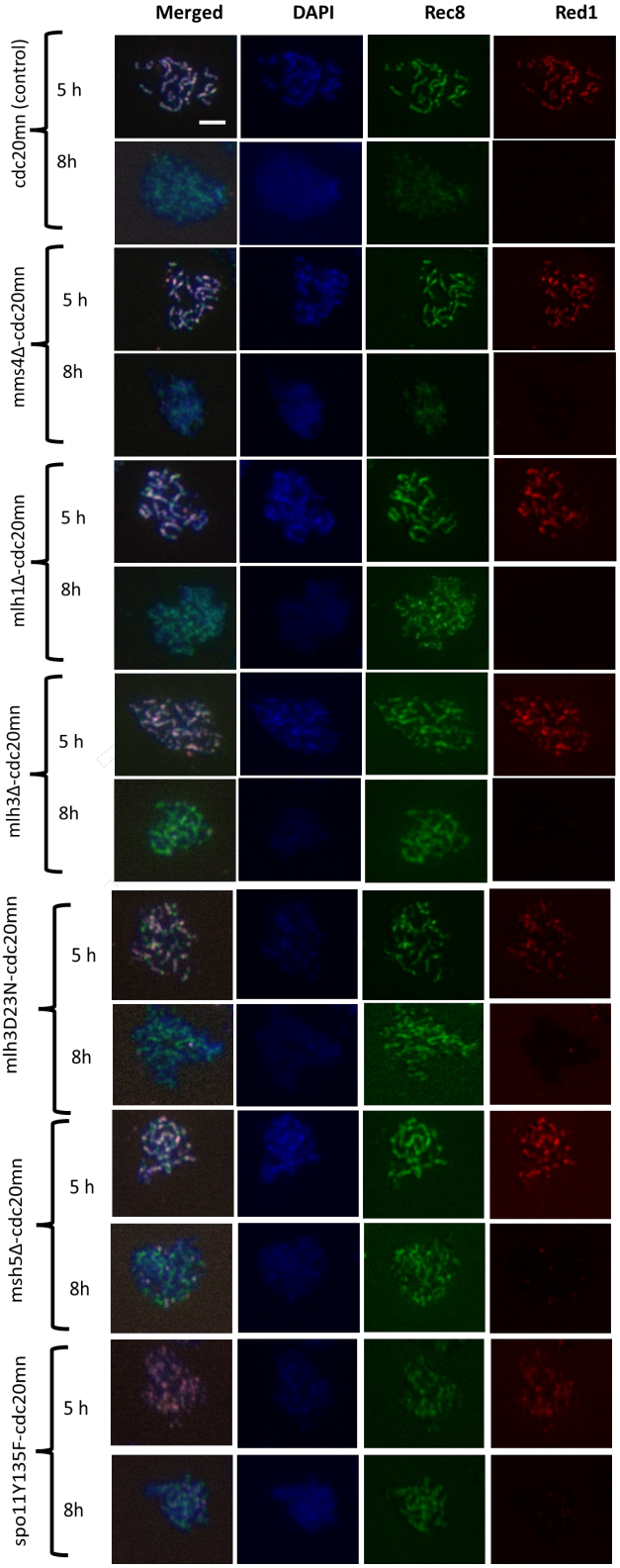

Figure 2a

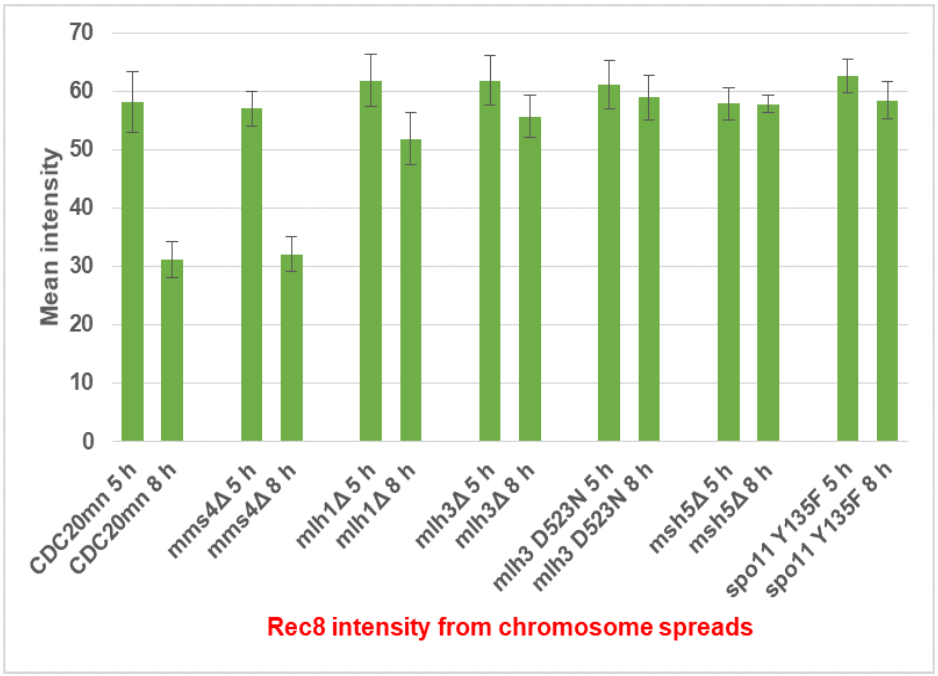

Figure 2b

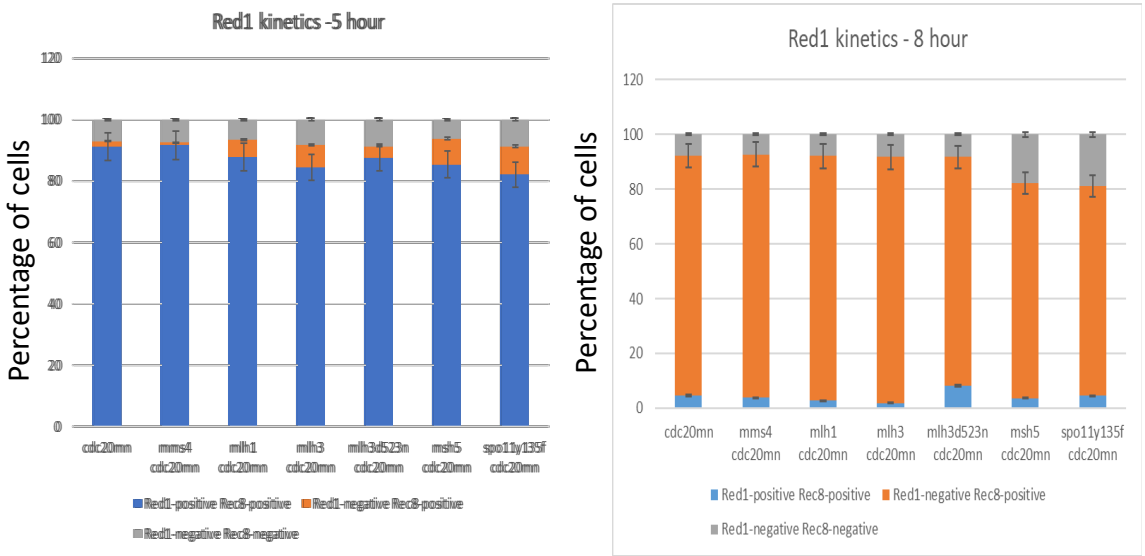

Figure 2c

Figure 2c

Figure 3

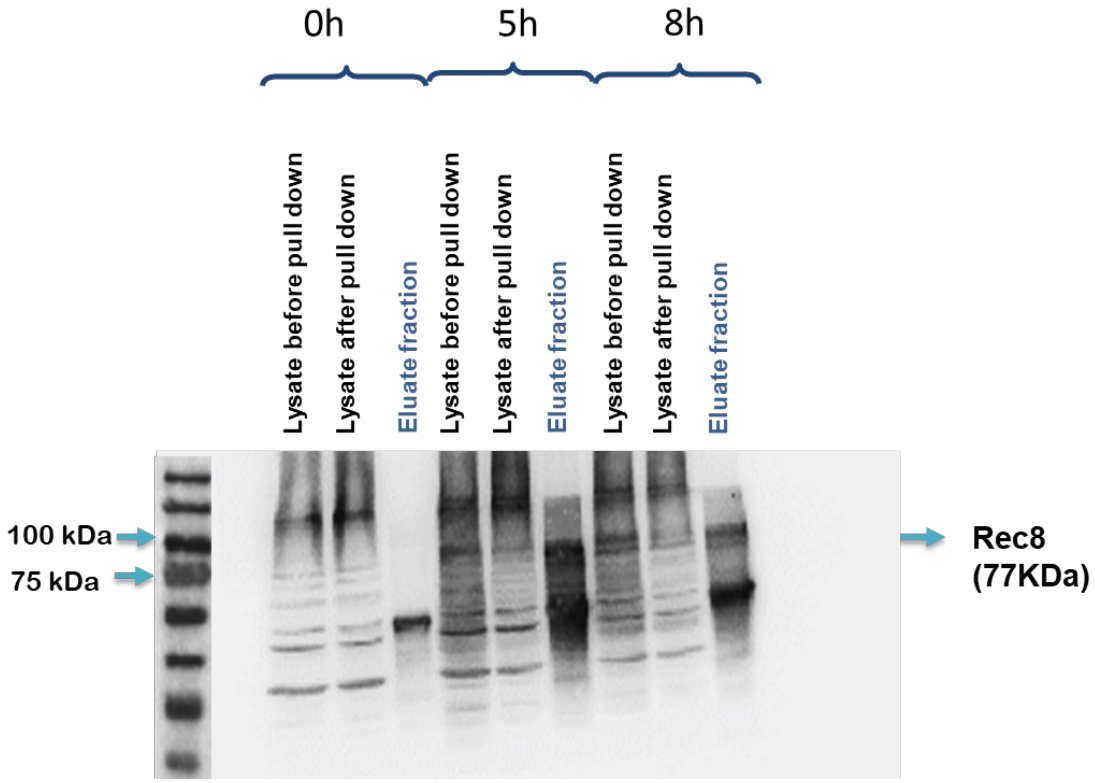
0h
5h
8h
Lysate before pull down
Lysate after pull down
Eluate fraction
Lysate before pull down
Lysate after pull down
Eluate fraction
Lysate before pull down
Lysate after pull down
Eluate fraction
100 kDa
75 kDa
Rec8
(77KDa)

Figure 4

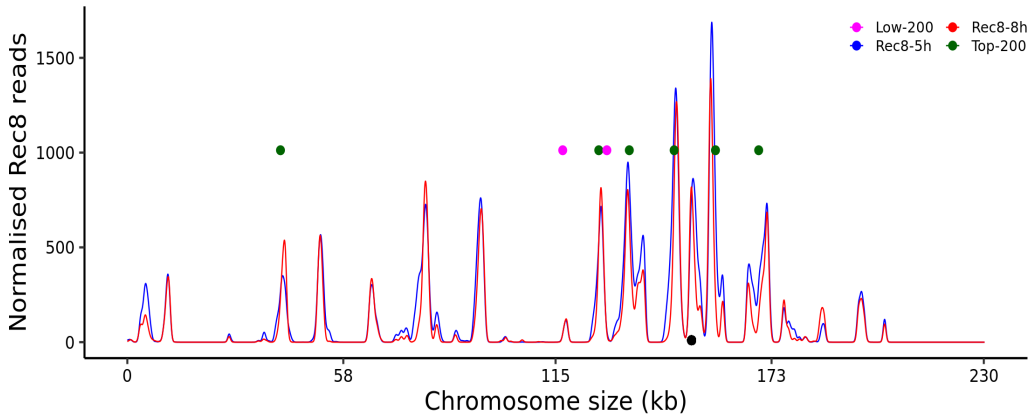

Chromosome I

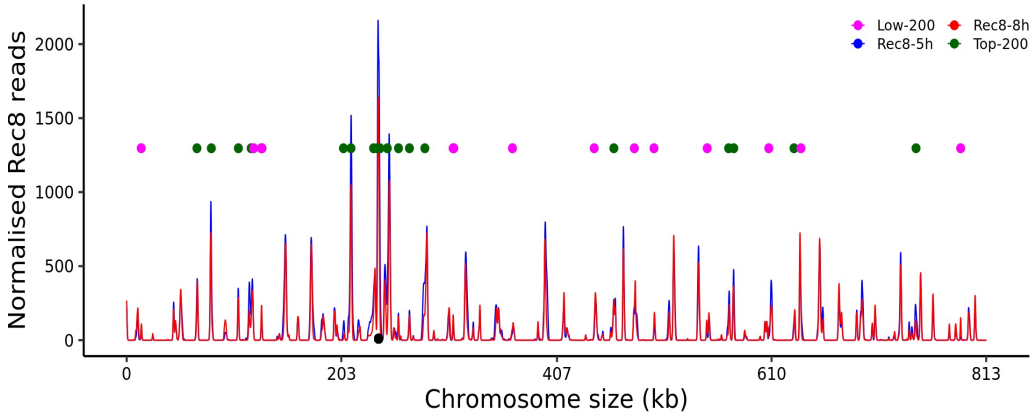

Chromosome II

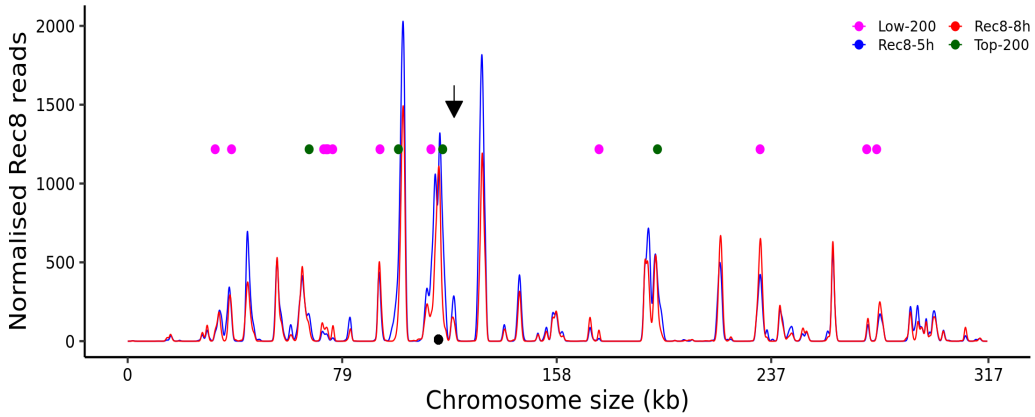

Chromosome III

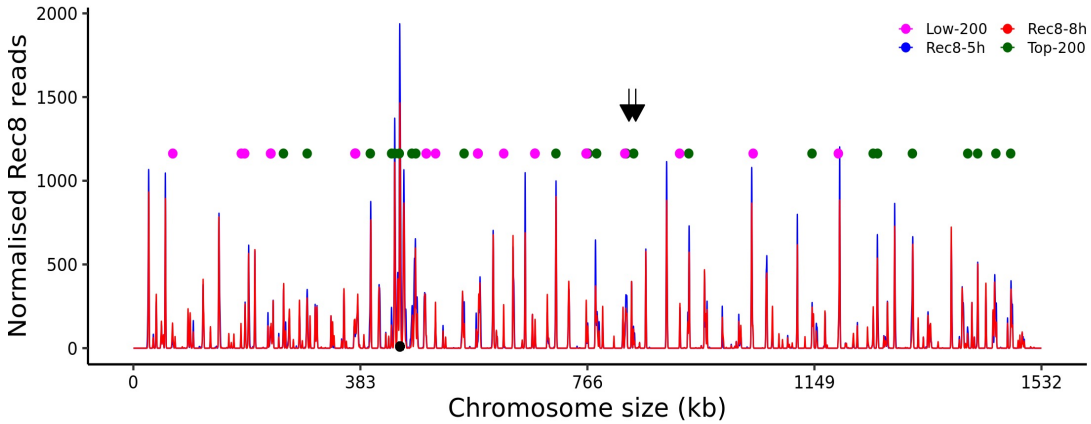

Chromosome IV

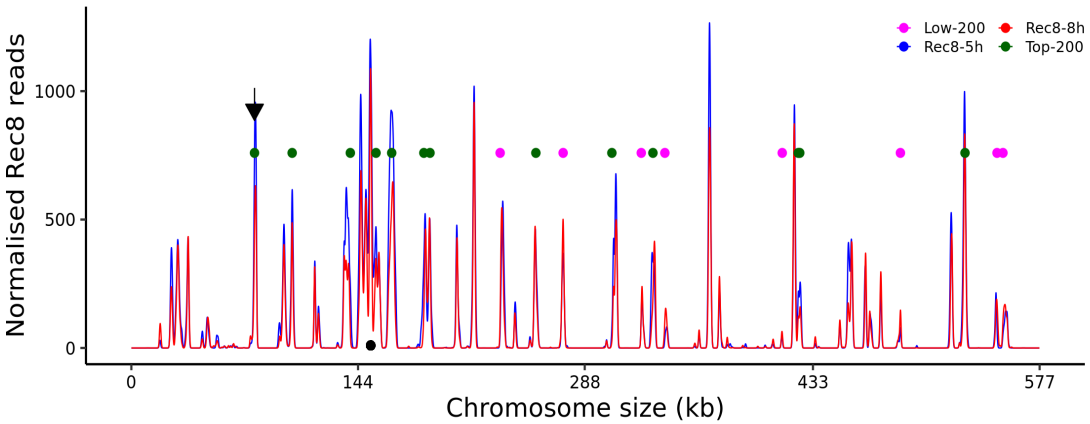

Chromosome V

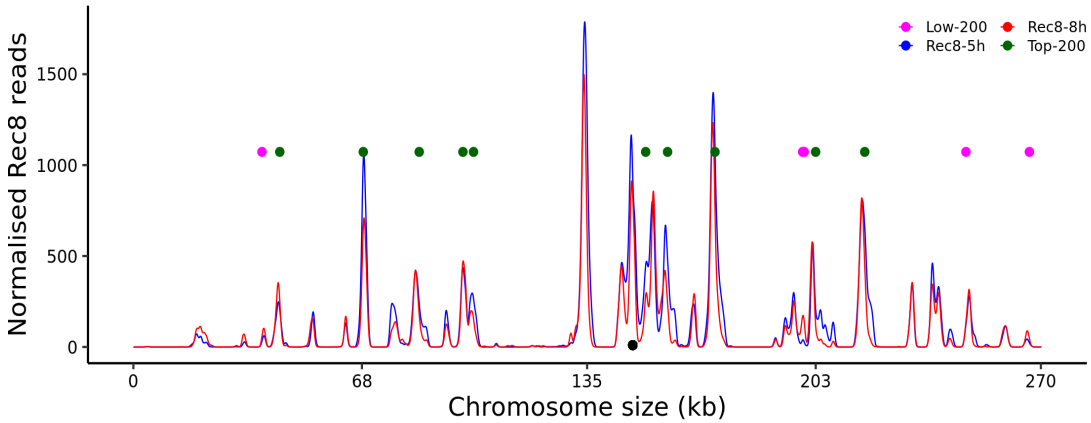

Chromosome VI

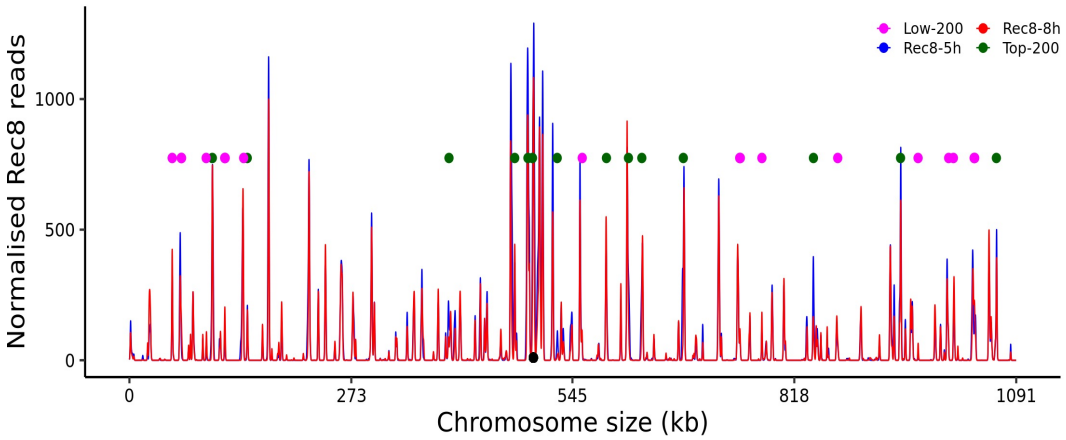

Chromosome VII

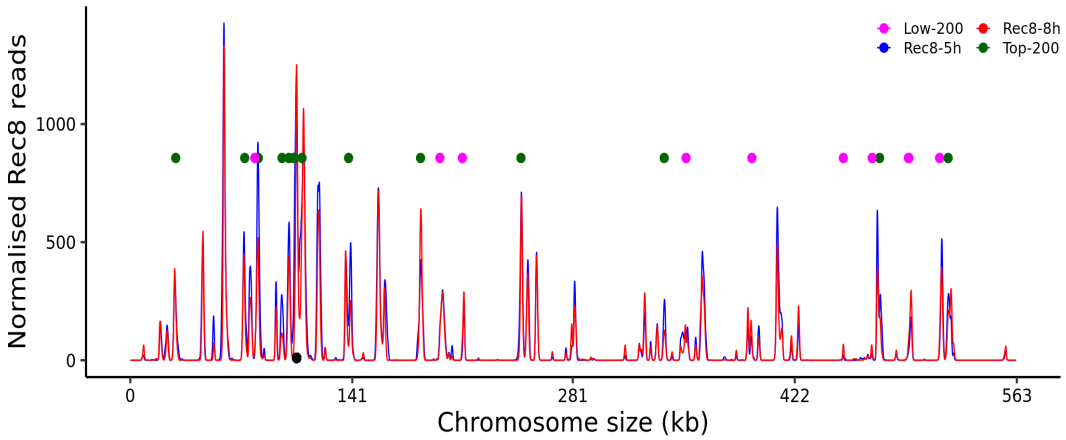

Chromosome VIII

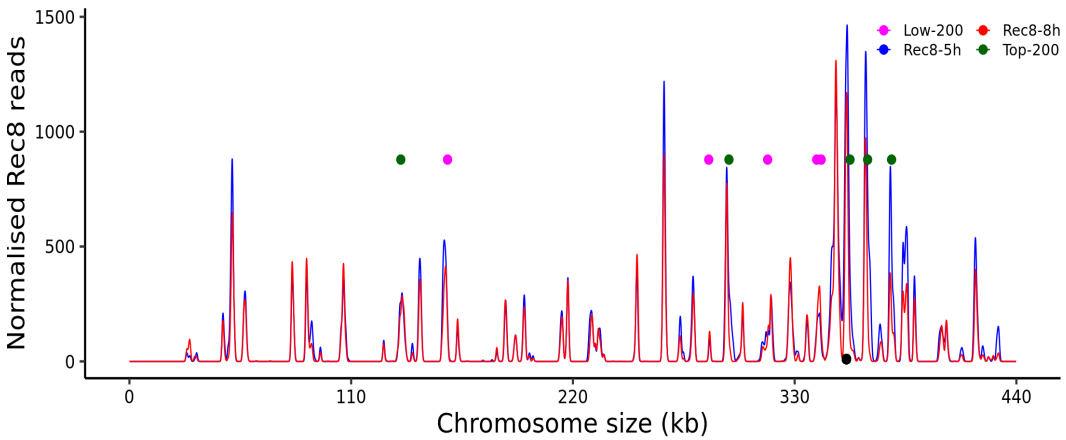

Chromosome IX

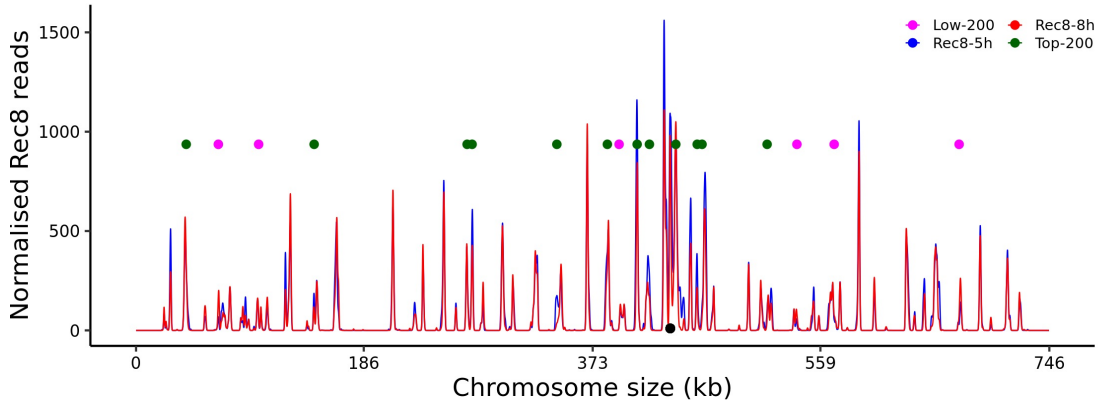

Chromosome X

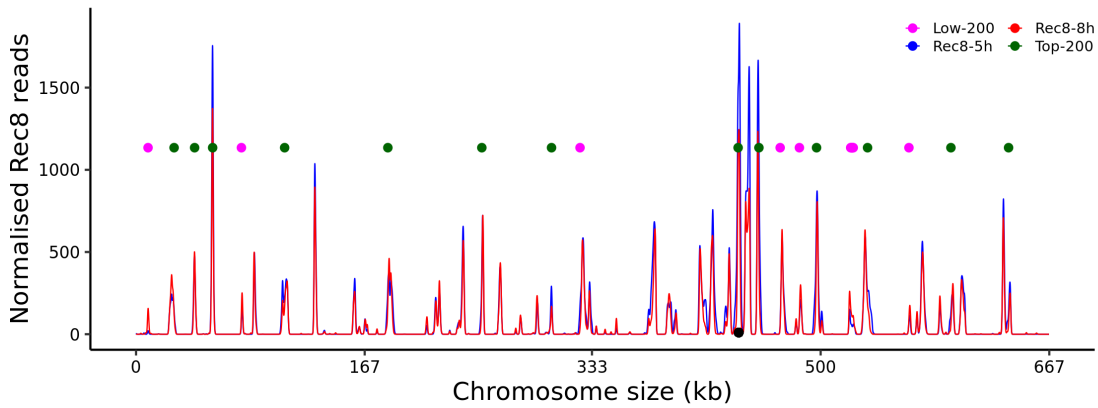

Chromosome XI

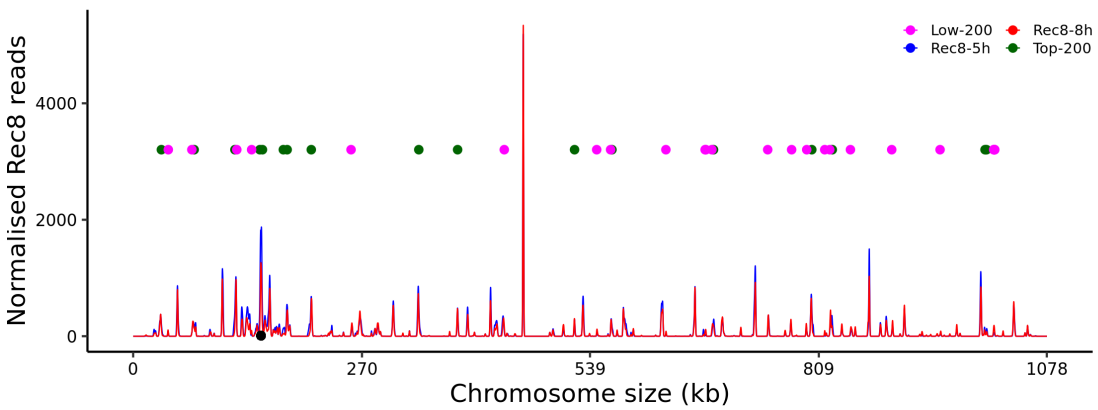

Chromosome XII

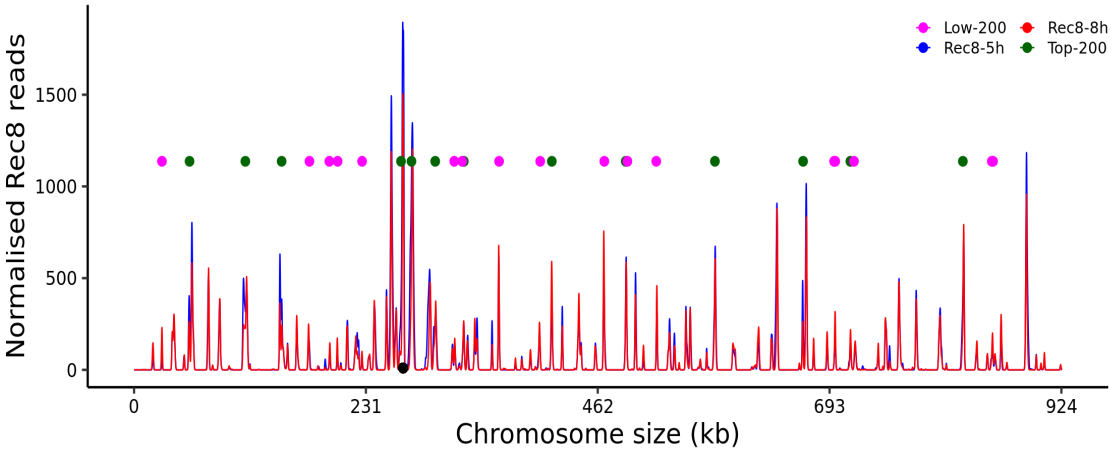

Chromosome XIII

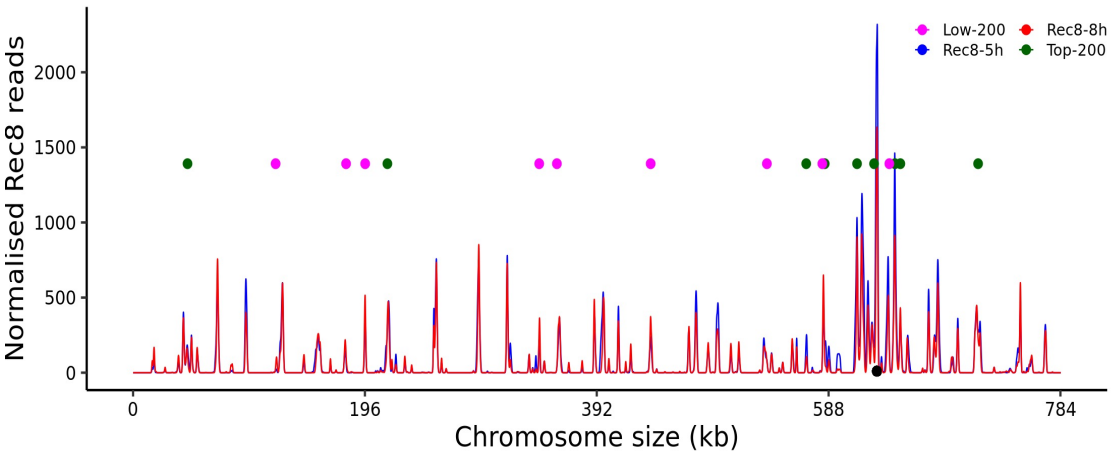

Chromosome XIV

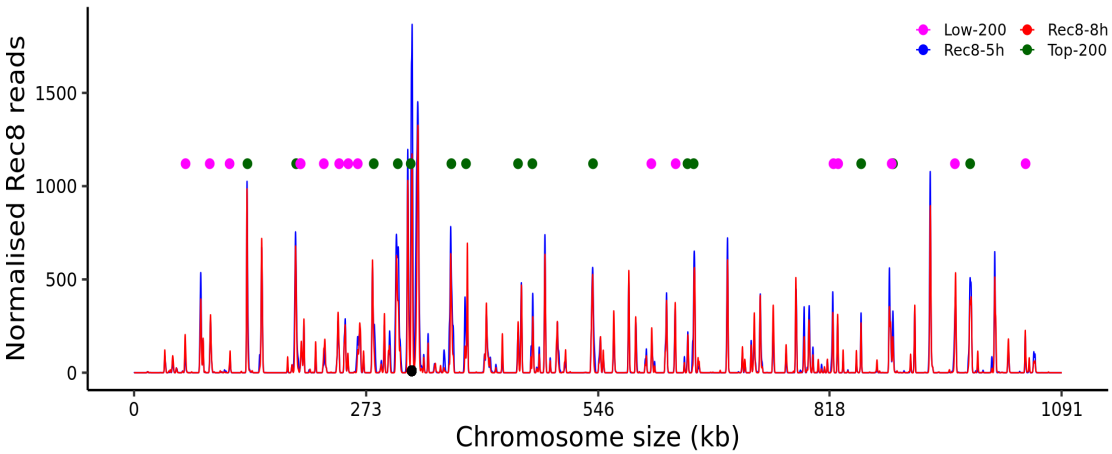

Chromosome XV

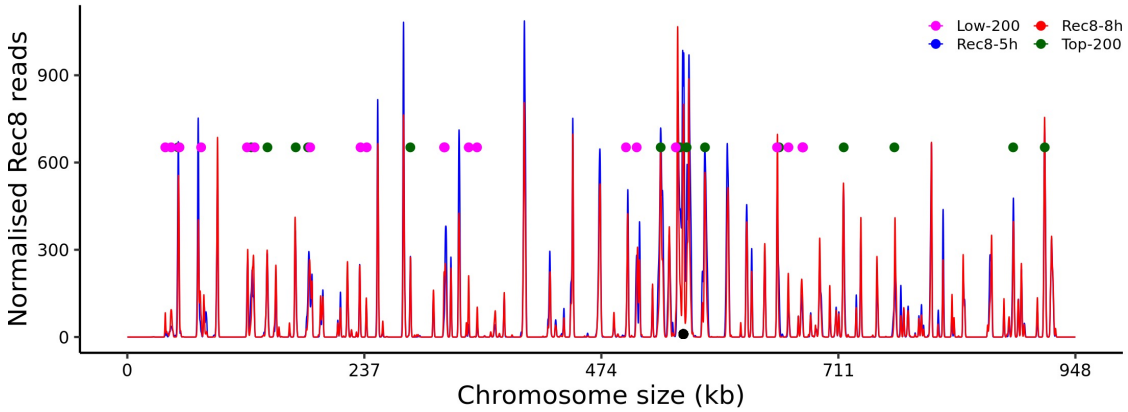

Chromosome XVI

Figure 4a

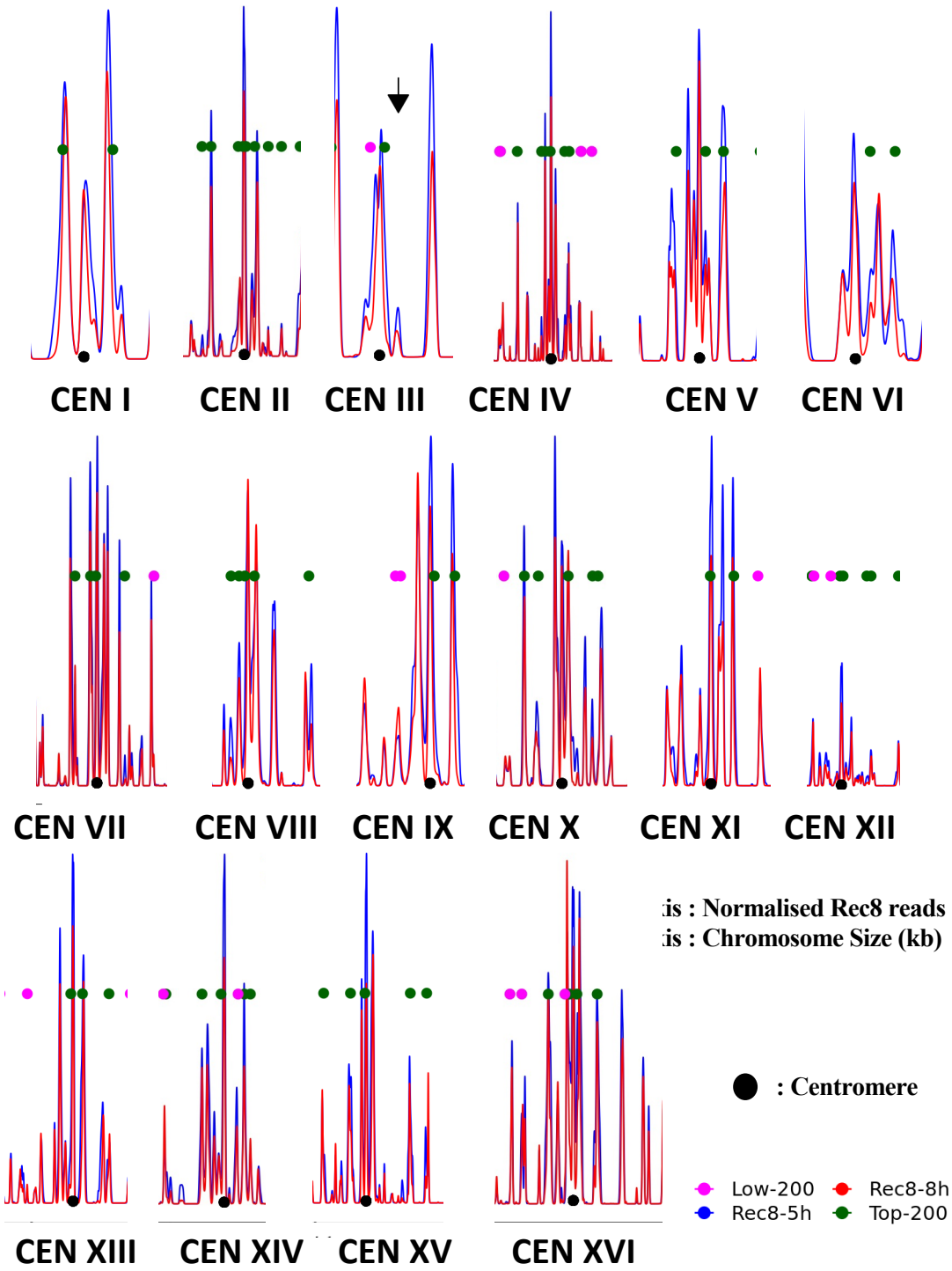
CEN I
CEN II
CEN III
CEN IV
CEN V
CEN VI
CEN VII
CEN VIII
CEN IX
CEN X
CEN XI
CEN XII
CEN XIII
CEN XIV
CEN XV
CEN XVI
is : Normalised Rec8 reads
is : Chromosome Size (kb)
: Centromere
Low-200
Rec8-8h
Rec8-5h
Top-200

Figure 4b

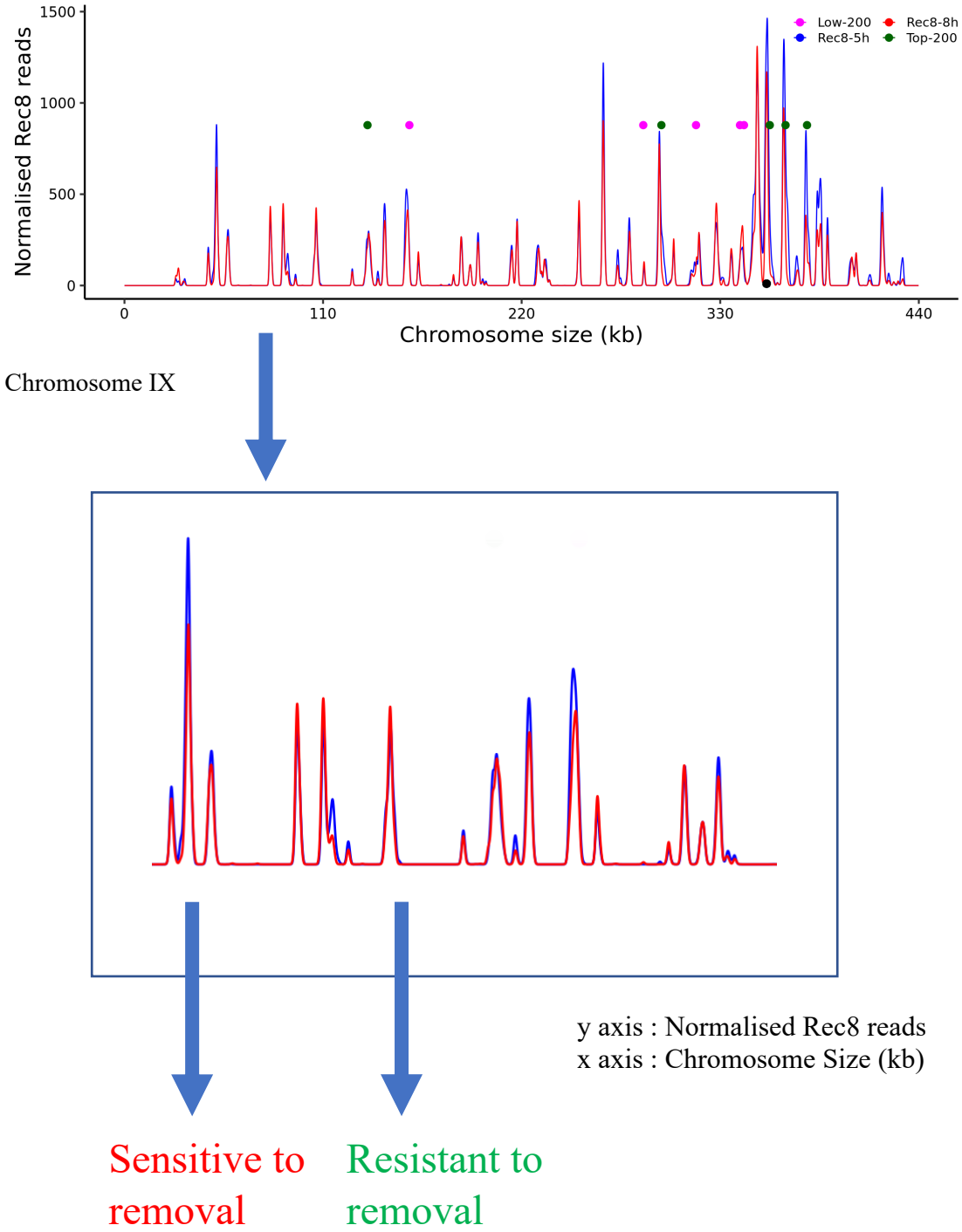
Normalised Rec8 reads
1500
1000
500
0
Low-200
Rec8-5h
Rec8-8h
Top-200
0
110
220
330
440
Chromosome size (kb)
Chromosome IX
y axis : Normalised Rec8 reads
x axis : Chromosome Size (kb)
Sensitive to removal
Resistant to removal

Figure 4c

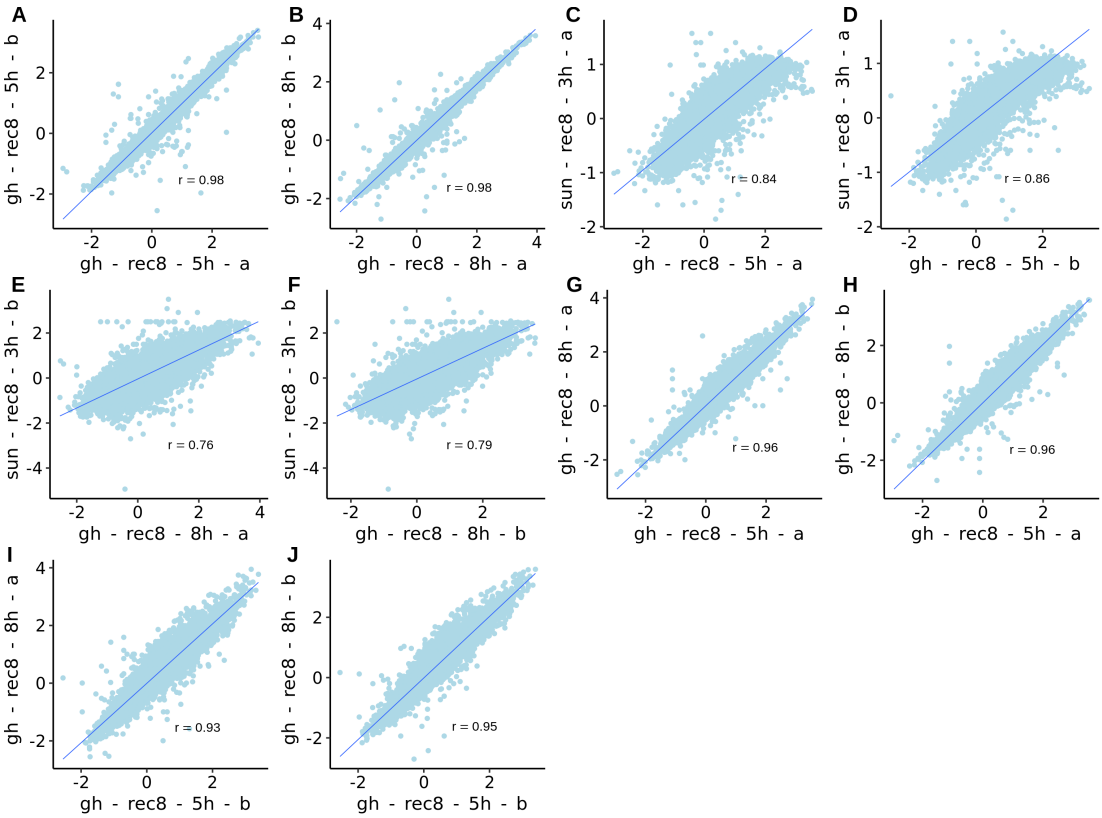

Figure 4d

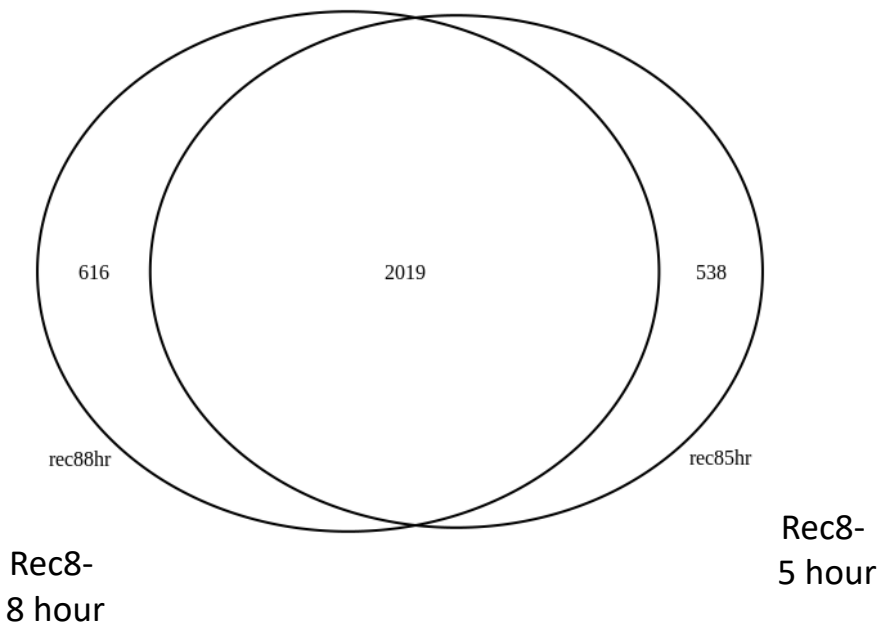

Figure 4e

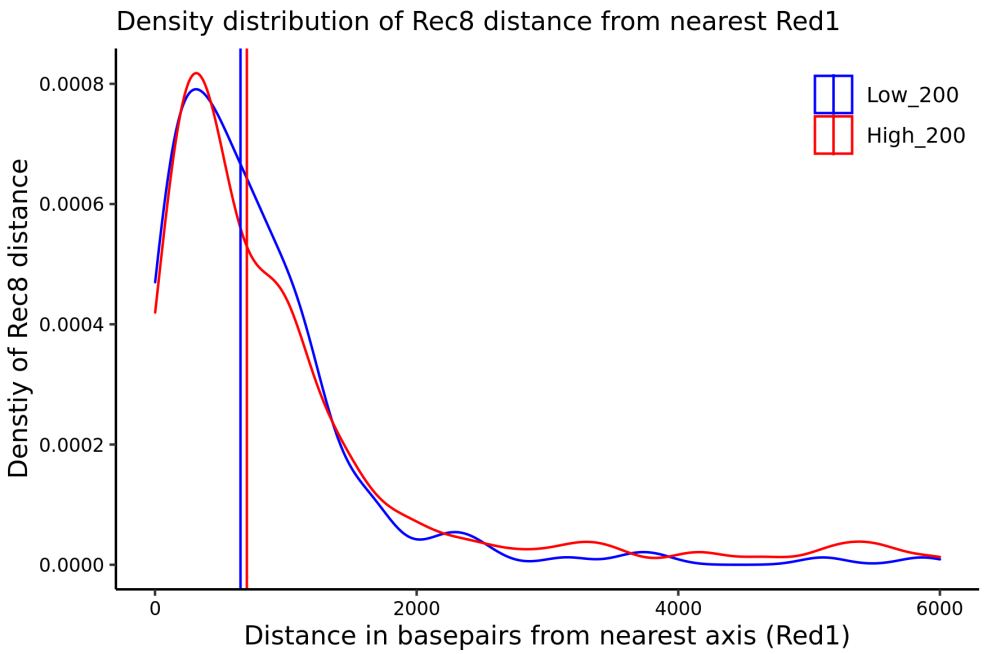

Figure 4f

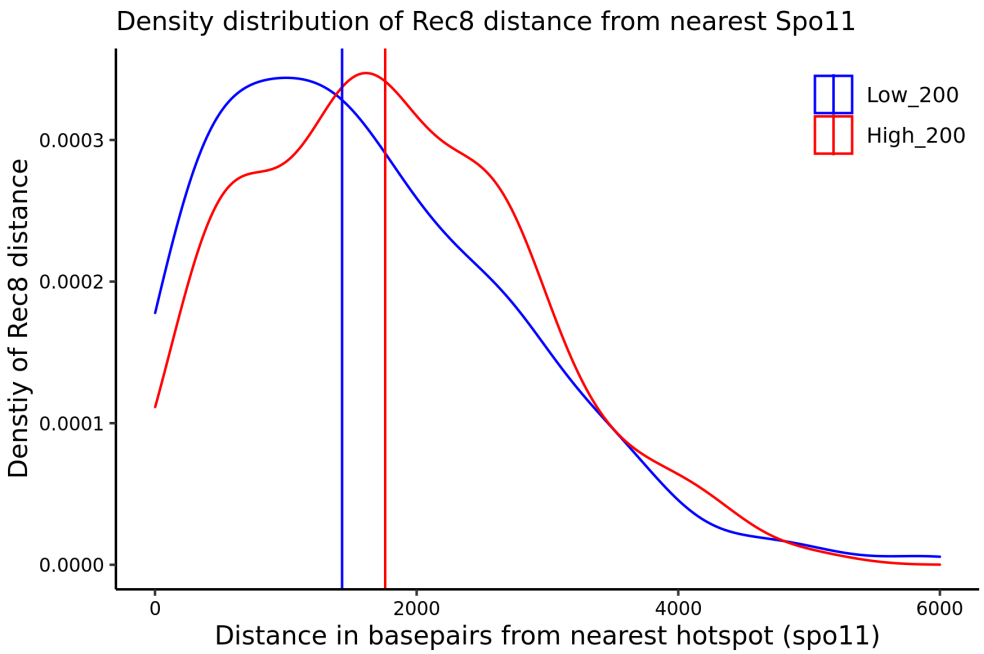

Figure 4g

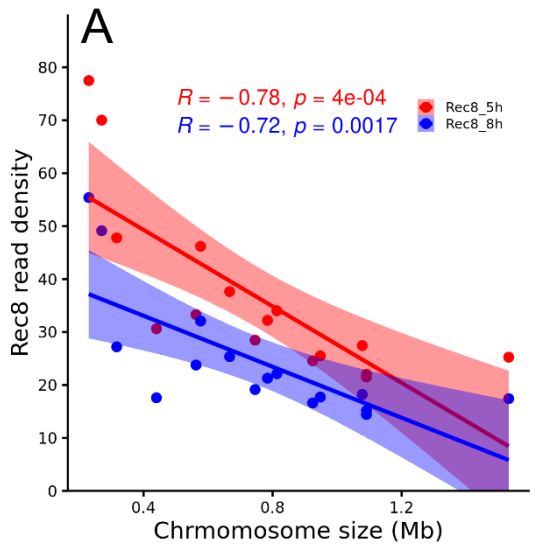

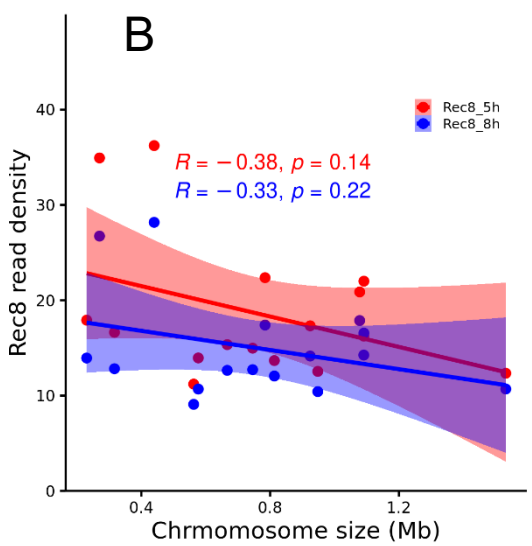

5h > 8h

5h = 8h

Figure 4h

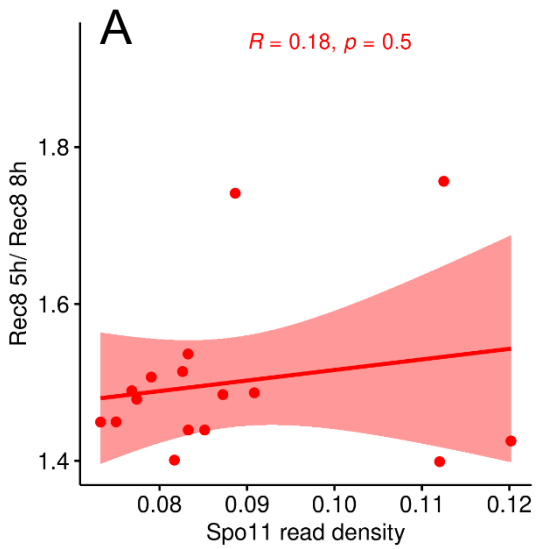

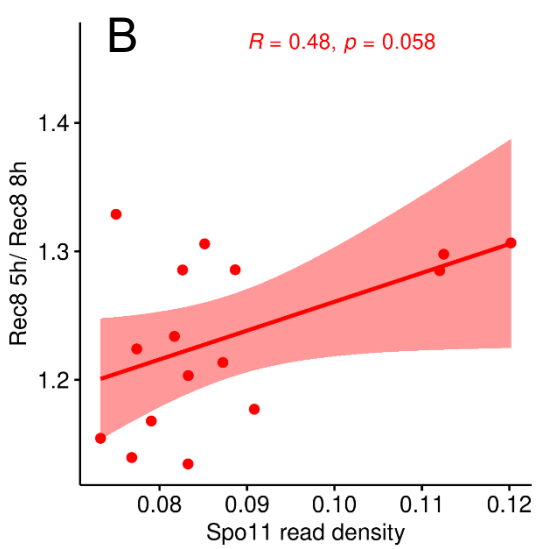

5h > 8h

5h = 8h

Figure 4i

Figure 5

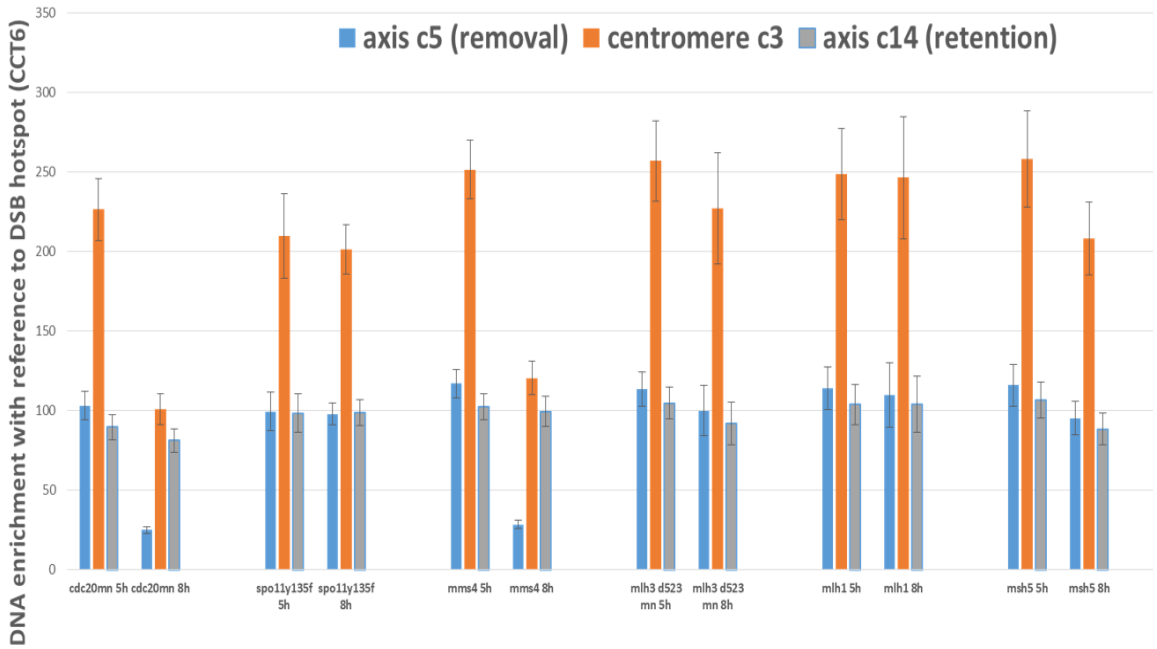
axis c5 (removal)
centromere c3
axis c14 (retention)
DNA enrichment with reference to DSB hotspot (CCT6)
350
300
250
200
150
100
50
0
cdc20mn 5h
cdc20mn 8h
spo11y135f 5h
spo11y135f 8h
mms4 5h
mms4 8h
mlh3 d523 mn 5h
mlh3 d523 mn 8h
mlh1 5h
mlh1 8h
msh5 5h
msh5 8h

Figure 6

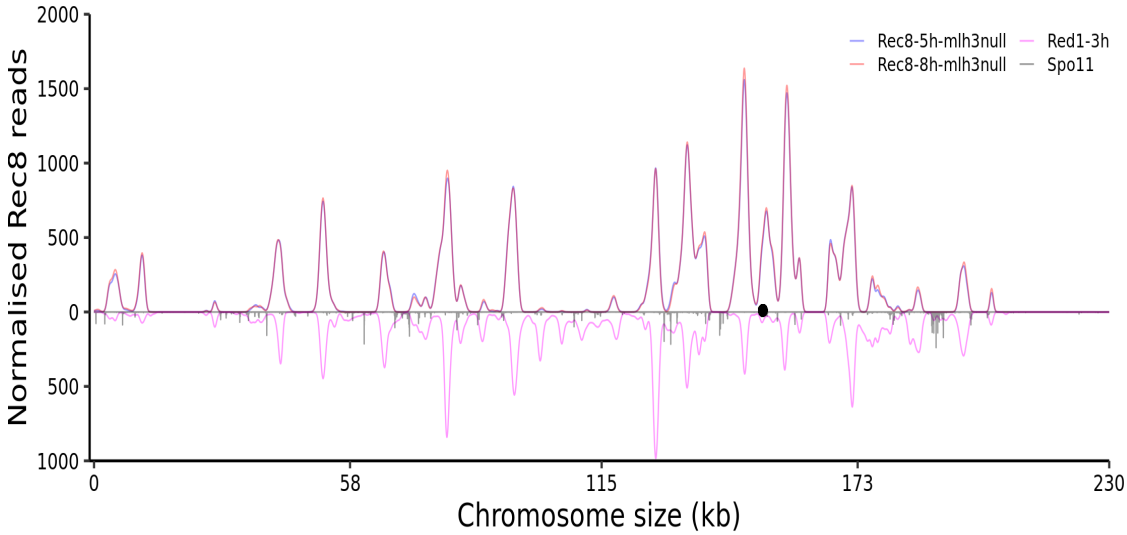

Chromosome 01

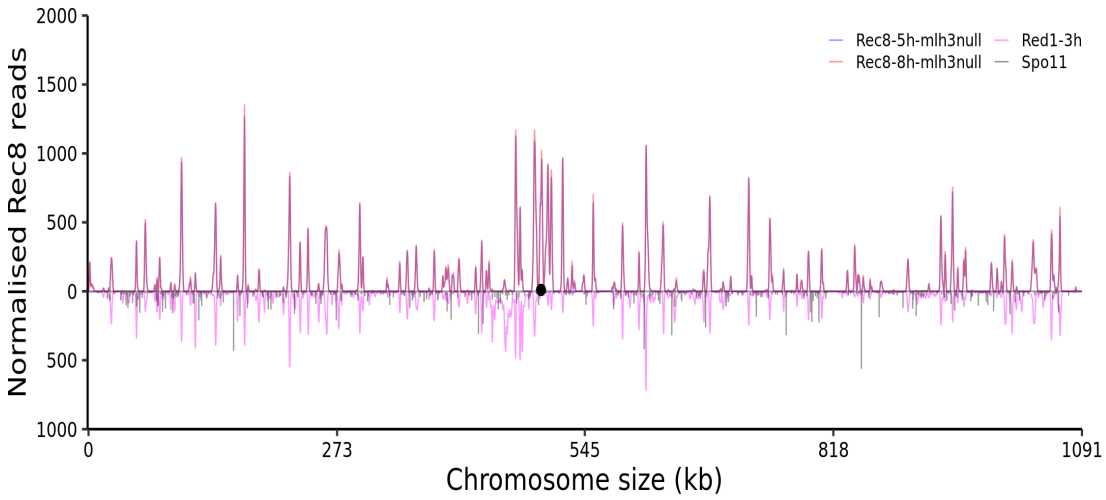

Chromosome 07

Figure 7

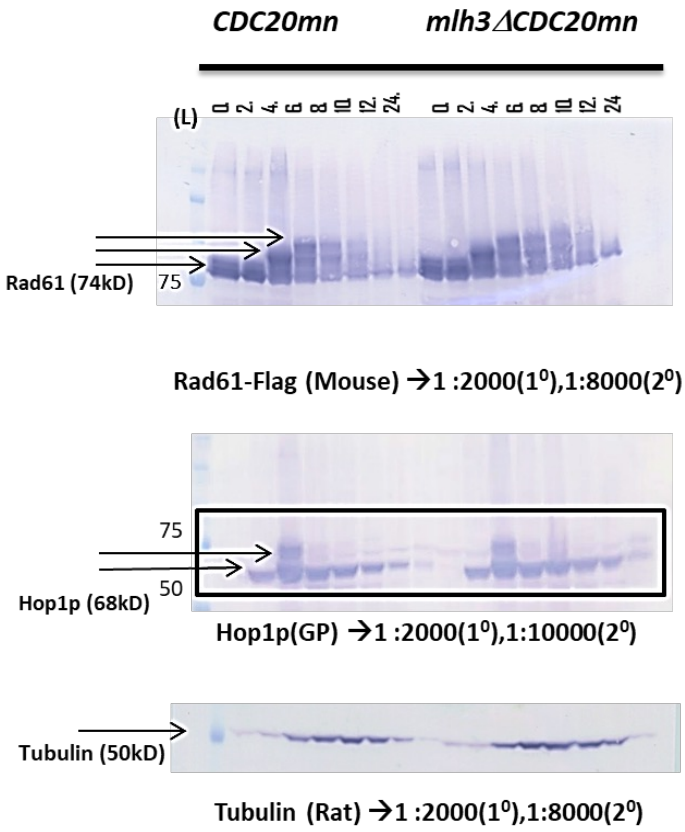

Figure 7a

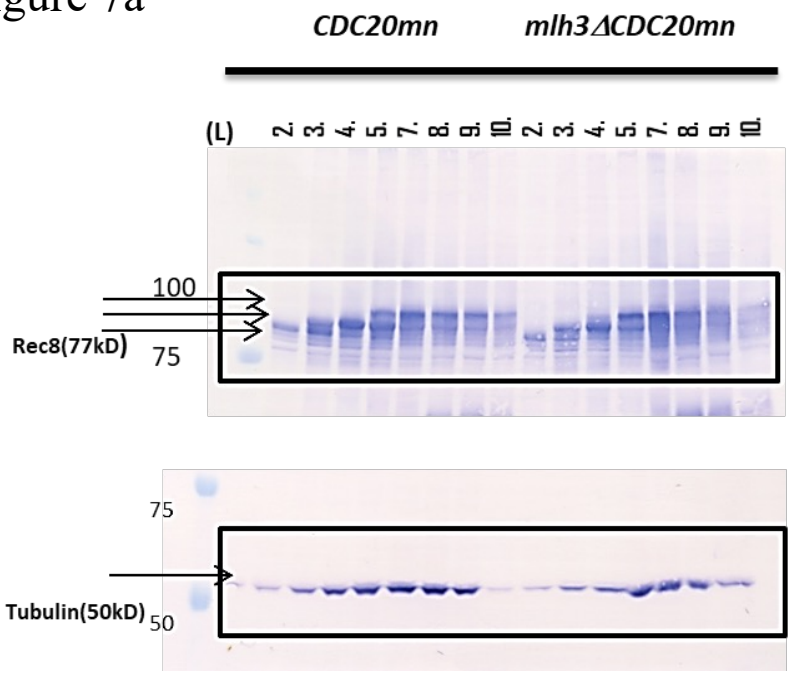

Figure 7b

Figure 8

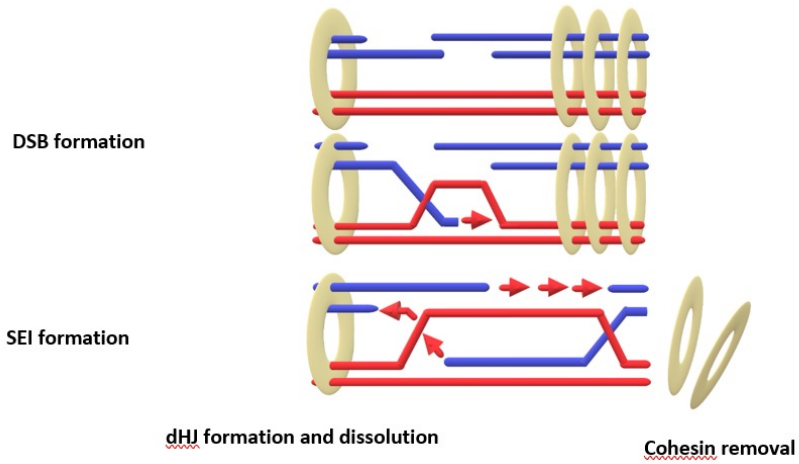

Figure 8a

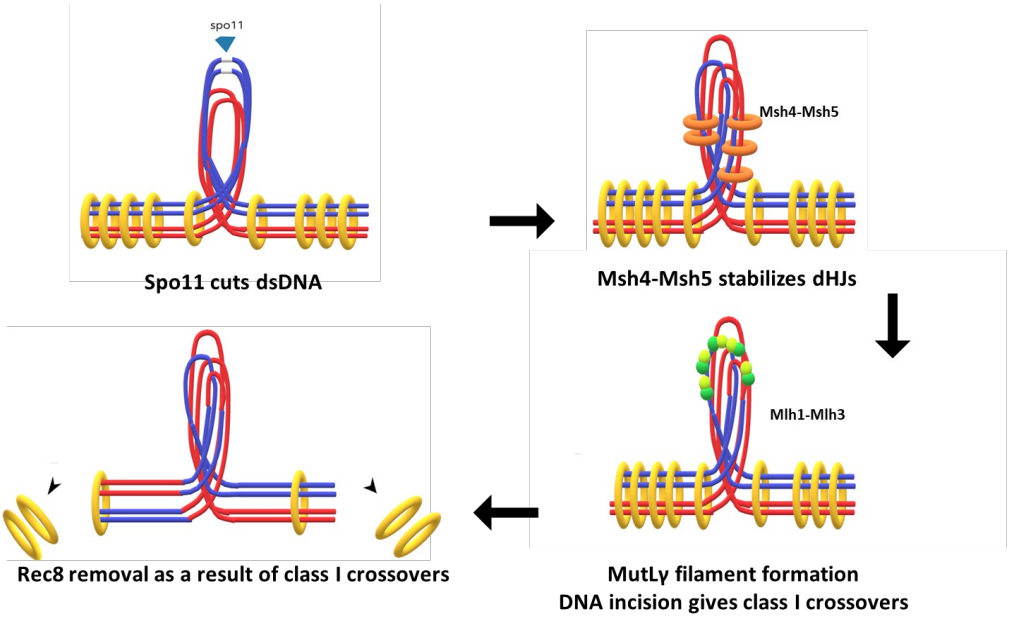

Figure 8b

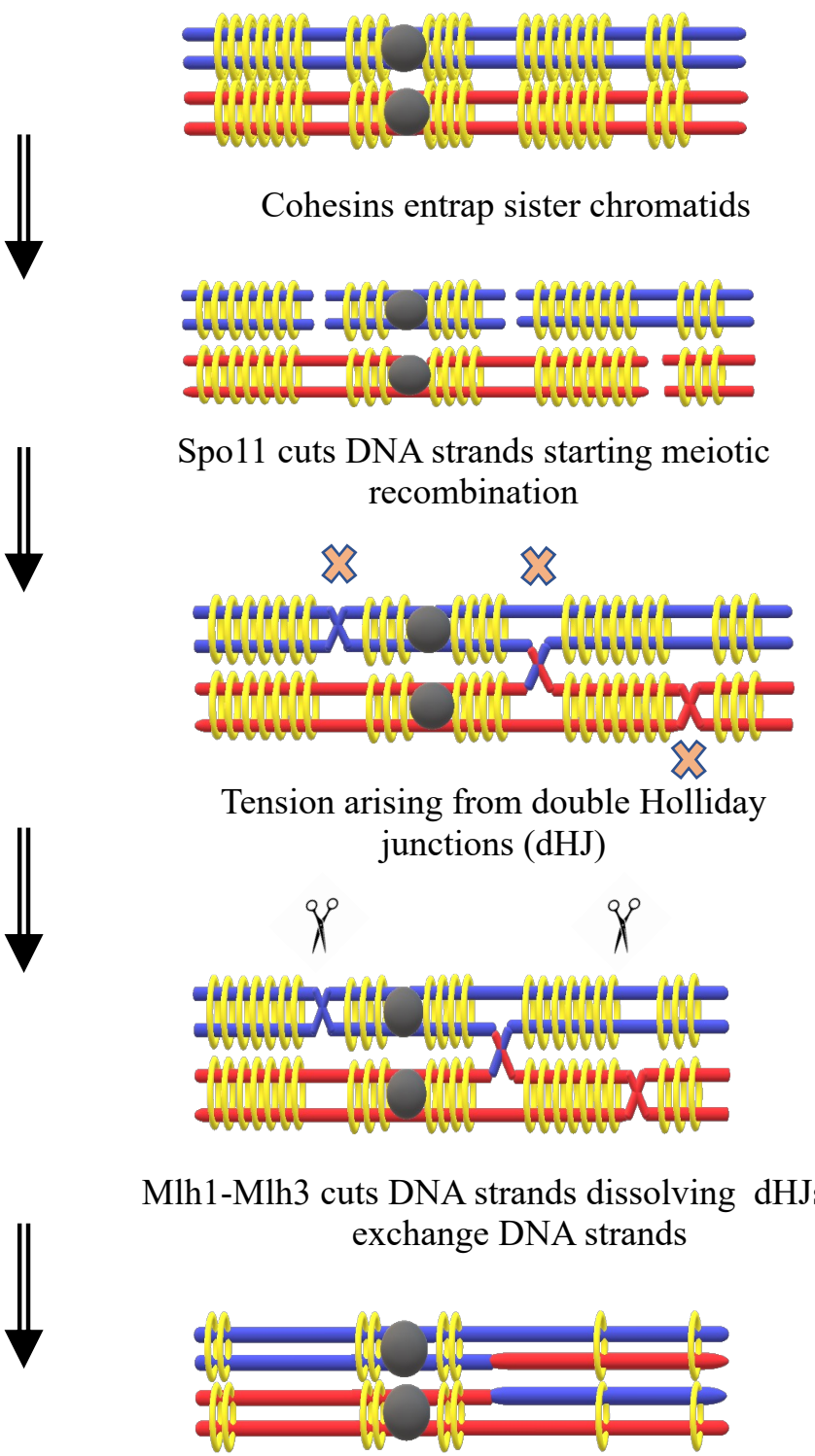

Cohesins entrap sister chromatids

Spo11 cuts DNA strands starting meiotic recombination

Tension arising from double Holliday junctions (dHJ)

Mlh1-Mlh3 cuts DNA strands dissolving dHJs and exchange DNA strands

Local tension release from Class I crossover formation result in global cohesin removal from arms and centromere

Figure 8c